Identification of Novel Niche Molecules Controlling Hematopoietic Stem Cell Behavior

Dissertation

Faculty of Biology

Ludwig Maximilian University

Munich

prepared at the

Research Unit Stem Cell Dynamics

Helmholtz Center Munich – German Research Center for Environmental Health

submitted by

Konstantinos D. Kokkaliaris, *MSc*

26 September 2013

Direct Adviser: Dr Timm Schroeder

Erste Gutachter: Prof Dr Heinrich Leonhardt

Zweiter Gutachterin: Prof Dr Barbara Conradt

Tag der mündlichen Prüfung: 12.9.2014

Part of this work has been published as follows:

Loeffler D., Kokkaliaris K.D., and Schroder T. (2011). Wnt to notch relay signaling induces definitive hematopoiesis. **Cell Stem Cell** 9(1): 2-4.

Kokkaliaris K.D., Loeffler D., and Schroder T. (2012). Advances in tracking hematopoiesis at the single-cell level. **Current Opinion in Hematology** 19: 243–249.

Montrone C., Kokkaliaris K.D., Loeffler L., Lechner M., Kastenmüller G., Schroeder T., and Ruepp A. (2013). HSC-Explorer: a curated database for hematopoietic stem cells. **Plos One** 8(7): e70348.

Swiers G., Baumann C., O'Rourke J., Giannoulatou E., Joshi A., Moignard V., Pina C., Kokkaliaris K.D., Yoshimoto M., Yoder M.C., Frampton J., Schroeder T., Enver T., Göttgens B., and de Bruijn M.F.T.R. Haemogenic endothelium: cells in transit. (in revision)

Hoppe P.S., Schwarzfischer M., Loeffler D., Kokkaliaris K.D., Endele M., Hilsenbeck O., Moritz N., Filipczyk A., Rieger M., Marr C., Schauberger B., Burtscher I., Kirstetter P., Bürger A., Lickert H., Nerlov C., Theis F.J. and Schroeder T. A stochastic PU.1 / Gata1 switch is not the basis for hematopoietic myeloid lineage choice (in revision)

Schwarzfischer M.*, Hilsenbeck O.*, Schauberger B., Hug S., Filipczyk A., Hoppe P.S., Strasser M., Buggenthin F., Feigelman J.S., Krumsiek J., Löffler D., Kokkaliaris K.D., van den Berg A.J.J., Endele M., Hasenauer J., Marr C., Theis F.J.*, and Schroeder T.* Reliable long-term single-cell tracking and quantification of cellular and molecular behavior in time-lapse microscopy (submitted)

1. Table of Contents

2. Abstract

Hematopoietic stem cells (HSCs) are the multipotent cells able to differentiate and daily produce a massive number of all mature blood cells (hematopoiesis), while maintaining their undifferentiated state long-term. This delicate balance between self-renewal and differentiation is regulated by intrinsic mechanisms and extrinsic signals. The main regulator of the extrinsic signals responsible for this balance is the anatomical microenvironment where HSC reside, the so-called HSC niche. Despite the fact that the concept of the niche is decades-old, its exact cellular and molecular composition as well as the underlying mechanisms controlling HSC fates remain unknown.

The main limitation for the improved clinical application of HSCs is our inability to maintain or ideally expand them in vitro without genetic modification. In vitro studies revealed that the clonal, fetal-liver derived stroma cell line AFT024 can maintain the number of co-cultured HSCs, even upon long culture periods, while another cell line failed (2018 stroma). However, the behavior of HSCs under self-renewing conditions and the key factors governing the HSC-niche interaction remain obscure. In the current study, we monitor HSCs and multipotent progenitor (MPP) cells in co-cultures with niche stroma cells by implementing continuous live-cell imagining, at the single-cell level. We report early differences in the behavior of HSCs co-cultured with the different stroma and present evidence for an AFT024-mediated pro-survival/proliferation effect upon co-cultured HSCs. Also, we show that AFT024 stroma promotes survival/proliferation of early MPPs. Conditioned media experiments and stroma-free cultures revealed cell adhesion as the predominant mechanism of this interaction. Finally, we propose that delta-like homolog 1 (Dlk1), dermatopontin (Dpt) and fibroblast activation protein (Fap) are necessary for HSC survival and proliferation and that Dpt alone is essential for the in vitro maintenance of HSCs in AFT024-based in vitro cultures.

3. Introduction

3.1. Hematopoietic stem cells: A historical overview and current concepts

Every second of our life, millions of cells die in different tissues of our body. Blood is such a tissue with high turnover rate, with 200 billion ($2x10^{11}$) erythrocytes and 2 billion ($2x10^{9}$) granulocytes dying every day. The same number has to be replenished to secure homeostasis (Dexter et al., 1984). Hematopoietic stem cells (HSCs) are the adult stem cells responsible for the lifelong production of all mature blood cells (multipotency), in a process called hematopoiesis. HSCs are also capable of maintaining their undifferentiated state even after numerous cell divisions (self-renewal), therefore avoiding exhaustion. It is widely accepted that HSCs are currently the best understood adult stem-cell system, mainly due to decades of research and the tens of thousands of scientific papers published on this topic.

3.1.1. The first discoveries

The first impetus for HSC research dates back to the late 19th century, when it was reported that mature blood cells vary in their morphology, therefore belonging to different lineages (Ehrlich, 1879). Some scientists believed that lymphoid and myeloid cells originate from a common precursor cell, which they called "stem cell" (Stammzelle) (Pappenheim, 1896; Maximov, 1909). Pappenheim, who is coined the term, also drew one of the first hematopoietic trees in 1905 (reviewed by Ramalho-Santos and Willenbring, 2007).

An important year for hematopoietic research was 1945, when exposure to nuclear bomb radiation caused severe hematopoietic failures to the exposed civilians in Hirosima and Nagasaki. A few years later, Jacobson and colleagues showed that mice which had their spleens shielded with lead, were protected from lethal doses of irradiation, suggesting that some spleen cells could reconstitute the blood system (Jacobson et al., 1949). In 1951, Lorenz and colleagues went one step further showing that injection of spleen or bone marrow cells successfully rescued recipient mice from fatal irradiation injury (Lorenz et al, 1951), thus paving the way for HSC transplantations (Figure 3.1). It is important to note that the

transplantation assays are still the gold-standard method for the assessment of HSC function. Following that observation, Barnes and Loutit, as well as Main and Prehn showed independently that what orchestrates the post-transplantation recovery of irradiated recipients is the transplanted cells (Barnes and Loutit, 1954; Main and Prehn, 1955) and not some "humoral" element in their spleen or bone marrow, as it was initially hypothesized (reviewed by Thomas, 2000; Little and Storb, 2002; Weissman and Shizuru, 2008).

The early 1960's were marked by major progress in the hematopoietic field due to the pioneering work of Till and McCulloch who reported the ability of transplanted bone marrow cells to form colonies in the spleen of lethally irradiated mice (Till and McCulloch, 1961). They described the first quantitative hematopoietic assay by reporting the linear correlation between the number of transplanted cells and the spleen colonies (104 bone marrow cells give rise to one spleen colony). Based on chromosomal markers, they identified the clonal origin of individual spleen colonies which were formed by the progeny of a single transplanted cell, the so-called spleen colony-forming cell or CFU-S (Becker et al., 1963). In addition, they proposed that the CFU-S were hematopoietic stem cells in which the decision between self-renewal and differentiation is stochastic (Till et al., 1964). Till later named his model as "Hematopoiesis is engendered randomly" or "HER", in response to Trentin's "HIM" model (see below). Finally, they reported the multipotency of the CFU-S, which could give rise to both, myeloid (granulocytes, megakaryocytes, macrophages), as well as erythroid colonies in the spleen of lethally irradiated recipients (Wu et al., 1967).

3.1.2. The "niche/microenvironment" era

In 1968, Wolf and Trentin sought to investigate the effect of stroma upon HSC differentiation potential. For this reason, they performed a key experiment in which plugs of bone marrow stroma from primary reconstituted mice were implanted into the spleen of secondary recipients (Wolf and Trentin, 1968). They reported that most of the bone-marrow colonies were granulocytic, whereas colonies residing in the spleen stroma were mostly erythroid. This observation combined with their previous data (Curry and Trentin, 1967; Curry et al., 1967) led them to the proposal of the "Hematopoietic Inductive Microenvironments" concept ("HIM" model), according to which the microenvironment can instruct the differentiation of the stem cell progeny towards a certain lineage (Curry et al., 1967; Trentin, 1971).

During the mid 1970's, Dexter made a major contribution to the field by establishing an ex vivo system capable of maintaining hematopoiesis for long culture periods (Dexter et al., 1973; Dexter et al., 1977). Dexter's long-term culture was based on the cultivation of bone marrow fractions consisting of both hematopoietic cells and heterogeneous stroma populations. Some of the main characteristics of his system were: 1) the lineage skewing towards granulopoiesis, 2) the absence of secreted-factor activity in the conditioned media (called colony stimulating activating − CSA) and 3) the importance of HSC-stroma interactions for the maintenance of hematopoiesis (no CFU-S maintenance in stroma-free cultures).

In addition to the data mentioned above, Schofield showed that the transplanted HSCs homing to the bone marrow support hematopoiesis more robustly than those homing to the spleen (Schofield, 1978). Based on these findings, as well as on Dexter's published work (Dexter et al., 1973; Dexter et al., 1977), Schofield introduced the concept of the HSC niche. He envisioned the niche as the anatomical microenvironment within which HSC reside and self-renew and out of which, they undergo differentiation (Schofield, 1978). That was the first time that a self-renewing anatomical environment was proposed (in addition to the "differentiation" niche introduced by Trentin). In a follow up study, Whitlock and Witte developed another ex vivo culture system allowing production of lymphoid cells (Whitlock and Witte, 1982).
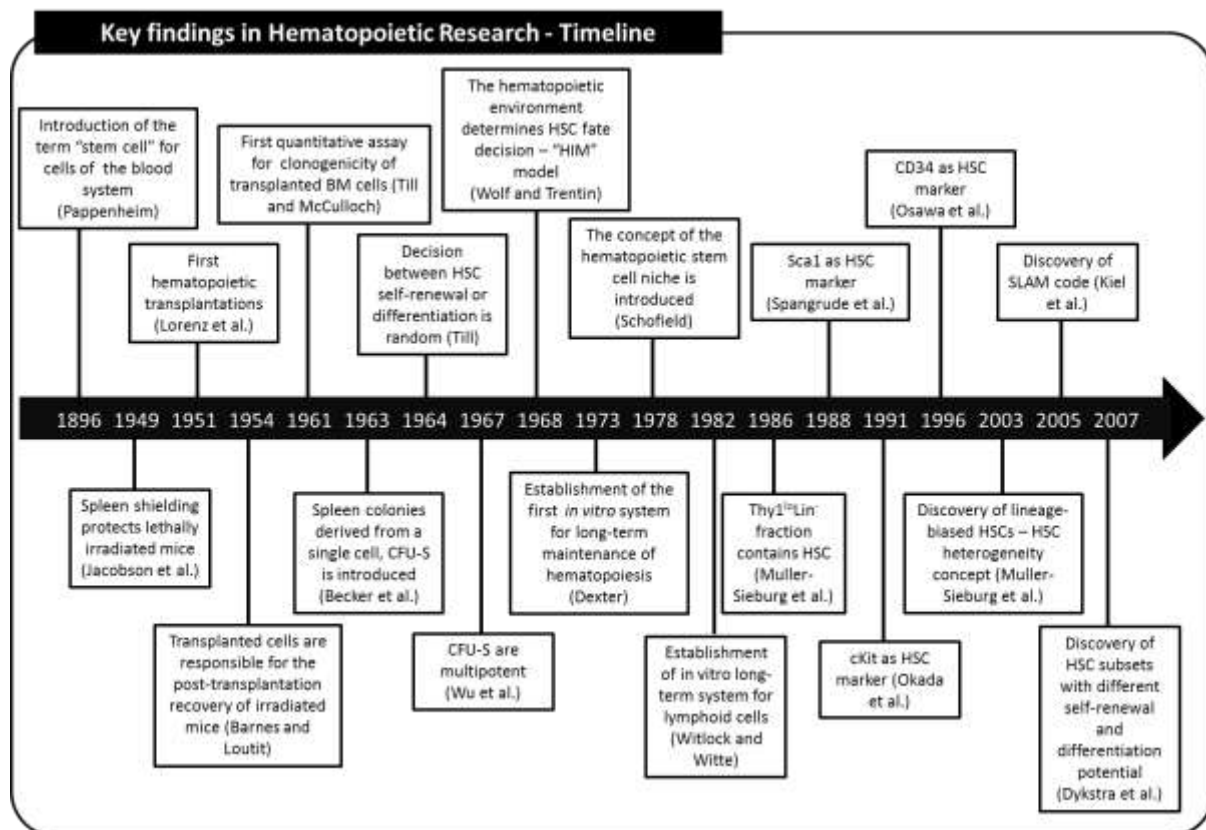
Figure 3.1. Historical overview of the key findings in the field of hematopoietic stem cell research.

3.1.3. Identifying markers for HSC enrichment/isolation

Despite the major advances in the hematopoietic field during the thirty years outlined above, the extremely low number of repopulating cells within the heterogeneous mix of bone marrow cells was still a significant hurdle for hematopoietic research. For scientific and therapeutic purposes, the need for HSC enrichment protocols became an issue of pivotal importance, therefore efforts were directed towards the identification of cellular properties that could distinguish stem cells from differentiated blood cells.

It is important to note that such efforts would have been impossible without two groundbreaking inventions coming from different fields: the development of the fluorescent-activated cell sorting (FACS) methodology by Leonard Herzenberg (Hulett et al., 1969) and the nobel-prize winning work from Georges Kohler and Cesar Milstein (Nobel Prize in Physiology or Medicine 1984, together with Niels Jerne), who introduced the concept of monoclonal antibodies against specific cellular antigens (Köhler and Milstein, 1975). The combination of those two technological advances allowed the isolation of cells with a defined

expression profile from a heterogeneous cell mixture and they are still a routine technique in almost all hematology laboratories.

One of the main groups contributed to the identification of markers for different hematopoietic populations (including HSCs) was the group of Irving Weissman. As he describes in one of his reviews (Weissman, 2002), the "key moment in the search for stem cells" was the finding that B-cell progenitors did not express the major marker of the B lineage, B220 (Muller-Sieburg et al., 1986). This led to the hypothesis that primitive blood cells would be negative for all markers expressed by terminally differentiated blood cells. For this reason, a cocktail of antibodies against surface proteins expressed by different types of mature blood cells (lineage cocktail) was utilized. Until today, a cell or a number of cells are experimentally defined as HSCs when their transplantation into lethally irradiated mice results in long-term survival of the recipients (longer than 16 weeks) and reconstitution of both the myeloid and the lymphoid lineage. To test the hypothesis, Muller-Sieburg transplanted lethally irradiated mice and found that all the HSC activity was indeed found in the Thy1^{low} lineage- (Lin-) fraction of bone marrow cells (Muller-Sieburg et al., 1986). It is important to note that Christa Muller-Sieburg was therefore the first to prospectively isolate HSCs.

Two years later, Gerald Spangrude (also from Weissman's group) introduced another marker (stem cell antigen 1, Sca1 or Ly-6 A/E) dividing further the Thy1^{low} Lin- compartment into two sub-populations, from which only the Sca1+ population contained HSCs (Spangrude et al., 1988). In the next years, more HSC markers were identified, such as c-Kit (kit oncogene) from the Suda lab (Okada et al., 1991) and CD34 from the Nakauchi lab (Osawa et al., 1996). Inevitably, different labs developed different sorting strategies to isolate HSCs (see Table 3.1): Thy1^{low} Sca1+c-Kit+ from the Weissman group, Hoechst dye efflux (defining the so-called side population - SP), Sca1+Lin- from the Mulligan group (Goodell et al., 1996), SLAM code from the Morrison lab (Kiel et al., 2005) and the E-SLAM code from the Eaves group (Kent et al., 2009). Interestingly, all those strategies yielded different HSC purities (number of sorted HSCs that indeed have HSC properties as shown by functional assays). Currently, the highest sorting purity (56%) has been achieved by Kent and colleagues, who used the endothelial protein C receptor (EPCR) in addition to CD45, CD48 and CD150 markers (abbreviated as E-SLAM) to isolate HSCs (Kent et al., 2009).

Immunophenotype	% purity	Reconstitution	Lab	First Author
Thy1^{lo} Sca1$^+$ Lin$^-$	ND	8-12 weeks	Weissman	Spangrude et al., 1988
KSL	ND	25 weeks	Suda	Okada et al., 1991
SP Sca1$^+$ Lin$^-$	ND	16 weeks	Mullingan	Goodell et al., 1996
CD34$^-$ KSL	21%	40 weeks	Nakaushi	Osawa et al., 1996
CD150$^+$ CD48$^-$ KSL	47%	16 weeks	Morrison	Kiel et al., 2005
CD150$^+$ CD48$^-$ CD41$^-$	45%	16 weeks	Morrison	Kiel et al., 2005
CD45$^+$EPCR$^+$CD48$^-$ CD150$^+$	56%	>16 weeks	Eaves	Kent et al., 2009

Table 3.1. Overview of the different immunophenotypes used for HSC isolation via flow cytometry and their respective purities. Abbreviations are Thy1: thymus cell antigen 1, theta, KSL: cKit+ Sca1+ Lineage-, SP: side population, ND: not determined.

This illustrates that even with the best currently available sorting method, almost every second cell is still not a stem cell. However, a technically demanding approach for calculating the purity of isolated HSCs was implemented (single-cell transplantations) in the studies achieved the highest purities (Kiel et al., 2005; Kent et al., 2009). Therefore it is not clear if the reported impurities originates from technical problems or really reflect inadequacies in the enrichment protocols. Lately, additional HSC-specific markers have been reported, such as CD49b which sub-divides the HSC compartment into long-term and intermediate-term reconstituting cells (Benveniste et al., 2010). In conclusion, the current "technical" heterogeneity within the isolated HSC populations underlines the necessity for single-cell level analysis, since population averaging can mask the behavior of single HSCs.

3.1.4. HSCs are not all the same: Functional heterogeneity in the HSC compartment

In addition to the "technical" heterogeneity due to the absence of exclusive HSC markers and technology-related limitations (precision of HSC sorting due to FACS

software/hardware or general handling), the HSC compartment itself is heterogeneous. The first report for such intrinsic heterogeneity regarding the differentiation potential of HSCs was published in 1990 (Jordan and Lemischka, 1990). HSCs have been classified into distinct subtypes based on reported heterogeneity in their differentiation potential (Muller-Sieburg et al., 2004; Dykstra et al., 2007), repopulation kinetics (Sieburg et al., 2006), self-renewal ability (Dykstra et al., 2007), proliferation kinetics or response to extrinsic factors (Muller-Sieburg et al., 2004; Challen et al., 2010).

Using the differentiation potential of HSC as a readout, Muller-Sieburg and colleagues identified three distinct subsets of HSCs: 1) the balanced HSCs capable of generating equal numbers of myeloid and lymphoid cells, 2) the myeloid-biased (My-bi) HSCs generating more myeloid than lymphoid cells and inversely 3) the lymphoid-biased (Ly-bi) (Muller-Sieburg et al., 2004). Notably, all three subsets are multipotent giving rise to all different blood lineages, but in different ratios. Further studies based on single-cell transplantation experiments revealed that transplanted HSCs reconstitute the hematopoietic system of host mice following 16 distinct repopulation patterns (Sieburg et al., 2006).

Dykstra and colleagues combined the self-renewal capacity of HSCs with their differentiation potential and identified four HSC subtypes; alpha (α) cells exhibit robust self-renewal capacity and a bias towards the myeloid lineage, beta (β) cells were also robustly self-renewing but balanced for lymphoid and myeloid lineages, the multipotent gamma (γ) cells with reduced self-renewal activity after 16 weeks (potentially downstream of beta) and the delta (δ) cells with limited self-renewal and skewed differentiation potential towards lymphoid cells (Dykstra et al., 2007).

Despite the solid proof for the functional heterogeneity of the HSC compartment, the current know-how in purifying individual HSC subtypes is limited. However, a study by Challen and colleagues revealed that the lower side population (SP) KSL cells show a bias towards the myeloid lineage, whereas the high SP KSL are lymphoid biased (Challen et al., 2010). In addition to Hoechst dye efflux, CD150 expression could further dissect the lower SP KSL population to cells with robust self-renewal and higher myeloid bias (CD150+ SP KSL). Recently, CD229 expression was also reported to distinguish those two HSCs subtypes (Oguro et al., 2013).

The two current models attempting to predict HSC behavior (stochastic or deterministic/environmental models) can also be applied to explain the observed HSC heterogeneity. According to the stochastic model, the decision between self-renewal or differentiation (from stem cells to progenitors) is random. Likewise, the downstream lineage choice could also occur randomly, therefore leading to balanced or biased HSC progeny. However, this concept is difficult to reconcile with a process as crucial and as tightly controlled as hematopoiesis. On the other hand, the notion that HSC behavior is determined by extrinsic cues requires either distinct in vivo microenvironments favoring one behavior over the other or a gradient of different niche factor(s) producing differential outcomes on HSCs. Although the idea of distinct HSC niches has already been proposed (Wilson and Trumpp, 2006), functional evidence is still lacking. An alternative model which could explain this heterogeneity is the Generation Age Hypothesis, according to which all HSCs have initially equal self-renewal capacity and differentiation potential (Rosendaal et al., 1976). Dividing HSCs gradually lose their robust self-renewal ability with cumulative cell divisions and therefore heterogeneity is introduced to the stem cell compartment (due to asynchronous division kinetics of HSCs). Although this hypothesis could successfully explain HSC subtypes with differences in their self-renewal potential, it does not explain the reported lineage bias.

3.1.5. The hematopoietic differentiation tree: from HSCs to mature blood cells

As mentioned above, hematopoiesis is the biological process through which all different types of mature blood cells are produced from multipotent HSCs. HSCs first differentiate to multipotent progenitors (MPPs) which still have the potential to form mature blood cells of all lineages (myeloid and lymphoid), but lack long-term self-renewing potential (Figure 3.2). Noteworthy, MPPs can be sub-divided into immunophenotypically distinct sub-populations differing in their repopulation potential and cell-cycle progression (Wilson et al., 2008). MPPs further differentiate into committed progenitors, either the common lymphoid progenitors (CLPs) or the common myeloid progenitors (CMPs). CLPs finally give rise to T, B or natural killer cells, whereas CMPs produce different granulocytes and monocytes (through e.g. the granulocyte/monocyte progenitors - GMPs) or erythrocytes and megakaryocytes/platelets (through the megakaryocyte/erythrocyte progenitors - MEPs).
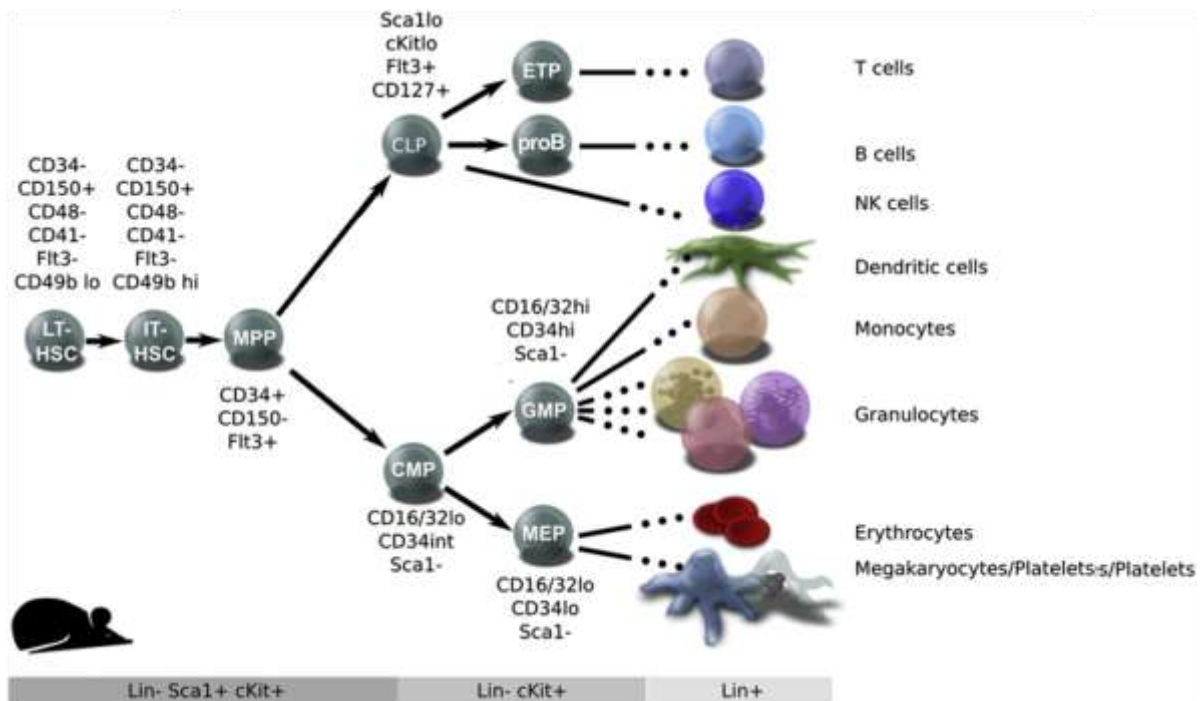
Figure 3.2. Depiction of the murine hematopoietic hierarchy showing distinct hematopoietic populations and their respective marker expression. Abbreviations are LT-HSC: long-term hematopoietic stem cell, IT-HSC: intermediate-term hematopoietic stem cell, MPP: multipotent progenitor, CLP: common lymphoid progenitor, CMP: common myeloid progenitor, ETP: earliest thymic progenitor, proB: B-cell progenitor, GMP: granulocyte/monocyte progenitor, MEP: megakaryocyte/platelet progenitor (picture modified from Doulatov et al., 2012).

3.2. HSCs in regenerative medicine: Clinical potential and current limitations

The unique ability of adult stem cells to reconstitute certain tissues by producing all mature cell types (multipotency) while maintaining their undifferentiated state (self-renewal), makes them an important tool for regenerative medicine. In the case of HSCs, autologous or allogeneic stem cell transplantations have been used against injury or blood disorders, such as anemias or different types of leukemias, lymphomas and myelomas (Anisimov et al., 2010). Importantly, HSC transplantations can be also implemented in cases of non-hematological conditions, such as Parkinson's disease (Anisimov, 2009), autoimmune diseases (Tyndall and Gratwohl, 1997) or cardiovascular repair after myocardial infarction (Harris et al., 2007). Lately, they have been used after cancer treatments (such as irradiation or chemotherapy) to improve hematopoietic recovery (Forsberg and Smith-Berdan, 2009; Wagers, 2012).

3.2.1. The clinical need for HSC maintenance/expansion in vitro

A critical factor for applying such approaches is the number of HSCs available for clinical use. Current isolation methods do not yield sufficient HSC numbers for therapeutic purposes. One method to circumvent this limitation is to manipulate HSC numbers during their in vitro cultivation. For this reason, a variety of cytokine combinations have been used, but often result in increased levels of dead and/or differentiated cells and a dramatic decrease of HSC numbers. It is only under few cytokine conditions that the numbers of HSCs can be maintained ex vivo, but only for very short culture periods (Ema et al., 2000).

Genetic manipulation of freshly purified HSCs is another alternative for maintaining or expanding their numbers in vitro. Work from Humphries group showed that over-expression of the homeobox transcription factor HOXB4 led to 40-fold expansion of HSC numbers (Antonchuk et al., 2002). In a follow-up study, even greater expansion over input cells was achieved (1000 to 10000 fold), by over-expressing the Nucleoporin98-Homeobox fusion construct (Ohta et al., 2007). However, direct genetic manipulation of transplanted HSCs is a highly controversial method, due to the unpredictable consequences of such manipulation in the human system (oncogenic transformation through insertional mutagenesis, leukemia).

In vivo, HSCs are always in association with stroma cells comprising the HSC niche. Based on this observation, stroma-based co-culture systems have been used to achieve long-term HSC maintenance or expansion, by mimicking the interaction of HSCs with their physiological microenvironment. Importantly, such culture systems allow indirect manipulation of HSCs, by manipulating their stroma counterparts.

Several stroma-based culture systems have been screened by independent groups for their potential to maintain or expand HSCs in vitro. However, a description of hematopoiesis during development as well as of the different in vivo niches (from which those systems were derived) is necessary, before analyzing the characteristics of the currently available stroma-based in vitro culture approaches.

3.3. Mammalian hematopoiesis during development: Different niches for HSCs

Hematopoiesis is a crucial procedure directly linked with organism's viability. For this reason, it is initiated early during embryogenesis and lasts until the death of the organism. During this time frame, HSCs sequentially reside in distinct tissues functioning as HSC niches (Figure 3.3A). The fact that HSCs are always associated with niche cells highlights the importance of the microenvironment in regulating hematopoiesis. Interestingly, HSCs exhibit different behaviors in the different niches suggesting that the microenvironment might influence HSC decisions. In the current chapter, I briefly present the different HSC niches during murine development and adulthood.

3.3.1. Embryonic hematopoiesis

3.3.1.1. The yolk sac

Mammalian hematopoiesis is initiated in the yolk sac (YS) with the generation of erythrocytes (to meet the growing need for tissue oxygenation), macrophages (for tissue remodeling and recycling) and megakaryocytes (for platelet formation and homeostasis) at embryonic day 7.5 (E7.5) in mice. This transient production of differentiated blood cells is known as the "primitive" wave of hematopoiesis and is replaced by the "definitive" wave, through which long-term reconstituting HSCs are generated. Interestingly, Yoder and colleagues showed that E9.0-E10.0 murine yolk sac also contains "definitive" hematopoietic cells capable of multilineage reconstitution of primary and secondary recipients (Yoder and Hiatt, 1997; Yoder et al., 1997). Although later studies challenged the lymphoid potential of those YS-derived definitive blood cells (Rampon and Huber, 2003), lineage tracing experiments have proven their contribution to the adult HSC pool in the murine bone marrow (Samokhvalov et al., 2007).

3.3.1.2. The aorta-gonad mesonephros (AGM) region

It is important to note that due to the early onset of circulation (E8.0-E8.5 in mice, Figure 3.3B), migration of repopulating hematopoietic cells may mask the site of their true emergence (Orkin and Zon, 2008). However, it is currently accepted that the first murine HSCs appear in the ventral wall of the dorsal aorta within the embryo proper (Godin et al., 1995), which together with the genital ridges and the mesonephros constitute the Aorta-

Gonad Mesonephros (AGM) region. The AGM region is capable of generating repopulating HSCs in the absence of the yolk sac, as shown by isolated organ cultures (Medvinsky and Dzierzak, 1996). Currently, it is believed that definitive (multipotent) hematopoietic cells arise in the YS and AGM region from specialized endothelial cells, the so-called hemogenic endothelium. The hematopoietic activity of the AGM region starts before E8, peaks at around E11 and then decreases due to the migration of HSCs to the fetal liver and potentially to placenta. Similar kinetics in the hematopoietic potential of the AGM region have also been described for the corresponding human developmental stages (Mikkola and Orkin, 2006).

3.3.1.3. The placenta

The next site of embryonic hematopoiesis is the placenta (from E10.5 until E13.5). The origin of placental HSCs is currently debated; whether they migrate via circulation or they are formed de novo in the placenta due to its hemogenic potential, or due to a combination of both scenarios. Nevertheless, transplantation experiments have shown that placental HSC are capable of long-term repopulation of recipient mice (Gekas et al., 2005; Ottersbach and Dzierzak, 2005).

3.3.1.4. The fetal liver

Around the same time frame (from E10.5), the fetal liver is another embryonic tissue functioning as a HSC niche. Unlike placenta where hematopoiesis diminishes quickly, the hematopoietic potential of the fetal liver persists until the end of the gestational life. At this stage, the stem cell pool increases in numbers (HSC expansion). This observed expansion is not related to de novo generation of HSCs, but to their extensive proliferation and self-renewing divisions. The fact that HSCs in the fetal liver are cell-cycle active, whereas in the bone marrow are mainly quiescent (see below) may reflect differences between the molecular composition of those niches. Unfortunately, the exact mechanism responsible for this expansion is currently unknown, despite efforts to recapitulate this phenomenon in vitro (Moore et al., 1997a). In an attempt to identify differences between fetal liver and adult HSCs, Kim and colleagues compared their gene expression profiles and identified that the transcriptional regulator Sox17 was exclusively expressed by the fetal liver HSCs (Kim et al., 2007). It was also shown that Sox17 is essential for the maintenance of fetal liver HSCs, since its conditional deletion severely impaired fetal, but not adult hematopoiesis. However,

this requirement for Sox17 during fetal hematopoiesis was cell autonomous and did not reflect any differences between fetal liver and the adult hematopoietic niches.

3.3.2. Adult hematopoiesis: The bone marrow and the spleen

A few days before birth, HSCs migrate from the fetal liver to the bone marrow, the main site of hematopoiesis in postnatal animals (Orkin and Zon, 2008). HSCs in the bone marrow are thought to be mainly quiescent and protected from signals inducing differentiation. Adult hematopoiesis also occurs in extramedullar sites such as the spleen, especially under stress conditions or injury. Details about the cellular composition and the molecular players of the bone marrow niche are described in the chapter below.
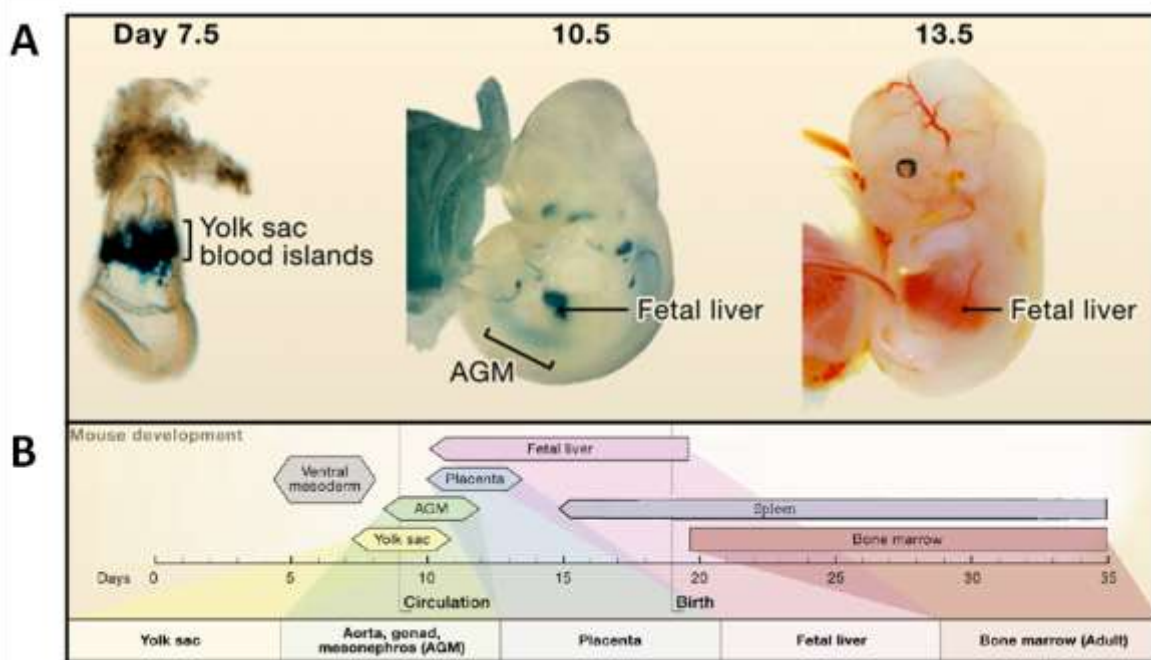
Figure 3.3. Sequential HSC niches during mouse development. A. Murine embryos in different developmental stages with HSC niches highlighted. **B.** HSC niches and their respective time windows in murine development (modified from Orkin and Zon, 2003).

3.4 Uncertainty about the in vivo bone marrow HSC niche(s)

In addition to the advances in isolating HSCs, considerable progress has also been made in identifying cell populations contributing to the in vivo HSC niche. Before describing the current concept for the bone marrow niche, it is important to mention the basics of bone

formation, since the exact anatomy, complexity and dynamics of its cellular components is often underestimated.

3.4.1. Bone formation (Skeletogenesis)

The skeleton (from the greek word skeletos (σκελετός) for dried body) is the organ providing support and structure to the body of all vertebrates (endoskeleton) and many invertebrates (exoskeleton), while protecting internal organs. Despite its reported complexity, it consists of two distinct tissues (cartilage and bone) and three cell types (chondrocytes, osteoblasts and osteoclasts) with different properties and functionality (Karsenty et al., 2009).

Developmentally, the process of bone formation (skeletogenesis) is divided into two main phases. Initially, mesenchymal cells form aggregates generating the scaffold for future skeletal tissue (Figure 3.4A). During the second phase, the centrally-located mesenchymal condensations differentiate into proliferative chondrocytes, the main cell type of the cartilage (E10.5). At the same time, cells in the periphery form a surrounding structure, the perichondrium. Few days later, some of the chondrocytes stop proliferating and undergo progressive maturation into pre-hyperthrophic, hypertrophic and terminally hypertrophic cells (Long and Ornitz, 2013). Hypertrophic chondrocytes regulate matrix mineralization and control the differentiation of perichondrial cells into osteoblasts, which later form the bone collar. Finally, the hypertrophic chondrocytes apoptose allowing osteoblasts and blood vessels to invade the central hypertrophic area of the cartilage (Figure 3.4A), where they form the primary spangiosa. It is important to note that the bone collar will develop into the cortical bone, while the primary spangiosa into trabecular bone (Kronenberg, 2003).

The procedure described above (mesenchymal cells differentiate first into chondrocytes and then to osteoblasts) is called endochondral ossification and it is the main mechanism for bone formation. In some bones however (parts of skull and clavicle), no (chondrocytic) intermediate step is required for the production of osteoblasts, which develop directly from mesenchymal cells (intramembranous ossification).

In adults, most bones share a characteristic architecture (from distal to proximal) with the epiphysis, the growth plate or epiphyseal line, the metaphysis and the diaphysis (Figure 3.4B). The epiphysis is the terminal region of long bones, where they often connect with adjacent bones through the joint. The growth plate is the skeletal region responsible for bone

lengthening. It consists of different types of chondrocytes which progressively apoptose. As soon as the bone has reached its final length, the growth plate is replaced by the epiphyseal line. The bone region proximal to the epiphyseal line is the metaphysis followed by the diaphysis which is located in the central part of the bone.

A cross section of a bone reveals two types of osseous tissue covered by an internal layer (endosteum) and an external layer of connective tissue (periosteum). The first type is the cortical bone facilitating most of the skeletal functions, due to its hardness and stiffness. The other type is the trabecular bone which is softer, heavily vascularised and more centrally located. It contains the bone marrow stroma which functions as the niche for hematopoiesis.
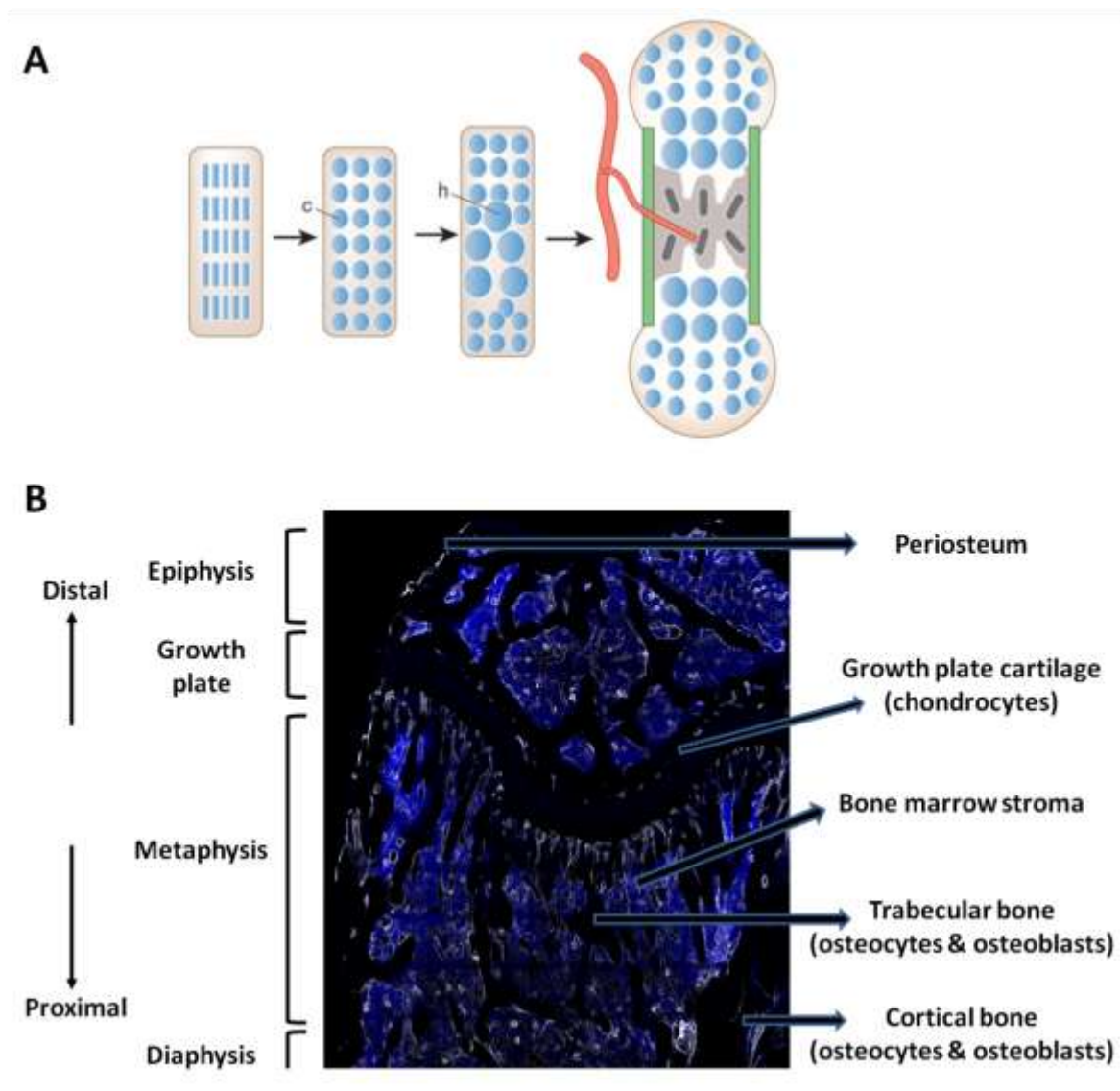
Figure 3.4. Bone development (endochondral ossification) and architecture. A. Initial condensations of mesenchymal cells differentiate into chondrocytes (c), whereas peripheral cells generate the perichondrium (brown line). Chondrocytes proliferate and mature into hypertrophic cells

(h) at the centre of the skeletal mould. Hypertrophic chondrocytes undergo apoptosis and blood vessels (red line) invade the central area of the bone resulting in the formation of the marrow and eventually of trabecular bone (dark grey). At the same time, the bone collar (green rectangular) will develop into cortical bone (panel modified by Kronenberg et al., 2003) **B.** Immunostaining of a section depicting half murine femur (thickness 100μm) with annotation of the different regions and cell types (blue is DAPI and white is CD31 antibody for blood vessels).

The current concept of the HSC niche dichotomizes the bone marrow into the endosteal and the vascular microenvironment. Despite the fact that anatomically the bone marrow is heavily vascularized with blood vessels being only few cell diameters away from the endosteum, the candidate niche populations mentioned below will still be classified according to the currently accepted model.

3.4.2. The endosteal niche

The endosteum is the anatomical area between the inner side of the bone and the bone marrow. Its importance in hematopoiesis has been documented since the mid-1970s, when transplanted CFU-S cells were found to preferentially home/reside in the endosteum rather than the central bone marrow of irradiated recipients (Lord et al., 1975; Gong, 1978). Anatomically, the endosteal surface is covered by a heterogeneous mix of bone-lining cells, a proportion of which are osteoid-depositing osteoblasts (Kiel and Morrison, 2008). Together with the osteoclasts, osteoblasts control the dynamic process of bone remodeling (formation versus resorption).

3.4.3. Cellular composition of the endosteal niche

3.4.3.1. Osteoblasts

Osteoblasts (from the greek words osto (οστό) for bone and vlastos (βλαστός) for blast/germ) are the cells orchestrating bone formation, through production and mineralization of extracellular matrix rich in collagen 1 and osteocalcin. In 2003, two groups proposed independently that osteoblasts are the key players of the bone marrow HSC niche. In both studies, increased numbers of osteoblasts (activation of the osteoblast-specific receptor from the parathyroid hormone - Pth (Calvi et al., 2003) or by the conditional inactivation of the bone morphogenic protein receptor type 1a (Bmpr1a) (Zhang et al., 2003)) led to a net increase of the HSCs numbers (KSL cells). Attempting to reveal the downstream signalling, Calvi and colleagues proposed that osteoblasts express Jagged 1 which binds to Notch

(expressed by HSCs) resulting in increased HSC proliferation (Calvi et al., 2003). Zhang et al on the other hand, proposed that the underlying mechanism is mediated through N-cadherin homophilic interactions (Zhang et al., 2003).

Despite their significant impact on the field, both studies and the proposed mechanisms were dealt with major skepticism. In terms of the experimental design, both studies have been criticized for limited specificity, since the described manipulations affected also other cell types in the bone marrow besides osteoblasts (Isern and Méndez-Ferrer, 2011). The fact that the conditional deletion of Jagged 1 from bone marrow cells had no effect on hematopoiesis, along with the ability of Notch-deficient HSC to reconstitute those mice (Mancini et al., 2005) strongly challenged Calvi's model. Also, Zhang's model has been challenged by a study from Morrison's group reporting undetectable N-cadherin expression in HSCs (Kiel et al., 2007). It is important to note that in addition to the underlying molecular mechanisms, the role of osteoblasts in maintaining HSCs in vivo has also been challenged. This criticism originated from the observation that mice with reduced numbers of osteoblasts (in biglycan deficient mice) had normal HSC numbers (Kiel et al., 2007).

It has been shown that osteoblasts produce several key factors controlling HSC maintenance, such as angiopoietin (Arai et al., 2004), the chemokine C-X-C motif ligand 12 (CXCL12) (Petit et al., 2002), osteopontin (Nilsson et al., 2005) and thrombopoietin (Yoshihara et al., 2007). However, whether osteoblasts are indeed the critical source of these factors in the bone marrow is still controversial, since conditional deletion experiments are still pending (Kiel and Morrison, 2008). The fact that hematopoiesis can occur in tissues devoid of osteoblasts (extramedullary hematopoiesis) suggests that osteoblasts are dispensable for HSC maintenance (Ellis and Nilsson, 2012). In line with this, confocal imaging of bone marrow sections revealed that around 60% of stained HSCs (CD150+CD48-CD41-Lin-) were found adjacent to sinusoids and only 20% to the endosteum (Kiel et al., 2005). However, since osteoblasts also produce soluble factors (as mentioned above), direct contact with bone marrow HSCs may not be a prerequisite for their contribution to the in vivo HSC niche.

In contrast, recent studies provided additional evidence for a functional role of osteoblasts in the HSC niche. Kieslinger and colleagues reported that ablation of early B cell factor 2 (Ebf2)-expressing immature osteoblasts negatively affected the numbers of HSCs and committed progenitor cells (Kieslinger et al., 2010). In addition, Sugimura et al showed

that N-cadherin expressing osteoblasts protect HSCs from activation via non-canonical Wnt signalling (flamingo and Frizzled receptor 8) (Sugimura et al., 2012).

3.4.3.2. Osteoclasts

Osteoclasts (from the greek words "οστό" for bone and "κλάσις" for fracture/break) are the cells responsible for bone resorption by removing the mineralized matrix deposited by osteoblasts. To achieve that, osteoclasts secrete proteases such as cathepsin K and matrix metallopeptidases (Mmp9 and Mmp13). During bone resorption, osteoclasts also release calcium ions from hydroxyapatite (calcium-phosphate ceramic) and enzymatically process CXCL12 (via cathepsin K) (Kollet et., 2006), an important molecule for HSC maintenance and function (Barker, 1994).

Current data suggest an important role of osteoclasts in hematopoiesis under steady-state conditions. Administration of bisphosphonate alendronate (ALN), an inhibitor of osteoclast-mediated bone resorption, results in decreased HSC numbers (defined as Flt3$^-$ KSL), loss of quiescence and delayed hematopoietic recovery upon transplantation in treated mice (Lymperi et al., 2011). Using a mouse model with defective osteoclastic activity (oc/oc mouse), Mansour and colleagues revealed that osteoclasts play an important role in the formation of the bone marrow niche and HSC homing, by controlling the differentiation of osteoblasts from mesenchymal progenitors (Mansour et al., 2012).

3.4.4. The vascular niche

The bone marrow vasculature contains different types of blood vessel structures and its architecture has been visualized through electron microscopy (Tavassoli, 1981) or injection of India ink into the circulation (Fliedner et al., 2002). In general, blood vessels are the main structures of the blood circulation and can be divided into three different types: the arteries (taking blood away from the heart), the veins (returning blood to the heart) and the capillaries (allowing the exchange of blood's components with body tissues). They all share common anatomy having three basic layers: the tunica intima (the inner layer of all vessels consisting of an endothelial layer being in contact with the blood flow and an internal layer of elastic tissue - elastic lamina), the tunica media (the middle layer with the smooth muscle cells) and the tunica externa (the outer layer of connective tissue). In the bone marrow, blood flows from the arteries to the capillaries, through small vessels called arterioles. Capillaries are themselves divided into three different types: the continuous, the fenestrated and the

sinusoids. Continuous capillaries are covered by a solid, uninterrupted layer of endothelial cells and allow diffusion of small molecules (ions). Fenestrated capillaries are characterized by the presence of gaps between endothelial cells, thus allowing small proteins to exit from the blood stream. Sinusoids which are very abundant in the bone marrow, are specialized capillaries with bigger pores (than fenestrated capillaries) enabling exchange of medium size proteins.

3.4.5. Cellular composition of the vascular endothelial niche

3.4.5.1. Vascular Endothelial cells

As previously mentioned, the bone marrow is a heavily vascularized tissue with numerous arterioles and capillaries providing oxygen and nutrients to the neighboring cells. The walls of blood vessels are composed of endothelial cells, which allow different levels of permeability. Billions of differentiated blood cells are directed to the circulation every day, through the extended network of sinusoidal blood vessels. It is currently thought that HSCs (similarly to differentiated cells) periodically pass the "barrier" of sinusoid endothelial cells, circulate in the peripheral blood and then return back to the bone marrow (Méndez-Ferrer et al., 2008).

Developmentally, endothelial cells are closely related to hematopoietic cells (Kennedy et al., 1997). In fact, it was recently shown that blood cells arise from hemogenic endothelium in vitro (Eilken et al., 2009). During embryonic development in both mice and humans, hematopoiesis occurs in the absence of bone tissue. After birth, HSCs have been found in extramedullary areas, such as the liver and the spleen. It is important to note that in several vertebrate species hematopoiesis is not associated with bones; in zebrafish for example the kidney and the thymus are the main hematopoietic sites (Murayama et al., 2006).

Morrison's group has provided proof for the connection between adult, bone marrow HSCs and endothelial cells. Their study showed that the 60% of bone marrow HSCs (CD150+CD48-CD41-Lin-) are adjacent to vascular endothelial cells, whereas 20% was found in the endosteum (Kiel et al., 2005). The authors also revealed that all HSCs were located within 5 cell diameter from sinusoids suggesting that endothelial cells are the key players in the in vivo bone marrow niche (Kiel et al., 2007). However, their results should be handled with care since they are based on frozen sections distorting the exact tissue morphology and architecture.

The described heterogeneity of the stem cell compartment, which consists of various subsets of HSCs distinct properties, might imply the existence of several different niches in the bone marrow. Additionally, what remains questionable and needs to be addressed is the current notion that more primitive HSCs reside in the endosteal niche, whereas activated ones are located in the sinusoid endothelium (Wilson and Trumpp, 2006).

3.4.6. Cellular composition of the perivascular niche

3.4.6.1. CXCL12-abundant reticular (CAR) cells

It has long been appreciated that hematopoietic cells are in close association with reticular cells in the bone marrow of rodents (Weiss, 1976). A more recent study reported that some reticular cells in the murine bone marrow express high levels of the chemokine CXCL12, hence their name CXCL12-adundant reticular (CAR) cells (Sugiyama et al., 2006). Interestingly, CAR cells have been found in both the endosteal and vascular region, a unique feature which could potentially link/unify those niches. The fact that 97% of HSCs (CD150+CD48-CD41-) were found adjacent to those cells in the bone marrow (Sugiyama et al., 2006), makes CAR cells the cell type with the most significant correlation with HSCs up to now. In a recent study, Omatsu and colleagues showed that ablation of CAR cells leads to a 2-fold decrease of HSC numbers, increase of their quiescence and a skewing towards the myeloid lineage (Omatsu et al., 2010). They also reported the ability of CAR cells to differentiate in vitro and in vivo to osteoblasts and adipocytes, a property compatible with stem or progenitor cell types.

3.4.6.2. Nestin+ mesencymal cells (MSCs)

Another cell type in the bone marrow known for its high CXCL12 expression are the nestin expressing (Nes+) mesenchymal cells (Méndez-Ferrer et al., 2010). The authors reported that ablation of Nes+ cells leads to loss of HSC function and impaired homing to the bone marrow. However, a recent study ablating CXCL12 from the Nes+ cells revealed minor or no effects upon HSC function and homing in the bone marrow (Ding and Morrison, 2013) arguing that CXCL12 is not the relevant molecule promoting HSC maintenance by the Nes+ cells.

3.4.6.3. Mature blood cells

Until recently, only non-hematopoietic cells were acknowledged as candidate niche elements for HSCs. However, recent studies provided evidence for the role of mature hematopoietic cells in the bone marrow niche. Megakaryocytes share the Tpo receptor (c-Mpl) with HSCs, thus antagonizing for Tpo's availability in the bone marrow. In cases of increased numbers of megakaryocytes, HSCs loose quiescence and eventually their self-renewal potential (De Graaf et al., 2010). Another mature blood type, macrophages, have been shown to influence HSC retention in the niche, since their ablation causes HSC mobilization (Winkler et al., 2010; Chow et al., 2011). It is important to note that despite the importance of the studies mentioned above, observed phenotypes can be the result of secondary effects (for example impaired bone remodeling having downstream effect on osteoblasts or other cell types).

3.4.6.4. Adipocytes

The adipocytes, the specialized fat-storing cells, is another cell type found in the adult bone marrow. The numbers of bone-marrow adipocytes are increased with age (Neumann, 1882) and obesity (Hamrick et al., 2004). Until recently, it was thought they only fill marrow space and have no role in hematopoiesis (Wang and Wagers, 2011). However, using the obese leptin-deficient (ob/ob) (Ingalls et al., 1950; Zhang et al., 1994) and leptin receptor-deficient mice (db/db), recent studies revealed impaired HSC function in vivo (Claycombe et al., 2008; Pietramaggiori et al., 2009). The negative effect of adipocytes in hematopoiesis was later confirmed by the work of Naveiras and colleagues. They reported a gradient of adipocytic tissue in the mouse spine, with thoracic vertebrae possessing low numbers (if any) and tail vertebrae being very rich. HSCs (Flt3-KSL) isolated from tail vertebrae (highly adipocytic) showed reduced repopulation potential upon transplantation when compared with the ones from the thoracic vertebrae (Naveiras et al., 2009). In the same study, it was also reported that genetic or chemical inhibition of adipogenesis partially restored the impaired HSC phenotype.

Considering the studies mentioned in this chapter, whether the in vivo BM niche consists of one or more HSC niches, their precise role on hematopoiesis, their exact cellular composition and the underlying molecular mechanisms are still controversial and require further clarification.

3.5. Establishing an in vitro HSC niche: Stroma cell types and molecular players

As mentioned above, stroma-based culture systems are a robust method to culture HSCs in vitro, since they mimic the interaction between HSCs and niche cells and allow indirect HSC manipulation. The pioneer of the in vitro culture of hematopoietic cells was T.M. Dexter (Dexter et al., 1973). Later efforts focused on the isolation of stroma cells from tissues known to function as hematopoietic niches during development. Below, several stroma cells lines isolated from different hematopoietic niches during murine development are described.

3.5.1. Yolk sac-derived stroma cell lines

In the mid 90's, Yoder and colleagues sought to understand the role of the yolk sac (YS) microenvironment in hematopoiesis, since this is the initial site where it arises. To address this, they established cell lines from the endodermal (YSE) and mesodermal (YSM) layers of murine yolk sac from E9.5 embryos (Yoder et al., 1994). Bone marrow (BM) cells were isolated from mice treated with 5-fluorouracil (5-FU) to enrich for more primitive/quiescent hematopoietic cells. Then, these cells were co-cultured with the different YS-derived stroma lines while were compared with BM-derived stroma (summary of all described cell lines in Table 3.3). The analysis showed that both YS stroma increased the proliferation of colony forming cells (Yoder et al., 1995). Interestingly, the authors reported that conditioned media supplemented with recombinant growth factor(s) could restore the observed effects in the absence of YS stroma.

3.5.2. AGM-derived stroma cell lines

The next hematopoietic site during embryonic development is the AGM region, which gives rise to the first hematopoietic cells with repopulation capacity (definitive hematopoiesis) in the mouse embryo (Medvinsky and Dzierzak, 1996). The proximity of hematopoietic cells with endothelial cells in the ventral wall of dorsal aorta, led Ohneda and colleagues to isolate endothelial cells from E11 mouse embryos and to screen their effect on co-cultured fetal liver CD34+KSL HSCs (Ohneda et al., 1998). Interestingly, they identified one endothelial cell line (DAS 104-4) able to maintain HSC numbers for 7 days of in vitro culture (as measured by primary transplantation for 15 weeks). Another line (DAS 104-8) promoted differentiation of co-cultured HSCs towards the myeloid lineage, which

necessitated cell-cell contact, was also established (Ohneda et al., 1998). Importantly, the secondary transplantations required to confirm maintenance of fetal liver HSCs were not performed. In a study published few months later, Xu and colleagues established another AGM-derived stroma cell line from E10.5 mouse embryos (AGM-S3), which supported differentiation of adult BM HSCs (KSL cells) and maintenance of human cord blood repopulating cells, as shown by transplantations in non-obese diabetic severe combined immunodeficient NOD/SCID mice as recipients (Xu et al., 1998). Despite confirming previous findings that mouse stroma can also support human hematopoiesis ex vivo (Sutherland et al., 1991; Issaad et al., 1993), important technical limitations regarding the purity of co-cultured human hematopoietic cells and the heterogeneity of the non-clonal stroma cells were not addressed.

It is important to note that the AGM region can be anatomically divided into two different, morphologically distinct regions (dorsal aorta/mesenchyme [AM] and urogenital ridges [UG]) with different hematopoietic potential. In an exhaustive study, Oostendorp and colleagues isolated 25 stroma cell lines from the different AGM compartments (AM and UG), the embryonic liver (EL) and the gastrointestinal region (GI) of E11 mouse embryos, which were subsequently cloned to generate 100 different subclone lines (Oostendorp et al., 2002). The potential of those lines to support colony forming cells (CFC) and to maintain repopulation potential of co-cultured adult HSCs (CD31+cKit+Ly6C-) was screened by long-term culture (LTC)-CFC assays. Two UG (UG26-1B6 and UG26-2D3) and one EL line (EL08-1D2) were the most potent lines, with UG26-1B6 being the more robust in supporting repopulating HSCs after 4 weeks of co-culture (6/13 repopulated mice) (Oostendorp et al., 2002).

In a follow-up study, Buckley and colleagues revealed that UG26-1B6 stroma maintained repopulating cells through secretion of Wnt5a in non-contact cultures, whereas EL08-1D2 require direct contact (Buckley et al., 2011). Addition of Wnt5a-neutralising antibody inhibited this potential of UG26-1B6 cells illustrating that Wnt5a is among the molecules responsible for this interaction (Buckley et al., 2011). However, due to the considerable heterogeneity of the starting hematopoietic population co-cultured with the UG26-1B6 stroma (Lin- cells), the effect of Wnt5a might be a result of an indirect effect rather than a direct one upon HSCs. A recent study further support this hypothesis, since the exogenous addition of Wnt5a in a cell population more enriched for HSCs (KSL cells) did

not maintain, but rather decreased the number of repopulating cells, in stroma-free cultures (Schaap-Oziemlak et al., 2013). The inability of Wnt5a to maintain HSCs in stroma-free cultures might mean that other secreted factors are also required. Alternatively, it might illustrate the importance of the presence of the stroma cells, even in the case of non-contact cultures, due to the presence of a cleaved form of membrane or extracellular-matrix related molecule. Another molecule reported to be involved in the interaction between AGM-derived stroma and hematopoietic cells was pleiotrophin (Ptn). Interestingly, it was showed that the loss of Ptn had a positive effect upon the maintenance of repopulating cells (Istvanffy et al., 2011).

Unfortunately, despite the expectation for potential HSC expansion mediated from AGM-derived niche cells, such an effect was not observed. Also, to our knowledge, no gene expression profile of those cell lines is currently available, thus impeding their efficient molecular manipulation in large-scale.

3.5.3. Fetal liver-derived stroma cell lines

In an attempt to establish a culture system for HSC expansion, Kateri Moore and colleagues dissected the fetal liver (FL) of murine embryos and generated 225 clonal stroma cell lines. These cells lines were immortalized (insertion of temperature-sensitive simian virus 40 large T antigen – SV40T) and screened for their potential to support hematopoiesis over long culture periods (Wineman et al., 1996). The initial screening included "cobblestone area forming cell" (CAFC) assays by co-cultivation of BM cells with the different FL derived stroma cell lines. Cobblestone areas (CA) have been shown to correlate with the primitiveness of the cobblestone forming units (CFU), more primitive cells will need longer time to generate CA (Ploemacher et al., 1989). In addition, the presence of CA 28 days after the initiation of the co-culture, has been reported to highly correlate with in vivo repopulation potential (Van der Sluijs et al., 1990; Ploemacher et al., 1991; Van Os et al., 2008).This laborious screening revealed only few stroma cell lines being capable of supporting hematopoiesis for long co-culture periods (>6 weeks). From those, only AFT024 cells could qualitatively and quantitatively maintain repopulating cells as shown by competitive transplantation experiments (Moore et al., 1997a). Interestingly, HSCs (or repopulating cells) cultured on AFT024 showed the same potency for long-term multilineage reconstitution (56 weeks) as freshly purified (uncultured) HSCs, thus illustrating the potential of AFT024 for qualitative and quantitative HSC maintenance. Additional cell lines with intermediate

potential to maintain repopulating cells were also identified, such as the 2012 line. Unfortunately, no proof of HSC expansion in co-culture experiments with fetal-liver derived stroma was reported, as initially expected.

In a follow-up study, Moore and colleagues attempted to shed light upon the molecular mechanism of the AFT024-drived maintenance of murine HSCs, by investigate the role of delta-like or pre-adipocyte factor 1 (dlk1) (see Table 3.2). DLK1 protein, a transmembrane glycoprotein with epidermal growth factor-like repeats, was identified to be expressed exclusively in the supportive stroma cells (Hackney et al., 2002). Addition of either the soluble or transmembrane form of dlk1 had no effect on the colony-formation of fetal liver (AA4.1+, Sca-1+, c-Kit+, Lin low/-) or bone marrow (KSL) HSCs cultured on semi-solid media. A 2-fold increase in the number of cobblestone area colonies (CAC) was reported upon exogenous addition of the soluble protein form, when HSCs were cultured with non-supportive stroma (BFC012) in Dexter-type co-cultures (Moore et al., 1997b). Also, a 4- to 6-fold increase was observed, when BFC012 cells over-expressing the transmembrane form of dlk1 were used as stroma. However, the maintenance of the CACs was transient and competitive transplantation experiments revealed low levels of maintenance of HSCs pre-cultured in dlk-expressing conditions (Moore et al., 1997b). These results led authors to hypothesize the existence of additional factors which are responsible for the AFT024-driven maintenance of co-cultured HSCs in vitro.

Importantly, there is strong evidence that the AFT024 stroma can also support the ex vivo maintenance of human HSCs. Cord blood- and bone marrow-derived CD34+CD38- cells were co-cultured on AFT024 or primary human stroma and their potential to generate cobblestone-area forming cells (CAFC) after long-term culture was monitored and compared. AFT024 cells were found more potent in maintaining human HSCs in vitro necessitating direct contact (Thiemann et al., 1998). These results were later confirmed by long-term culture initiating-cell experiments (LTC-IC), a more objective method in vitro assay to estimate HSC potential. Bone marrow-derived CD34+Lin- human cells that were cultured on AFT024 stroma for 5 weeks, showed a 3-fold higher potential to generate LTC-IC colonies than those cultured on the murine bone-marrow cell line M2-10B4 (Punzel et al., 1999a). Although CAFC and LTC-IC assays are currently the best in vitro methods to estimate the numbers of HSC in a heterogeneous population, they do not measure engraftment and self-renewal potential. Such properties required in vivo transplantation experiments. Nolta and

colleagues compared the potential of the AFT024 and the human stroma to support human HSCs, by performing transplantations using a xenograft mouse model (beige/nude/xid mouse - bnx). Cord-blood derived human CD34+CD38- HSCs co-cultured with AFT024 stroma for two or three weeks showed at least 2-fold higher percentage of engraftment, 12 months after transplantation (Nolta et al., 2002). Also, the number of primitive cells (CD45+CD34−CD38− and CD45+CD34−Lin−) present in the bone marrow of mice transplanted with human cells maintained on AFT024 stroma was 3-fold higher.

In an attempt to reveal the molecular mechanism involved in the AFT024-driven maintenance of human HSCs in vitro, Punzel and colleagues reported that a higher percentage of CD34+ cells were in cycle when co-cultured in contact with AFT024 (29,8% ±1,7%) compared to M2-10B4 stroma (21,2% ±2,3%). Based on those differences, they suggested that M2-10B4 stroma leads to reduced LTC-IC potential of cultured cells by blocking cell-cycle progression (Punzel et al., 2002). Protein expression analysis revealed size differences on heparan sulfates (HS) produced by both cells types (AFT024 have bigger HS), leading them to postulate the involvement of large size O-sulfated HS in the cell-cycle progression of human HSCs. It is important to note that direct contact was reported as the predominant mechanism (Punzel et al., 2002) confirming earlier studies (Thiemann et al., 1998). However, the notion that AFT024 maintain human HSCs through direct contact or cell-matrix interactions has been challenged by later studies. CD34+ umbilical cord blood-derived human cells were cultured on transwells in the presence of stem cell factor (SCF), thrombopoietin (Tpo), interleukin 7 (IL-7) and fms-related tyrosine kinase ligand (Flt3L), without contacting the AFT024 stroma (Lewis et al., 2001). After 14 days in culture, the progeny of those cells or non-cultured, freshly purified cells were transplanted into non-obese diabetic/severe combined immunodeficiency (NOD-SCID) mice. The levels of engraftment were found similar, whereas the frequency of repopulating cells was increased by 2 folds in the cultured cells. These results suggest that AFT024 non-contact cultures can also maintain if not expand human CD34+ cells for culture periods not exceeding two weeks (Lewis et al., 2001).

Similar results were published few years earlier by the Verfaillie group, in which the reported poor ability of non-contact AFT024 cultures to maintain LTC-ICs was significantly improved by the addition of a cocktail of human cytokines (GM-CSF, G-CSF, SCF, LIF, MIP-1a, IL-6) (Punzel et al., 1999b). Finally, Hutton and colleagues reported that the bone

morphogenic protein 4 (BMP4), a secreted protein which is abundant in the AFT024 condition media, played a key role in the reported interaction. Blocking of the BMP4-downstream signalling abated the reported effect of AFT024 stroma on cord blood HSCs, arguing against the necessity of direct contact for the maintenance of human HSCs by the AFT024 stroma (Hutton et al., 2006).

HSPC Immunophenotype	Species	Stroma	Culture Conditions	Duration	Readout	Mechanism	Molecular Player	Study
AA4.1+ KSL (FL)	Mouse	AFT024	DMEM with FCS, HS, 2-Me, HC	4-7 weeks	Competitive transplantation, secondary transplantation, CAFC, CFU	ND	ND	Moore et al., 1997a
KSL (BM)	Mouse	AFT024	DMEM with FCS, HS, 2-Me, HC	4-7 weeks	Competitive transplantation	ND	ND	Moore et al., 1997a
AA4.1+ KSL (FL) or KSL (BM)	Mouse	AFT024, dlk expressing BFC012	DMEM with FCS, HS, 2-Me, HC	2 weeks	CAFC, Competitive transplantation	DC	Dlk	Moore et al., 1997b
CD34+CD38- (BM or CB)	Human	AFT024, primary human stroma	IMDM with IL-3, IL-6, SCF	3 weeks (CB) or 4 weeks (BM)	CFU, CAFC, immunophenotype	DC	ND	Thiemann et al., 1998
CD34+Lin- (BM)	Human	AFT024, M2-10B4	IMDM with FCS, HS, L-Glutamine, HC, P/S (+MIP1a, IL-3)	5 weeks	LDA LTC-IC	ND	ND	Punzel et al., 1999a
CD34+Lin- (BM)	Human	AFT024, M2-10B4	IMDM with FCS, HS, L-Glutamine, HC, P/S, GM-CSF, G-CSF, SCF, LIF, MIP-1a, IL-6	5 weeks	LDA LTC-IC	SF	ND	Punzel et al., 1999b
CD34+ (UCB)	Human	AFT024, no contact	RPMI with FL, SCF, IL-7, P/S	1-2 weeks	LDA LTC-IC, CFC Engraftment (NOD/SCID mice)	SF	ND	Lewis et al., 2001
CD34+ (UCB)	Human	no stroma	RPMI with FCS, G-CSF, MIP-1a, IL-6, MCP-1, VEGF, IL-8, N-desulfated-O-sulfated heparin, Tpo, FL, SCF, IL-7	1-2 weeks	LDA LTC-IC, CFC Engraftment (NOD/SCID mice)	SF	ND	Lewis et al., 2001
CD34+CD38-	Human	AFT024, human BM stroma	IMDM with FCS, BSA, 2-Me, HC, L-Glutamine, P/S, +IL-3, IL-6, SCF	2-3 weeks	Engraftment & multilineage reconstitution (bnx mice)	ND	ND	Nolta et al., 2002
CD34+Lin-	Human	AFT024, M2-10B4	IMDM with FCS, HS, L-Glutamine, HC, P/S, MIP1a, IL-3	5 weeks	LTC-IC	DC	Large-size O-sulfated heparan	Punzel et al., 2002
CD34+CD38- (CB)	Human	AFT024, no contact	RPMI-1640 with FCS, Flt-3l, SCF, Tpo	2 weeks	LTC-IC, immunophenotype, engraftment & multilineage reconstitution (NOD/SCID mice)	SF	BMP4	Hutton et al., 2006

Table 3.2. Experimental details of studies using the AFT024 co-culture system . Abbreviations are: HSC immunophenotype column (FL: fetal liver, BM: bone marrow, CB: cord blood, UCB: umbilical cord blood, AA4.1: cell surface antigen AA4 or CD93, KSL: cKit+ or Kit oncogene, Sca1+ or stem cell antigen 1, Lineage-), Culture conditions column (FCS: fetal calf serum, HS: horse serum, 2-Me: 2-Mercaptoethanol, HC: hydrocortisone, BSA: bovine serum albumin, IL-3: interleukin 3, IL-6: interleukin 6, IL-7: interleukin 7, IL-8: interleukin 8, SCF: stem cell factor, MIP1a: macrophage inflammatory protein 1-alpha, FL or Flt-3l: fms-related tyrosine kinase 3 ligand, MCP-1: monocyte chemoattractant protein 1, VEGF: vascular endothelial growth factor, Tpo: thrombopoietin), Readout

column (CAFC: cobblestone area forming cell, CFU: colony forming unit, LDA LTC-IC: limiting dilution long-term culture initiating cell, NOD/SCID: non-obese diabetic/severe combined immunodeficiency), Mechanism column (ND: not determined, DC: direct contact, SF: secreted factor(s)).

Collectively, these data illustrate that the AFT024 stroma cell line is capable of maintaining primitive murine and also human HSCs over long-culture periods ex vivo. Stroma-free or non-contact AFT024 cultures of human HSCs require exogenous addition of cytokines to yield similar results as the contact cultures. Despite those extensive studies, the exact mechanism and the molecules responsible for their supportiveness remain controversial.

3.5.4. Bone marrow-derived stroma cell lines

In addition to cell lines derived from embryonic tissue, bone marrow stroma cells isolated from newborn (PA6, OP9) or adult mice (MS-5) have also been studied. In the early 80's, Kodama and colleagues isolated calvaria from P1 (postnatal day 1) newborn mice and established the pre-adipocytic MC3T3-G2 cell line, which was later sub-cloned to seventeen different lines (Kodama et al., 1982a). From those, the MC3T3-G2/PA6 line (a subclone of a heterogeneous population of bone marrow cells) was initially selected based on its high potential for adipocytic differentiation in response to administration of glucocorticoids (Kodama et al., 1982a). In a follow-up study, Kodama illustrated the potential of the MC3T3-G2/PA6 line to increase the numbers of CFU-S cells (currently thought to correspond to multipotent progenitors, MPPs) through direct contact with co-cultured bone marrow cells (Kodama et al., 1982b). Few years later, sub-clones of the MC3T3-G2/PA6 cell line (MC3T3-G2/PA6/S-2 and MC3T3-G2/PA6/S-12) failing to support long-term hematopoiesis were also identified (Kodama et al., 1992). Recently, Shimizu and colleagues performed a microarray analysis (Affymetrix Gene Chip Mouse Genome 430 2.0 array) comparing the parental line MC3T3-G2/PA6 with the two sub-clones lines. The analysis revealed 144 genes being down-regulated in both non-supporting lines (Shimizu et al., 2008). Selected gene over-expression (1110007F12Rik) in the non-supporting lines slightly rescued their hematopoietic potential (although results were not statistically significant). Despite the importance of those findings the non-clonal nature of the parental MC3T3-G2/PA6 stroma cell line again precludes efficient molecular manipulation and questions sensitivity in the performed high-throughput analysis.

Another widely known line derived from mouse calvaria is the OP9 stroma. This line was generated from B6C3F1 osteopetrotic mice (op/op) with a mutation in the gene coding for the macrophage colony stimulating factor (M-SCF) protein (Kodama et al., 1994). These mice lack osteoclasts and have deficient phagocytes. OP9 stroma has been used for the multilineage hematopoietic differentiation of co-cultured mouse embryonic stem (ES) cells in the absence of additional cytokines (Nakano et al., 1994; Nishikawa et al., 1998). These results led researchers to hypothesize that the OP9 stroma should express some of the genes necessary for the regulation of hematopoiesis. Indeed, Ueno and colleagues illustrated the potential of OP9 to support co-cultured KSL cells and also identified a mammalian homologue of a *Drosophila melanogaster* gene (mKirre) as one of the key molecules involved in the this interaction (Ueno et al., 2003).

An interesting approach was followed by Itoh and colleagues who generated the MS stroma cell lines by irradiating the adherent layer during a long-term bone marrow culture assay (Itoh et al., 1989). The authors established different MS lines starting from single cells (MS-1 to -7) from which MS-5 cells were the most potent in supporting expansion of CFU-S and granulocyte-macrophage colony forming cells (GM-CFC) for over 2 months in vitro (cell-cell contact required). MS-5 cells produce extracellular matrix proteins, such as laminin, collagen I and fibronectin (Itoh et al., 1989) and important cytokines such as granulocyte-macrophage colony stimulating factor (GM-CSF), interleukin 6 (IL6) and stem cell factor (SCF) (Suzuki et al., 1992).

Line	Stage	Organ	Age	Clonality	Hematopoietic cells	Phenotype	Mechanism	Duration	Microarray Data	Initial Study
YSE, YSM	Fetal	Yolk sac	E9.5	Not clonal	5-FU treated BM	Increased proliferation	SF	2 weeks	NA	Yoder et al., 1994
DAS 104-4	Fetal	AGM	E11	Not clonal	CD34-KSL	HSC maintenance	CC	1 week	NA	Ohneda et al., 1998
AGM-S3	Fetal	AGM	E10.5	Not clonal	KSL	HSC differentiation	CC	>2 weeks	NA	Xu et al., 1998
UG26-1B6 UG26-2D3	Fetal	AGM	E11	Clonal	CD31+cKit + Ly6C-	HSC maintenance	SF	4 weeks	NA	Oostendorp et al., 2002
EL08	Fetal	Embryonic liver	E11	Clonal	CD31+cKit + Ly6C-	HSC maintenance	CC	4 weeks	NA	Oostendorp et al., 2002
AFT024	Fetal	Fetal liver	E14.5	Clonal	KSL	HSC maintenance	CC	6 weeks	A	Moore et al., 1997
MC3T3-G2/PA6	Adult	Bone marrow	P1	Not clonal	BM	Expansion of CFU-S	CC	1 week	A	Kodama et al., 1982
OP9	Adult	Bone marrow	P1	Not clonal	KSL	Hematopoietic ES differentiation	SF*	3 weeks	NA	Kodama et al., 1994
MS-5	Adult	Bone marrow	Adult	Not clonal	Non adherent cells after long-term BM culture	Expansion of CFU-S	CC	<2 months	NA	Itoh et al., 1989

Table 3.3. Detailed outline of stroma cell lines isolated from different regions during mouse development and their reported effect upon hematopoietic cells. Abbreviations are SF: secreted factor, SF*: cleaved extracellular domain of a membrane protein, DC: direct contact, E: embryonic or days post coitum - dpc, P: postnatal or days after birth, NA: not available.

3.5.5. AFT024: a stroma cell line supporting robust HSC maintenance, while allowing efficient molecular manipulation

Most of the in vitro systems described above consisted of heterogeneous stroma cell populations (Table 3.3). The importance of the AFT024-based in vitro culture system lies in the clonality of the stroma cell compartment. This is a prerequisite for the identification of the molecular mechanisms involved, since the existence of different cell types (stroma heterogeneity) might lead to experimental inconsistencies and technical variation. This critical difference enabled in-depth genomics analysis revealing unique molecules differentially expressed between AFT024 and the non-supportive lines. In a follow-up study, the molecular profile of the supporting stroma cell line (AFT024) was identified through functional genomics approach (Hackney et al., 2002). For this reason, cDNA libraries from the supportive (AFT024) and a non-supportive stroma cell line (2018) were sequenced and compared. Further bioinformatics analysis enabled functional annotation of all the sequences found preferentially or exclusively in supportive cells, thus revealing the molecular profile of

AFT024 (http://stromalcell.mssm.edu/). An additional follow-up study utilized a high-throughput analysis (Affymetrix microarrays) further confirming and updating the molecular signature of the AFT024s (Charbord and Moore, 2005). This published list of genes expressed in AFT024 cells allows molecular manipulation of the supportive stroma in order to identify the key molecule(s) responsible for the in vitro maintenance of HSCs. Taking into consideration the properties and available data of all stroma cell lines described above, it is obvious that AFT024 stroma cells was the most potent line to be used in this study due to its clonal origin and available gene expression profile.

Unfortunately, the studies mentioned above provided limited or no information regarding the effect upon HSC behavior. Also, the molecular mechanism through which the AFT024 stromal cell line supports the *in vitro* maintenance of HSCs is currently unknown. The main limitation of those studies is that their results were based on endpoint analysis conducted on heterogeneous populations of blood cells. Such analysis cannot reveal the sequence of fate-choice events of single cells over time and is thus not informative regarding the underlying molecular mechanism or the effects of molecular manipulations.

Continuous observation of living cells is necessary when studying dynamic biological processes. A time-lapse imaging approach with single-cell resolution would allow monitoring HSCs' behavior upon co-culture with the AFT024 stroma. Without single-cell observation, opposing interpretations could be used to explain the finding that the number of HSCs with long-term repopulation capacity is maintained when co-cultured with AFT024: increased levels of cell division and/or reduced levels of apoptosis or even complete absence of HSC divisions would be a possible explanation of the published experimental data. In addition, due to the size of the published gene lists (Hackney et al., 2002), conventional methodology including long co-cultures in vitro (4-6 weeks) and subsequent primary (>16 months) and secondary (4 months) in vivo transplantation experiments hinders high-throughput screening of individual molecules. Therefore, a high resolution and high throughput in vitro imaging system had to be utilized.

3.6. Time-lapse imaging: a brief historical perspective

Time-lapse imaging is a powerful technique allowing continuous observation of dynamic processes. The ancestor of the modern time-lapse imaging is chronophotography (from the greek words chronos (χρόνος) for time, photos (φωτός) genitive of phos (φως) for

light and grafi (γραφή) for drawing) invented by the French physicist Étienne-Jules Marey around 1880. The term describes a series of photos acquired with determined time intervals in order to analyze a continuous motion into individual still images. Marey's inventions allowed him to depict animal movements that were too fast for the human perception, such as the movement of wings during a pelican's flight or horse's leg during gallop. He achieved this by acquiring 12 pictures per second all depicted in a single picture. His passion for physiology led him to propose during an International Physiology Congress (1898, Cambridge) the creation of an International Commission aiming at the standardisation of available instruments for physiology studies. He became the president of this commission and the building hosting the commission's meetings was named after him (Marey Institute, Parc de Princes, Paris).

Marey's inventions quickly paved the way for continuous observation in the microscale. Time-lapse microcinematography was then introduced to enable imaging through a microscope. The principle was almost identical than chronophotography; imaging microscopic subjects with pre-defined time interval and projecting multiple images per second into a film. The first time-lapse microcinematography movie of growing bacteria was acquired by Bull and Pizon in 1904 (Talbot, 1931; Burton, 1962). A few years later (1907), the first time-lapse movie of fertilization and embryonic development of sea urchin eggs was recorded by Julius Ries (Ries, 1907). Ries projected to his medical students a 14-hour long developmental process into a 2-minute movie, which he used to demonstrate that all cells in an organism are derived from other cells (Landecker, 2009). However, the name which is historically more related to microcinematography is that of Jean Comandon. Comandon, a French medical doctor, established his own microcinematography lab in 1907, where he recorded movies of syphilis spirochete infecting blood cells (Gastou and Comandon, 1909; Roux et al., 2004) and the first movie monitoring the dynamic process of cell division (reviewed in Landecker, 2009).

Modern time-lapse imaging required major advances in many different scientific fields, such as the in vitro cultivation of mammalian cells, different image acquisition methods (phase contrast, fluorescence microscopy), discovery of fluorescent dyes/proteins/antibodies, invention of mechanical parts (filter cubes, charge-coupled device cameras, fluorescent light sources), progress in computer sciences (software for high throughput acquisition and image analysis). Currently, successful incorporation of those

advances enables biologists to monitor dynamic processes at the single cell level with high temporal resolution. However, commercially available hardware and software for multi-positional time-lapse imaging of single cells and most importantly for post-acquisition processing and analysis of cell progeny have limited functionality and flexibility.

3.6.1. Continuous time-lapse imaging with single-cell resolution is indispensable when studying the behavior of living cells

The need for continuous observation of dynamic biological processes has long been appreciated by natural scientists. For example, in 1882 Ilya Metchnikov hypothesized that cells of a transparent starfish larva would respond to inserted rose thorns. Indeed, after hours of continuous observation through his microscope, Metchnikov witnessed larva cells actively migrating and surrounding the intruding thorns (Metchnikoff, 1887) thus giving birth to the field of immunology. Noteworthy, he was later rewarded with the Nobel Prize (Nobel Prize for Physiology or Medicine, 1908) for his work on phagocytosis and immunity (for more details see Tauber, 2003; Dunn and Jones, 2004).

Comprehensive understanding of dynamic processes, such as the behavior of living cells, requires continuous monitoring over time (Schroeder, 2008; Kokkaliaris et al., 2012). Many modern analyzes are based on snapshots of heterogeneous populations, which may easily mask the behavior of individual cells with low frequencies. Snapshot analyzes conducted at the single-cell level (FACS, immunohistochemistry) overcome this limitation, but fail to illustrate the dynamics of cellular and molecular behaviors over time leading to conflicting interpretations (Schroeder, 2008; Schroeder, 2011). For these reasons, continuous time-lapse imaging with single-cell resolution is indispensable when studying living cells (Kokkaliaris et al., 2012). Ideally, such analysis should be implemented in living organisms, since cells could then be observed under physiological conditions. However, due to technical limitations (limited penetration depth of current imaging technology, need for animal immobilization), such in vivo analysis is not feasible for periods more than few hours. On the contrary, in vitro time-lapse imaging of single cells allows long-term monitoring of cellular and molecular behaviors for weeks.

The bioimaging technology established in the Schroeder lab (Schroeder, 2005; Eilken et al., 2009; Rieger et al., 2009) offers a series of advantages, such as: 1. flexibility in multi-positional time-lapse imaging 2. automated acquisition of different fluorescent wavelengths

3. equal time intervals between different cycles 4. long-term imaging of living cells for periods over 2 weeks 5. manual or automated restoration of the progeny of single cells (cell tracking) in different wavelengths 6. functional monitoring and annotation of different cellular properties (division, cell death, migration, speed, etc) 7.background correction algorithms 8. single-cell quantification of fluorescent markers and 9. statistical analysis of cellular behaviors. This technology consists of three main parts, the time-lapse imaging software (Timm's Acquisition Tool, TAT), the tracking software (Timm's Tracking Tool, TTT) with the QTFy algorithm and the staTTTS tool for statistical analysis. Taking advantage of such cutting-edge technology will enable to elucidate the behavior of hematopoietic stem cells and all their progeny followed for up to two weeks continuously and at the single cell level.

4. Goals of the thesis

Ex vivo maintenance of HSCs is a prerequisite for their improved clinical application in regenerative medicine against blood disorders and injury. It has been reported that AFT024 stroma cells promote HSC self-renewal in vitro for long co-culture periods. However, the behavior of single HSCs as well as the molecules involved in this interaction are unknown.

In my thesis, I plan to first identify the behavior of HSCs under maintenance conditions, by implementing continuous time-lapse imaging at the single-cell level. In addition, unravelling the mechanism of the interaction between HSC and stroma cells is required. This will enable me to efficiently screen candidate molecules with selected properties in order to identify the key factor(s) governing HSC maintenance in AFT024-based co-cultures in vitro.

5. Results

5.1. Identifying the behavior of single HSCs under conditions promoting in vitro HSC maintenance

5.1.1. Continuous time-lapse imaging and single-cell tracking allows long-term observation of individual HSCs and their progeny in vitro

The technology developed in the Schroeder lab allows both long-term, continuous observation of living cells through long-term bioimaging and tracking of single cells and their progeny through the tracking software TTT (Timm's Tracking Tool). This enabled me to perform high-throughput imaging of living murine HSCs co-cultured with a panel of irradiated stroma cells, with high temporal resolution for up to two weeks in vitro (Figure 5.1).
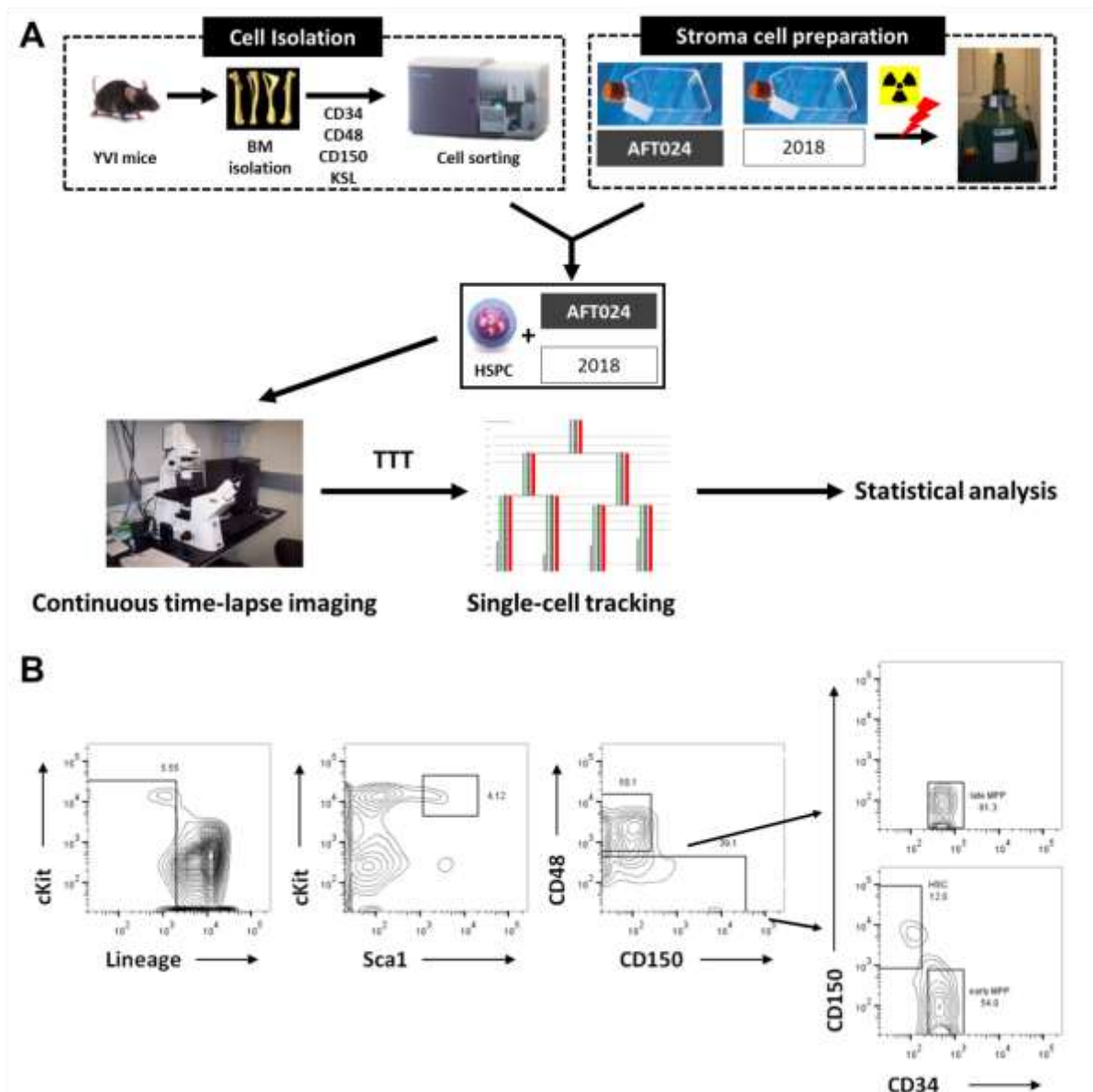
Figure 5.1. Schematic representation of the experimental approach followed in the current study. A. Left: Method for isolation of the bone marrow-derived HSCs and MPP populations from transgenic mice expressing yellow fluorescent protein (YFP) under the chicken beta actin promoter (B6J;129-Tg(CAG-EYFP)7AC5Nagy/J, with C57Bl/6J background).   Bone marrow cells with selected immunophenotypes were sorted by flow cytometry. Top right: stroma cell preparation. Stroma cells were irradiated to prevent future divisions. Later, primary blood cells and irradiated stroma cells were co-cultured and imaged for up to 2 weeks. The history of initially plated blood cells was then reconstructed in cellular pedigrees ('trees') through the TTT software. B. Flow cytometry analysis showing the sorting scheme for HSC and MPP isolation.

HSCs were isolated from transgenic mice ("YVI mice") with ubiquitous expression of the yellow fluorescent protein (YFP) to facilitate efficient cell tracking in visually complex co-culture with the stroma cells (Figure 5.2A). Freshly isolated and plated HSCs (so-called "generation 0" cells) and their progeny (cells of later generations) were monitored (phase

contrast pictures every 7-10 minutes, fluorescent pictures every 14-20 minutes) and their genealogy was re-constructed in tree structures (Figure 5.2B). Such trees provide information about the cell fates of the entire cell progeny of a "generation 0" cell, as well as the kinetics (absolute time after the culture initiation) when those fates occurred. Three distinct cell fates were quantified through this approach: i) cell division, ii) cell death and iii) cells that survived without division (non-dividing cells).
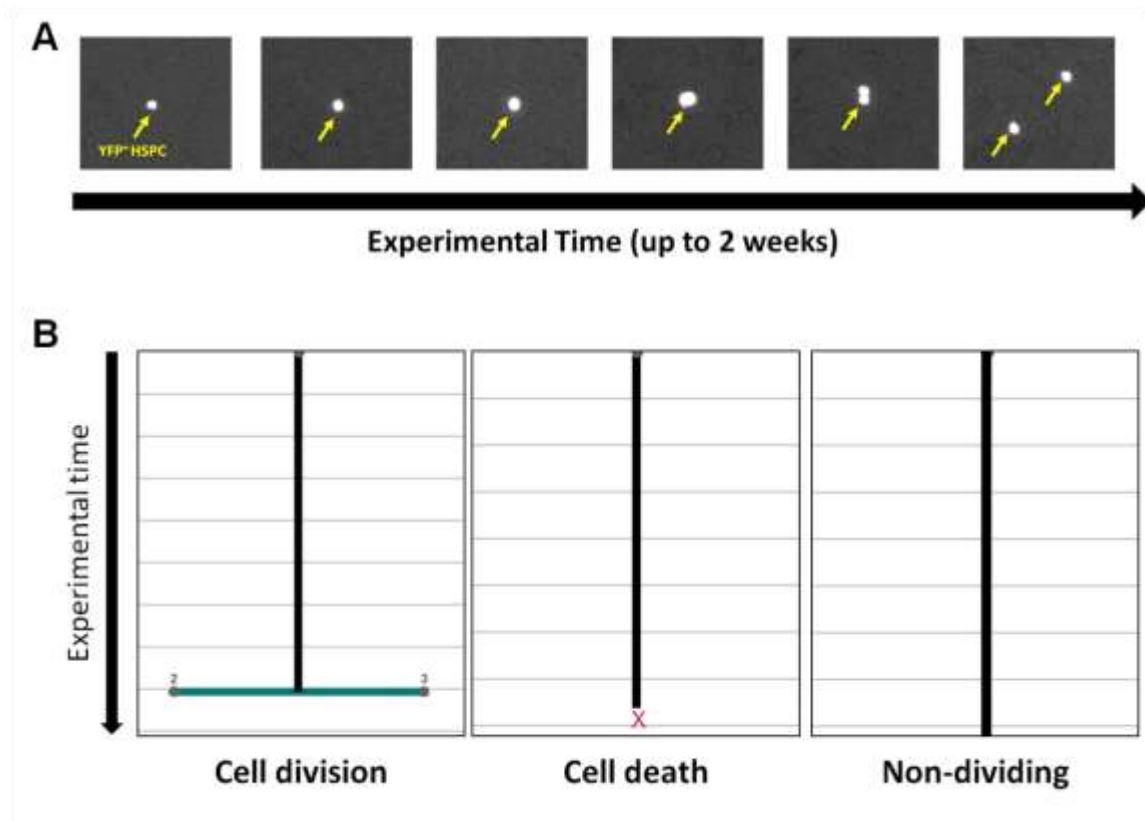
Figure 5.2. Continuous time-lapse imaging allows monitoring of the cell fates of single, living cells for long culture periods in vitro. A. Fluorescent pictures of YFP expressing blood cells co-cultured with non-fluorescent stroma cells were acquired with 10 to 15-minute intervals continuously for up to 2 weeks. **B.** Example trees depicting the history of initially plated cells over experimental time were generated by single-cell tracking. Three cell fates were monitored: cell division, cell death and surviving cells without any divisions until the end of the movie.

5.1.2. Continuous time-lapse imaging reveals the behavior of single HSCs co-cultured in different stroma microenvironments

As mentioned in the introduction, the fetal-liver derived stroma cell line AFT024 is capable of maintaining HSC numbers in long-term, Dexter-type co-cultures. In contrast, the "sister" stromal lines 2018 and BFC012, which were derived from the same experiment as AFT024 cells, failed to maintain HSCs (Moore et al., 1997a). These findings illustrate that cultured HSCs follow distinct cell fates depending on their micro-environment. However, previous studies analyzing the composition of these cultures only at very few time points (snapshot analysis) failed to identify the environment-specific HSC behavior. To be able to qualitatively and quantitatively assess those differences, continuous single-cell analysis is required to avoid population averaging, especially in a population with known heterogeneity, such as the HSCs (Jordan & Lemischka, 1990; Muller-Sieburg et al., 2004; Sieburg et al., 2006; Dykstra et al., 2007). In addition, only through continuous monitoring of living cells their behavior can reliably be identified and quantified (timing of cell division or cell death).

Indeed, HSCs showed distinct cell behaviors upon co-culture with the different stroma (Figure 5.3A). Three different fates were analyzed: cell division, cell death and cells that survived without division until the end of the time-lapse experiment (Figure 5.3B). The majority of the HSCs co-cultured with AFT024 divided (80,0%±8,0%), whereas 15,8%±7,8% died in generation 0. In conditions not supporting HSC maintenance (with 2018 or BFC012 stroma), the majority of HSCs died in generation 0 (71,6%±5,8% and 78,8%±4,2 respectively), and only a small proportion divided (26,2%±4,0 and 21,3%±2,5 respectively) resulting in a clear in vitro readout system. A small proportion of single HSCs (5,6%±3,8) survive without division until the end of the time-lapse movie. Interestingly, HSCs cultured on the stroma with the intermediate supportive capacity (2012 stroma) also showed intermediate levels of division/cell death suggesting that stroma's capacity to maintain repopulating cells correlates with their initial survival rates.
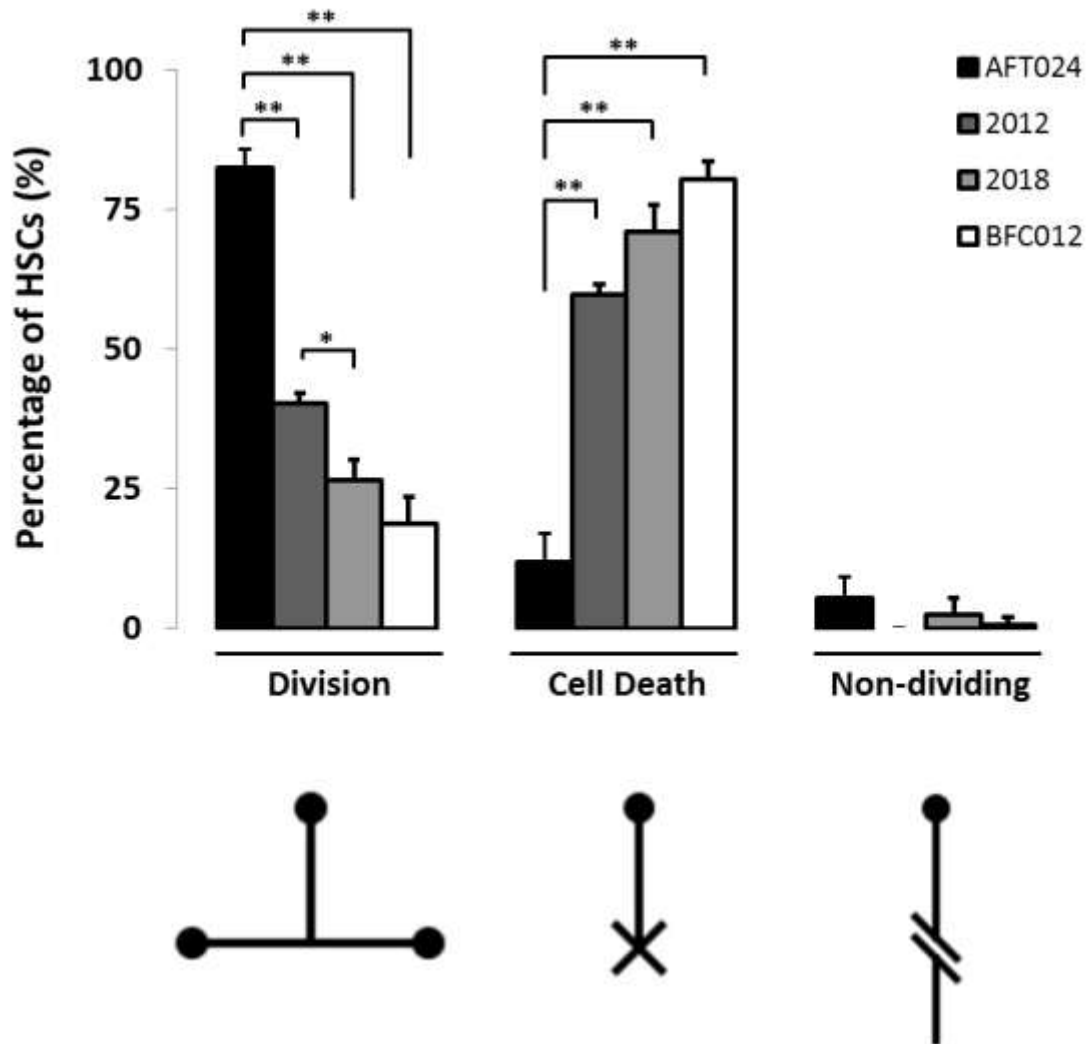
Figure 5.3. HSCs' survival correlates with stroma's ability to support self-renewal. Percentage of single HSCs following different fates (division, cell death or non-dividing cells) upon co-culture with AFT024 supportive stroma (black bars), 2012 intermediate-supportive stroma (dark grey bars), 2018 non-supportive stroma (light grey bars) and BFC012 non-supportive stroma (white bars) in generation 0. Mean of 7 experiments for HSC co-cultured on AFT024 cells (290 trees), 3 experiments on 2012 cells (112 trees), 5 experiments on 2018 (264 trees) and 4 experiments on BFC012 (160 trees). Error bars are ±SD, **p<0,01 and *p<0,05 .

5.1.3. Stability of the stroma-mediated effects on HSCs behavior over generations

The high temporal resolution imaging approach applied in this study, allowed us to follow the fates of the progeny of "generation 0" cells with high precision. Comparing cell fates over several generations revealed only minor changes in the levels of environment-dependent cell division or cell death for cells of later generations (Figure 5.4). "Generation 0"

HSCs cultured on AFT024 share similar frequencies of cell division (80,0% ±8,0%) with cells of later generations (77,0% ±5,5 for generation 1 and 68,0% ±8,2% for generation 2) (Figure 5.4A). The same holds true for the cell-death rates (Figure 5.2B). Interestingly, cells co-cultured with the 2012 or BFC012 stroma demonstrated the same behavior; the rate of dividing or dying cells is stable regardless of the generation. These data suggest that the effects of Dexter-type co-cultures upon HSCs fates are stable for at least the first three generations of in vitro culture.
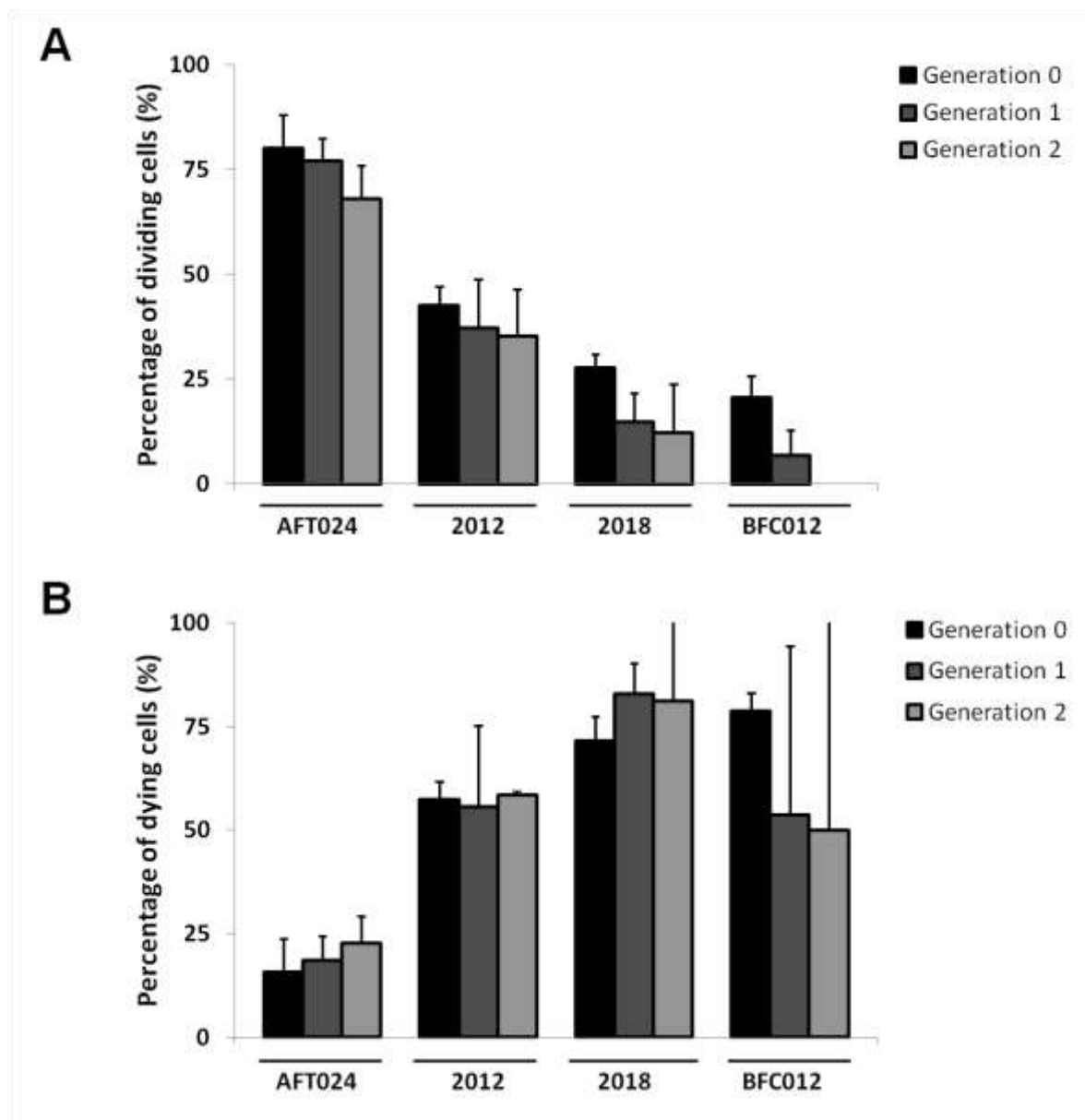
Figure 5.4. Stroma-dependent cell-fate decisions of single HSCs and their progeny do not change over generations. A. Percentage of dividing cells in the different stroma cell lines per generation. Mean ±SD of 290 trees from 7 experiments for cells on AFT024, 112 trees from 3

experiments on 2012, 264 trees from 5 experiments on 2018 and 160 trees from 4 experiments on BFC012. **B.** Dying cells is shown in the bar graph. Mean ±SD.

5.1.4. The genetic background of HSCs has minor effects on stroma-dependent cell-fate decisions

In order to validate these results, HSCs isolated from a different reporter mouse line (mT/mG), but with the same genetic background as YVIs (C57BL/6J), were co-cultured with stroma cells revealing similar cell-fate behaviors (divisional rates were 78,4%±4,8% compared to 80,0%±8,0% on control)(Figure 5.5). Also, to identify potential differences due to genetic background variation, the same analysis was conducted with HSCs isolated from YVI mice with mixed background (75% CD1, 25% C57Bl6), showing elevated cell-death (24,7%±9,0% compared to 15,8%±8,0% in YVI-C57Bl/6J) and reduced division levels (66,5%±6,1% compared to 80,0%±8,0%)(Figure 5.5).
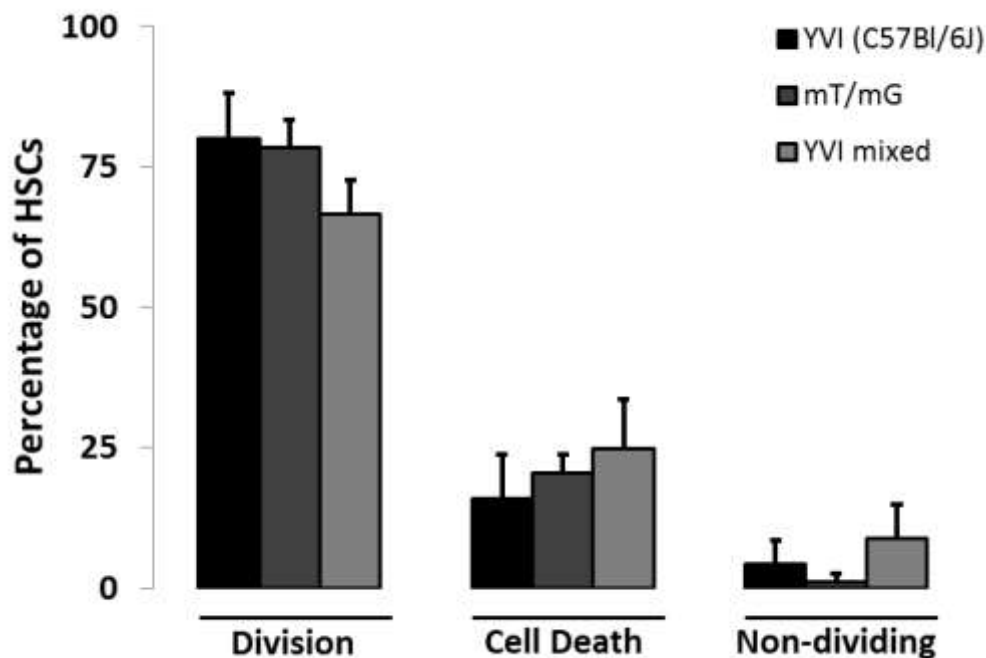
Figure 5.5. Genetic background has minor effects on the cell fates of co-cultured HSCs. Bar graphs are representing the percentage of single HSCs following different fates (division, cell death or non-dividing cells) upon co-culture with AFT024 supportive cells. Data from single HSCs isolated from YVI backcrossed with C57Bl/6J (black bars, 7 experiments, 290 trees), from mT/mG mice with

C57Bl/6J background (dark grey bars, 3 experiments, 125 trees) or YVI mice with mixed background (light grey bars, 6 experiments, 312 trees) are plotted. Error bars are ±SD.

5.1.5. Early differences in HSC division and cell-death kinetics on different stroma allow the establishment of a fast readout system

In addition to monitoring the cell fates of individual cells, continuous time-lapse imaging can also provide us with the kinetics of the observed fates. Such analysis revealed that more than 96% of the HSC co-cultured with AFT024 stroma cells (n=7, 290 total trees) divided within the first 7 days of co-culture, with the main population dividing between 30 and 80 hours (50% of HSCs divided at 50,4 hours, $T_{50\%}^{AFT024\text{-}Gen0}$) (Figure 5.6A). Likewise, the large proportion of HSCs co-cultured on 2018 died within the first 7 days (Figure 5.6B). Overall, individual cell-fate decisions in either condition occurred within the first 7 days of co-culture allowing the establishment of a fast readout system for studying the effects of stroma manipulation on HSC fates. It is important to note that this readout system offers a significant advantage over the conventional methodology, which includes long-term cultivation of isolated cells (4 to 6 weeks) and subsequent transplantation (at least 16 weeks) to reveal potential differences.
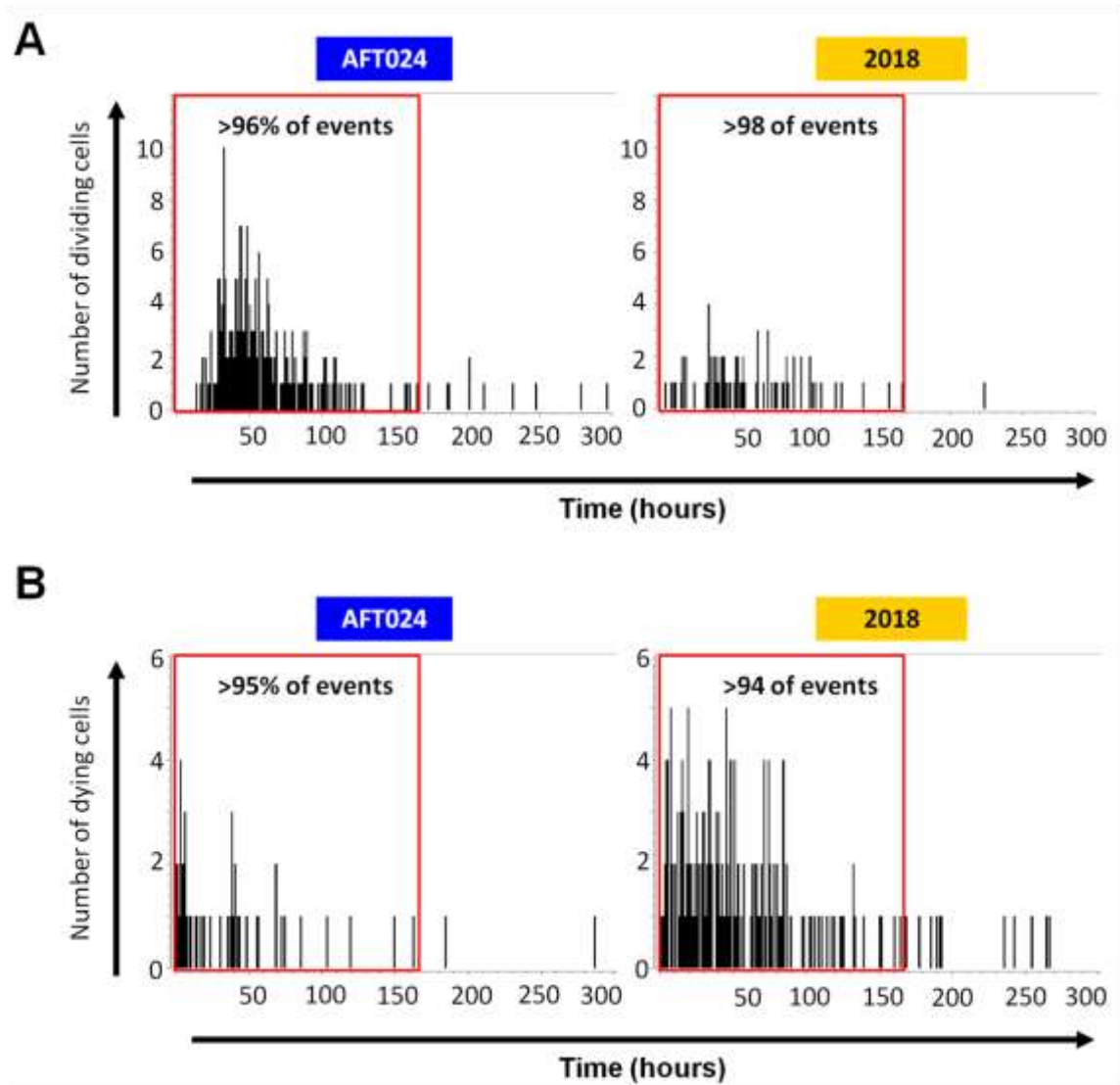
Figure 5.6. Kinetics of HSC fates co-cultured with the different stroma cells. A. Histograms depicting the divisional kinetics of freshly purified HSCs (Generation 0) co-cultured on AFT024 (left side) or 2018 stroma cells (right side). **B.** Histograms depicting the cell-death kinetics of freshly purified HSCs (Generation 0) co-cultured with AFT024 or 2018. The events occurred within the first 7 days are highlighted by the red frame. Five independent experiments, with 188 and 261 HSC trees for AFT024 and for 2018 co-culture, respectively. Individual bars represent the number of cells undergoing cell division at a specific time point.

5.1.6. Identical influence of different stromal lines on HSC cell-cycle progression

As mentioned above, long-term continuous time-lapse imaging and single-cell tracking allow following the fates and the kinetics of single cells and their progeny over different generations. Monitoring the fates of HSCs on different stroma over the first

generations revealed that 50% of generation 0 HSC cultured on AFT024 stroma ($T_{50\%}^{AFT024-Gen0}$) divided after 50,4 hours, whereas the respective value for HSCs cultured on 2018 is 52,1 hours ($T_{50\%}^{2018-Gen0}$). In generation 1, the $T_{50\%}^{AFT024-Gen1}$ value was 94,9 hours (after cell isolation) compared to the $T_{50\%}^{2018-Gen1}$, which was 99,7 hours (Figure 5.7A). In generation 2, the $T_{50\%}^{AFT024-Gen2}$ value was 160,1 hours versus approximately 150 hours on 2018. Similar analysis on HSCs co-cultured with the intermediate supportive 2012 stroma revealed similar kinetics for at least the first two generations (the $T_{50\%}^{2012-Gen0}$ was 58,8 hours, the $T_{50\%}^{2012-Gen1}$ approximately 92 hours and the $T_{50\%}^{2012-Gen2}$ was 124 hours) (Figure 5.7B). This shows that the divisional kinetics of HSCs under co-culture with different stromata are similar for the initial generations (except generation 2 between HSC cultured on AFT024 or 2012). However, comparison with stroma-free cultures revealed faster kinetics for dividing HSCs, since the $T_{50\%}^{stroma\ free-Gen0}$ value was 34,9 hours, the $T_{50\%}^{stroma\ free-Gen1}$ value was 56,2 hours and the $T_{50\%}^{stroma\ free-Gen2}$ value was 77,7 hours (Figure 5.7C). These results imply that although the cell fates of HSCs are influenced by the type of the microenvironment (different stroma cell lines), the cell cycle progression is influenced by stromal co-culture, but is independent of the tested stroma types.

A

Percentage of divided HSCs (%) vs Experimental time (h)

Legend:
- Generation 0-AFT024
- Generation 0-2018
- Generation 1-AFT024
- Generation 1-2018
- Generation 2-AFT024
- Generation 2-2018

B

Percentage of divided HSCs (%) vs Experimental time (h)

Legend:
- Generation 0-AFT024
- Generation 0-2012
- Generation 1-AFT024
- Generation 1-2012
- Generation 2-AFT024
- Generation 2-2012

C

Percentage of divided HSCs (%) vs Experimental time (h)

Legend:
- Generation 0-AFT024
- Generation 0-stroma free
- Generation 1-AFT024
- Generation 1-stroma free
- Generation 2-AFT024
- Generation 2-stroma free

Figure 5.7. The divisional kinetics of HSCs over different generations are independently of the co-cultured stroma. A. Generation-based comparison of divisional kinetics between HSCs cultured on AFT024 (7 experiments, 232 trees) and 2018 stroma (5 experiments, 74 trees). **B.** Similar analysis comparing the kinetics between HSCs cultured on AFT024 and 2012 (3 experiments, 54 trees) or **C.** stroma-free conditions in serum-free media supplemented with stem cell factor (SCF) and thrombopoietin (THPO) (3 experiments, 124 trees).

5.2 The effect of AFT024 stroma upon less primitive hematopoietic populations

We next sought to investigate the effects of the Dexter-type co-cultures on different multipotent progenitor cell populations (MPPs). The current marker combinations used for HSC isolation result in a heterogeneous mix of cells containing only 50% HSCs (Kiel et al., 2005). It is postulated that the remaining 50% of non-stem cells mainly consist of some kind of progenitor cells. Therefore, these experiments would allow us to identify the specificity of the AFT024-mediated effects on the stem cell compartment.

5.2.1 AFT024-based cultures also promote survival of co-cultured MPP populations

For this reason, we sorted different MPP populations and co-cultured them with the fetal-liver stroma. Early MPPs were identified as CD150+ CD48- CD34+ KSL and late MPPs as CD150-CD48+CD34+ KSL. Our experimental approach revealed that 54,5%±6,0% of early MPPs divided when co-cultured with the AFT024 stroma, and 45,1%±5,2% died (Figure 5.8A). In contrast 18,6%±16,8% of the late MPP divided on AFT024 with the remaining 81,5%±16,8% dying. As shown in figure 5.8B, the majority of early/late MPPs died at the initial generation, when co-cultured with the 2018 stroma.
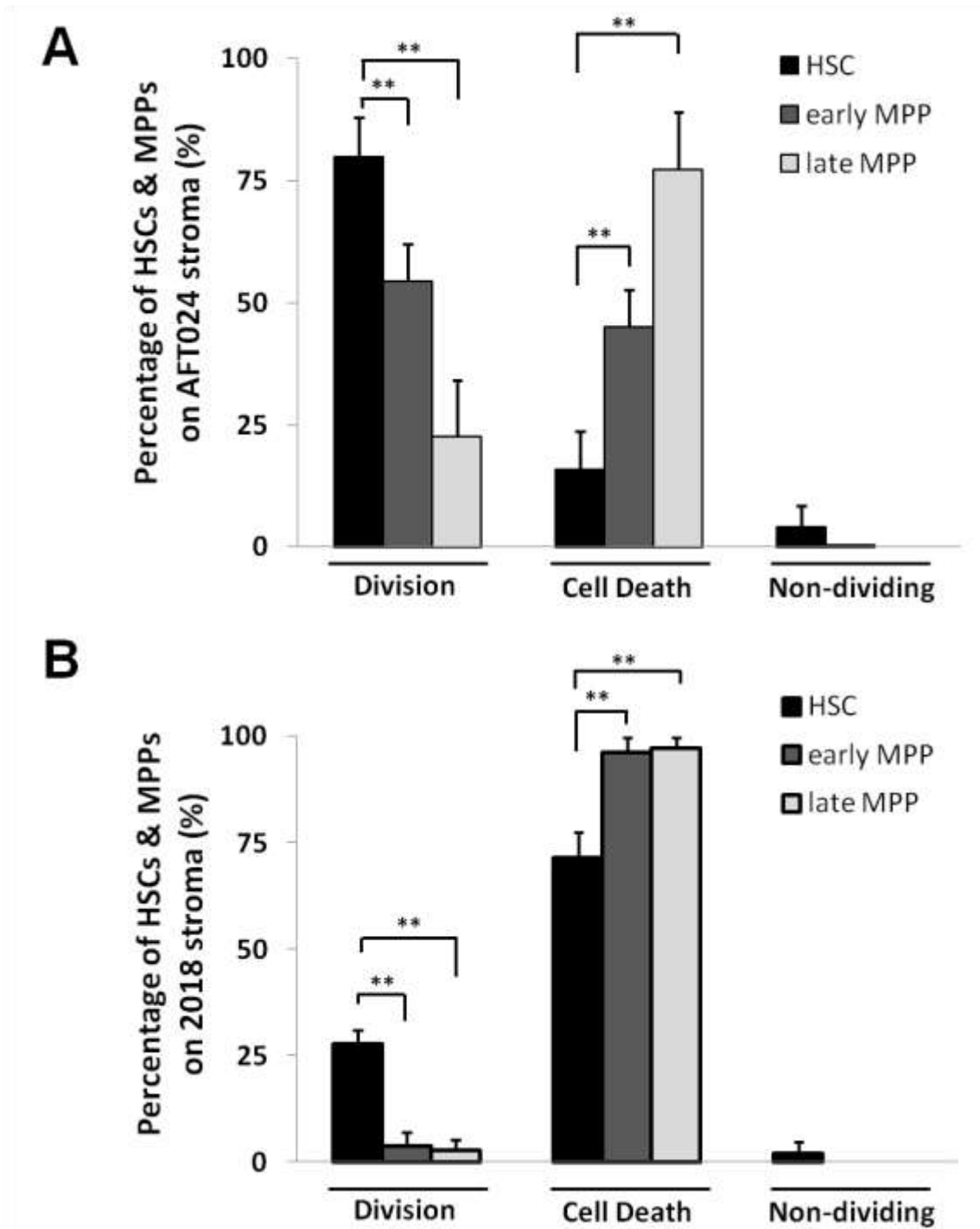
Figure 5.8. AFT024-based culture support intermediate levels of survival of co-cultured MPPs.
A. Bar graphs represent the percentage of single HSC (CD150+CD34-CD48-KSL) and MPP populations (early MPPs are CD150-CD34+CD48-KSL, late MPPs are CD150-CD34+CD48+KSL) following different fates (division, cell death or non-dividing cells) upon co-culture with AFT024 supportive cells in generation 0. Mean ±SD of 4 experiments with 213 early MPP trees, and 3 experiments with 150 late MPP trees. **B.** The same analysis on 2018 stroma. Mean ±SD of 3 experiments with 257 early MPP trees and 184 late MPP trees. **p<0,01.

Analysis of later generations showed high levels of division, (76,6% ±7,0% of generation 1 and 80,9% ±8,1% of generation 2) for early MPPs (Figure 5.9A). The progeny of late MPPs also showed high divisional rates, with 73,6% (±30,7%) and 88,2% (±11,5%) of cells dividing in generation 1 and 2 respectively. The complementary analysis of the cell-death rates confirmed that after the initial high frequencies of dying cells (Generation 0), co-cultured cells had similar levels of observed cell death in later generations (Figure 5.9B). These results imply the presence of an early selection mechanism based on the primitiveness of the co-cultured hematopoietic cell populations. After this selection, the progeny of surviving cells is then equally supported in AFT024 co-cultures.
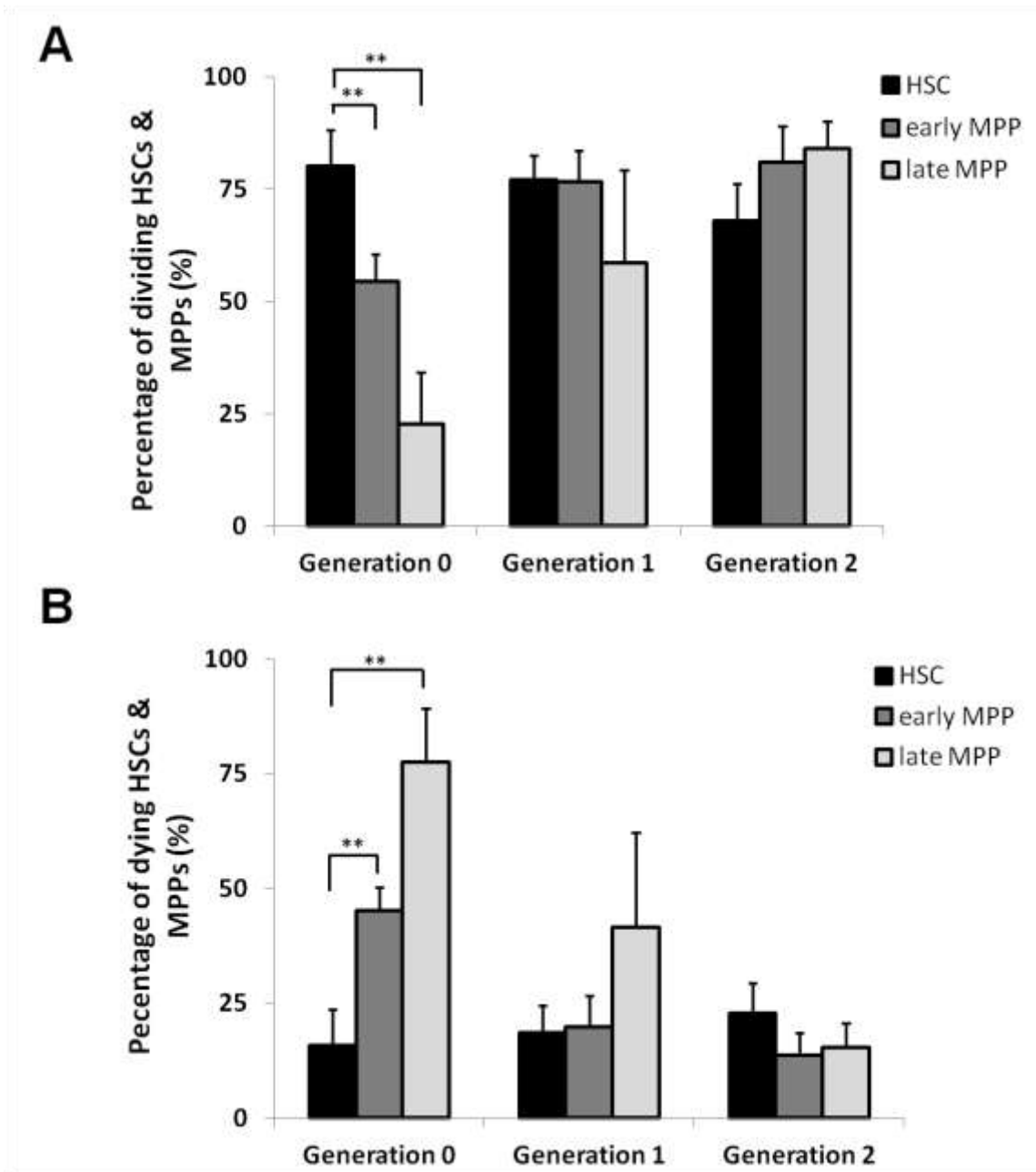
Figure 5.9. AFT024 co-cultures also support survival of progenitor cells, after initial selection.
A. Bar graphs represent the percentage of single dividing HSC (CD150+CD34-CD48-KSL) and MPP populations (early MPPs are CD150+CD34-CD48+KSL, late MPPs are CD150-CD48+CD34+KSL) upon co-culture with AFT024 supportive cells over different generations. They are the mean of 4 experiments for early MPP trees (213 early MPP trees for generation 0, 227 trees for generation 1 and 321 for generation 2) and 3 experiments for late MPP (150 late MPP trees for generation 0, 59 trees for generation 1 and 82 for generation 2). **B.** The same analysis for dying HSCs and MPP cultured on 2018 stroma over different generations. Bars are the mean of 4 experiments for early MPP trees and 3 experiments for late MPP. Error bars are ±SD, **p<0,01.

5.2.2 HSCs and MPPs divisional and cell-death kinetics on AFT024 and 2018 stroma

The comparison of the HSC and MPP fates cultured on AFT024 stroma over different generations revealed that the main differences occurred in the percentage of dividing/dying cells in generation 0. However, such analysis provides no information about the experimental time required for cells to divide or die. For this reason, I further analyzed the divisional and cell-death kinetics of HSCPs and MPPs cultured under supportive conditions, in order to identify potential differences.

According to our analysis, 50% of generation 0 HSC on AFT024 stroma needed 50,4 hours ($T_{50\%}^{HSC-Gen0}$) to divide, whereas early and late MPPs needed 40,1 hours ($T_{50\%}^{early \; MPP-Gen0}$) and 31,3 hours ($T_{50\%}^{late \; MPP-Gen0}$), respectively (Figure 5.10A). This suggests that more primitive cells require longer time periods before they divide. This trend was less obvious in generation 1, in which HSCs needed 94,9 hours to divide further, early MPPs 84,5 hours and late MPPs 86.9 hours. Finally, in generation 2, HSCs required 160,1 hours before their second division, early MPPs 140 hours and late MPPs 137,9 hours. Analysis of the cell-death kinetics confirmed the finding that more primitive cells also require longer time to cell death , since generation 0 HSCs died at 30 hours, early MPPs at 7,7 and late MPPs at 4,1 hours (Figure 5.10B). Furthermore, generation 1 HSCs died at around 113,9 hours, early MPPs at 79,8 hours and late MPPs at 4,1 hours. Finally, generation 2 HSCPs died at 172,8 hours, early MPPs at 128,3 and late MPPs at around 120 hours. These results illustrate that AFT024 co-cultures synchronise the cell-cycle progression of co-cultured HSCs and MPPs after their first division.
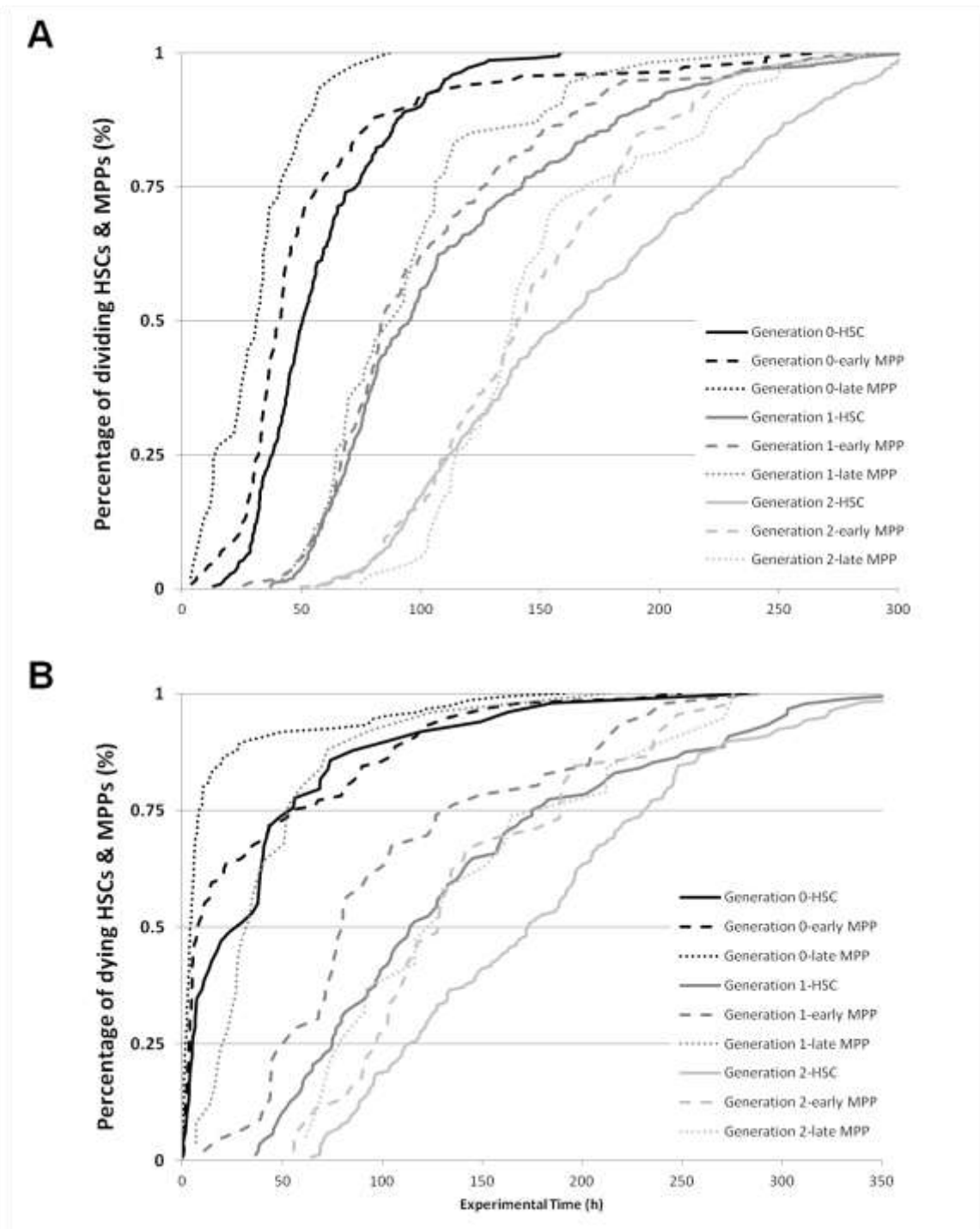
Figure 5.10. Divisional and cell-death kinetics correlate with the primitiveness of the co-cultured population, with less primitive cells having faster kinetics. A. Generation-based comparison of the divisional kinetics between HSCs (7 experiments, 232 trees), early MPPs (3 experiments, 116 trees) and late MPPs (3 experiments, 45 trees) on AFT024 stroma over the initial three generations. **B.** Similar analysis comparing the kinetics between HSCs (3 experiments, 54 trees), early MPPs (3 experiments, 96 trees) and late MPPs (3 experiments, 149 trees) cultured on AFT024 stroma.

5.3 Is cell-to-cell contact required for the effect of AFT024 stroma?

The unique molecular signature of the HSC maintaining stroma (AFT024) was revealed by functional genomics (cDNA subtracted library) and bioinformatics analysis (Hackney et al., 2002). It was later confirmed by microarray experiments (Charbord and Moore, 2005). These analyzes revealed almost 1000 genes preferentially or exclusively expressed by the AFT024 stroma when compared with non-supportive lines (2018, BFC012). The reported genes were classified in different categories, such as genes coding for membrane molecules, extracellular matrix-related proteins, secreted factors, cytoskeleton-related proteins and transcription factors. However, given the large number of differentially expressed genes, the selection of relevant molecules for HSC maintenance requires additional filtering mechanisms. Elucidating the necessity of secreted factors versus adhesion molecules would allow better filtering of the long list of candidate genes and more efficient stroma manipulation.

5.3.1 Absence of active migration towards the AFT024 stroma

Among the differentially expressed genes, several chemokines were reported. Chemokines are secreted proteins with the ability to trigger active migration (chemotaxis) towards the secreting cell. In order to functionally investigate whether AFT024 stroma secretes chemokines (or other molecules) capable of attracting HSCs, HSCs were plated on sparsely seeded AFT024 stroma and monitored through time-lapse microscopy. As a positive control, HSCs were plated on sparsely seeded PA6 stroma, where they were monitored to actively migrate towards PA6 cells (Figure 5.11, Dirk Loeffler, personal communication). On the contrary, no migration of HSCs was observed towards AFT024 cells. In addition, HSCs plated on gelatin-coated surface between AFT024 and 2018 showed no migration towards AFT024 stroma. Collectively, we report no detectable chemokine activity from the AFT024 stroma on freshly shorted murine HSCs, therefore excluding the possibility that they play a key role in the reported interaction.
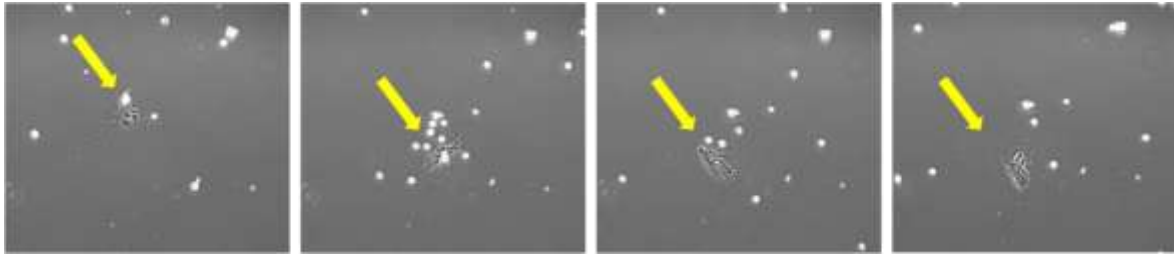
Figure 5.11. Example of active migration of HSCs towards PA6 stroma cell. Continuous time-lapse imaging of sparsely seeded PA6 cells (highlighted by the yellow arrow) co-cultured with HSCs (bright dots). Image was acquired with a 10x Plan-Neoluar objective. Phase contrast images were acquired and kindly provided by Dirk Loeffler.

5.3.2 AFT024 conditioned media exhibit minor effects upon HSC cell fates

To identify whether cell to cell contact or signaling by soluble factors is the predominant mechanism through which AFT024 stroma maintains HSCs, I performed experiments with exchange of conditioned media. In those assays, media from cultured AFT024 stroma (conditioned media) was collected and used to substitute media of co-cultures of HSCs with the 2018 cells (Figure 5.12A). Co-cultures without media exchange were used as controls.

Our analysis showed that 34,3% ±3,5% versus 26,2%±4,0% of HSCs divided with conditioned media versus control. 65,2%±2,9% died (versus 70,8%±5,4% in the control) and 0,5%±1,0% survived without division (versus 3,0%±3% in the control) (Figure 5.12B). Similarly, 28,4%±3,2% of HSCs exposed to 4 days AFT024-conditioned media divided, 70,3%±2,1% died and 1,3%±0,5% survived without dividing. These results from the 2-day conditioned media revealed a slight increase in the divisional rates of "generation 0" HSCs in AFT024 conditioned medium leading to the conclusion that factors secreted by the AFT024 stroma can improve HSCs' survival, although the effect is only minor. Further analysis of later generations revealed no statistically significant increase of the survival rates of HSC progeny (Figure 5.12C). Interestingly, the percentage of cell death decreased in the presence of AFT024 conditioned media for cells in generation 1 and 2 (Figure 5.12D). However, the reduced levels of dying cells did not lead to dividing cells, but to cells that survived without further division (possibly senescent cells).

These results illustrate that factor(s) secreted from the AFT024 stroma have only minor effects on the survival and proliferation of freshly purified HSCs and their progeny.

The main mechanism supporting HSC survival and cell cycle progression maintenance by AFT024 stroma therefore is through cell adhesion. However, since the stability of potential secreted factors contained in the conditioned media can be irreversibly damaged during isolation, additional assays were necessary to confirm these results.
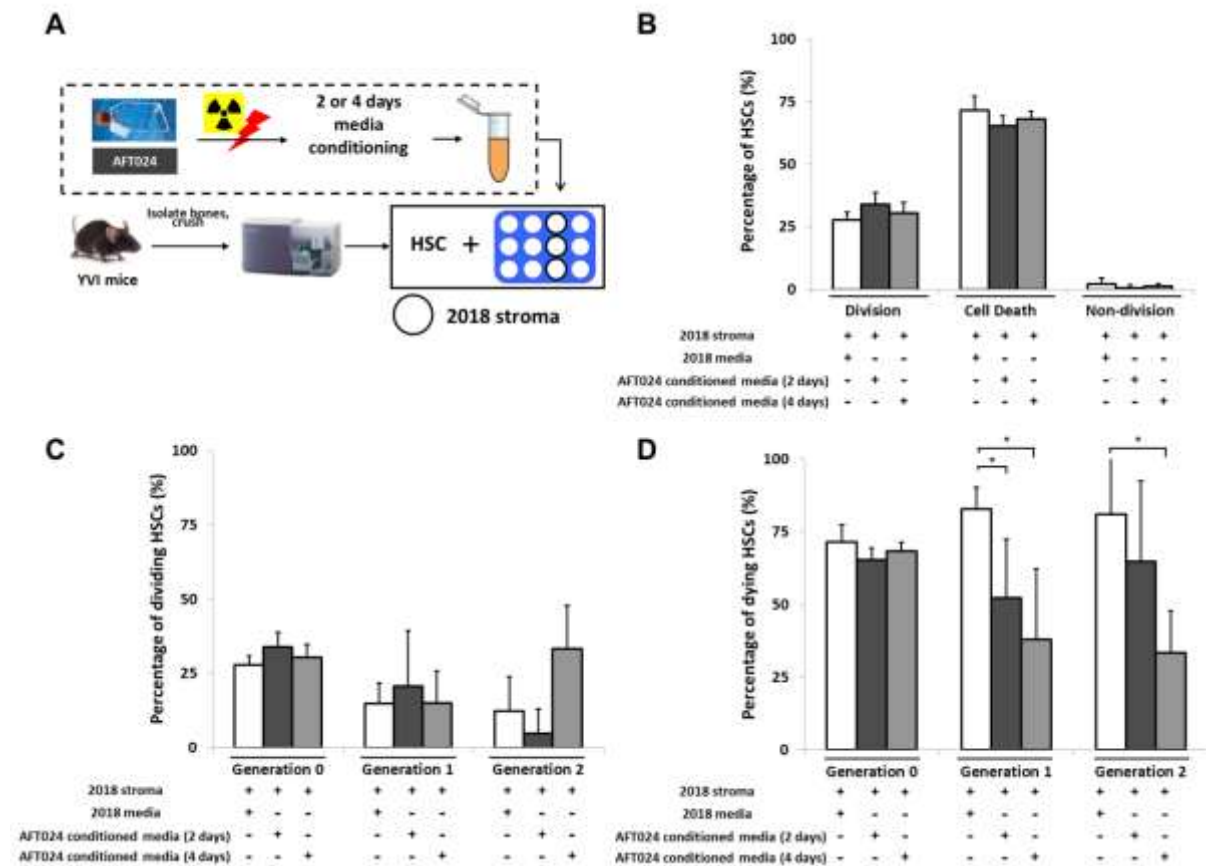
Figure 5.12. AFT024-derived secreted factors have only limited influence on HSCs fates. A. Schematic representation of the experimental approach. **B.** Percentage of tracked HSCs (generation 0) following different fates (division, cell death or non-dividing cells) in co-cultures with 2018 stroma in the presence or absence of conditioned media from AFT024 stroma cells. Mean of 5 experiments of 264 trees for HSCs cultured on 2018 stroma without media change (white bars), 3 experiments of 127 trees for HSCs cultured on 2018 stroma with AFT024 conditioned media for 2 days (dark grey bars) and 3 experiments of 165 trees for HSCs cultured on 2018 stroma with AFT024 conditioned media for 4 days (light grey bars). **C.** Generation-based analysis depicting the numbers of HSCs and their progeny that divided over the first three generations under conditions mentioned in panel B. **D.** Similar analysis as in panel B with the number of HSCs and their progeny that died over the first 3 generations. Error bars are SD.

5.3.3 Cell adhesion is the predominant mechanism mediating the AFT024 effect on HSCs

To cope with the potential stability issues of the secreted factors contained in the collected conditioned media, I applied an alternative method of stable media conditioning. HSCs were cultured on 2018 stroma, while being exposed to media stably conditioned by AFT024 cells. A silicon insert was used to physically separate the two different stroma types (Figure 5.13A). Freshly isolated HSCs were then cultured on top of the 2018 stroma plated inside the silicon insert, while being exposed to the media produced and conditioned from the AFT024 stroma. It is important to note that the inner surface of the silicon insert is 0,42cm^2, while the culture area of the entire well (of a 12-well plate) is around 8 times bigger (3,5cm^2).

HSCs cultured in contact with 2018 while exposed to AFT024-conditioned media showed a 1,5-fold increase in survival/proliferation (dark grey bar – Figure 5.13B) and reduced levels of cell death. In more detail, 42,1%±2,7% of HSC divided (versus 27,9%±3,2% in the control), 56,8%±4,5% died (versus 71,6%±5,8%) and 1,08%±1,86% survived without division (versus 3,0%±3,0%). Further analysis of later generations showed no significant increase in the levels of division for generation 1, since 19,0%±6,4% cells divided (Figure 5.13C, grey bars) compared to in the control (14,9%±6,8%) (Figure 5.13C, white bars) and generation 2 cells (19,1%±8,3% versus 12,3±11,6% in the control), suggesting that factor(s) secreted by AFT024 have only a transient positive effect upon HSC proliferation.

Generation-based analysis of the cell-death rates showed a trend of reduced number of dying cells, however results were not statistically significant. In generation 1, the percentage of dying cells was 65,0%±23,0% (versus 82,8%±7,6% in the control) with that of generation 2-dying cells being 42,9%±28,6% (versus 81,0%±20,7% in the control) (Figure 5.13D). These results, thus, confirm that our previous finding from the conditioned media experiments that: 1. AFT024-secreted factors can only partially rescue HSC survival and 2. adhesion molecule(s) are the main mediators of the AFT024-mediated maintenance of co-cultured HSCs.
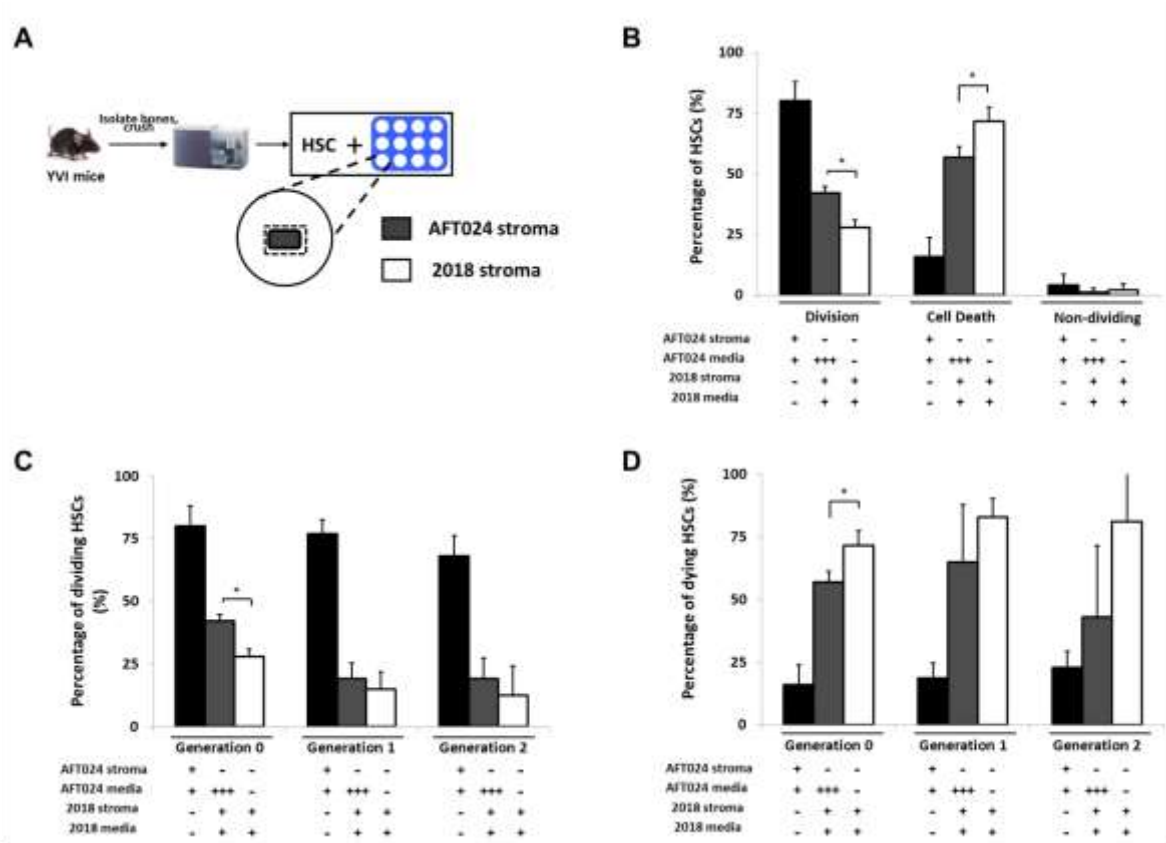
Figure 5.13. AFT024-derived secreted factor(s) partially rescue survival of co-culture HSCs. A. Graphical presentation of the experimental approach. **B.** Bar graphs depicting the percentage of "generation 0" HSCs following different cell fate under co-culture with AFT024 stroma only (n=7, 290 trees, black bars), 2018 stroma only (n=5, 264 trees, white bars) or on 2018 stroma with AFT024 stably conditioned media (n=3, 194 trees, grey bars). **C.** Bar graphs representing the percentage of dividing HSCs and their progeny cells for the first three generations after plating under the conditions mentioned above. **D.** Similar analysis of the percentage of dying cells over different generations. Errors bars are ±SD, *p<0,05.

5.3.4 AFT024 stroma cells are essential for HSC survival

To further investigate the importance of cell adhesion for HSC survival and subsequently for AFT-mediated maintenance, I performed stroma-free HSC cultures using fresh or conditioned Dexter media. In those experiments, HSCs were cultured without stroma in media conditioned by AFT024 (three or four days). In some cases, different coating proteins (gelatin, fibronectin) were used to minimize migration during the time-lapse imaging. All HSCs plated in gelatin-coated wells, fibronectin-coating wells or non-coated wells with fresh media died in generation 0. The same was observed for HSCs cultured in AFT024-conditioned media on fibronectin-coated wells (98,89% death), gelatin-coated wells (100% death, n=1, 9 trees) or uncoated plates (100% death, n=2, 63 trees) (summarized in

Figure 5.14A). In addition, all generation 0 HSCs cultured in 2018-conditioned media also died (Figure 5.14A, white bars). These results clearly illustrate the importance of the stroma and the prevalence of adhesion molecules as the key mediators of the AFT024-driven maintenance of HSCs in vitro.

Interestingly, analysis of the cell-death kinetics revealed differences between the different conditions. HSCs cultured with the AFT024-conditioned media survived longer before they eventually died suggesting that the AFT024-produced secreted factors can delay but not inhibit HSC death. In conclusion, adhesion to the stroma is essential for long-term survival and proliferation.
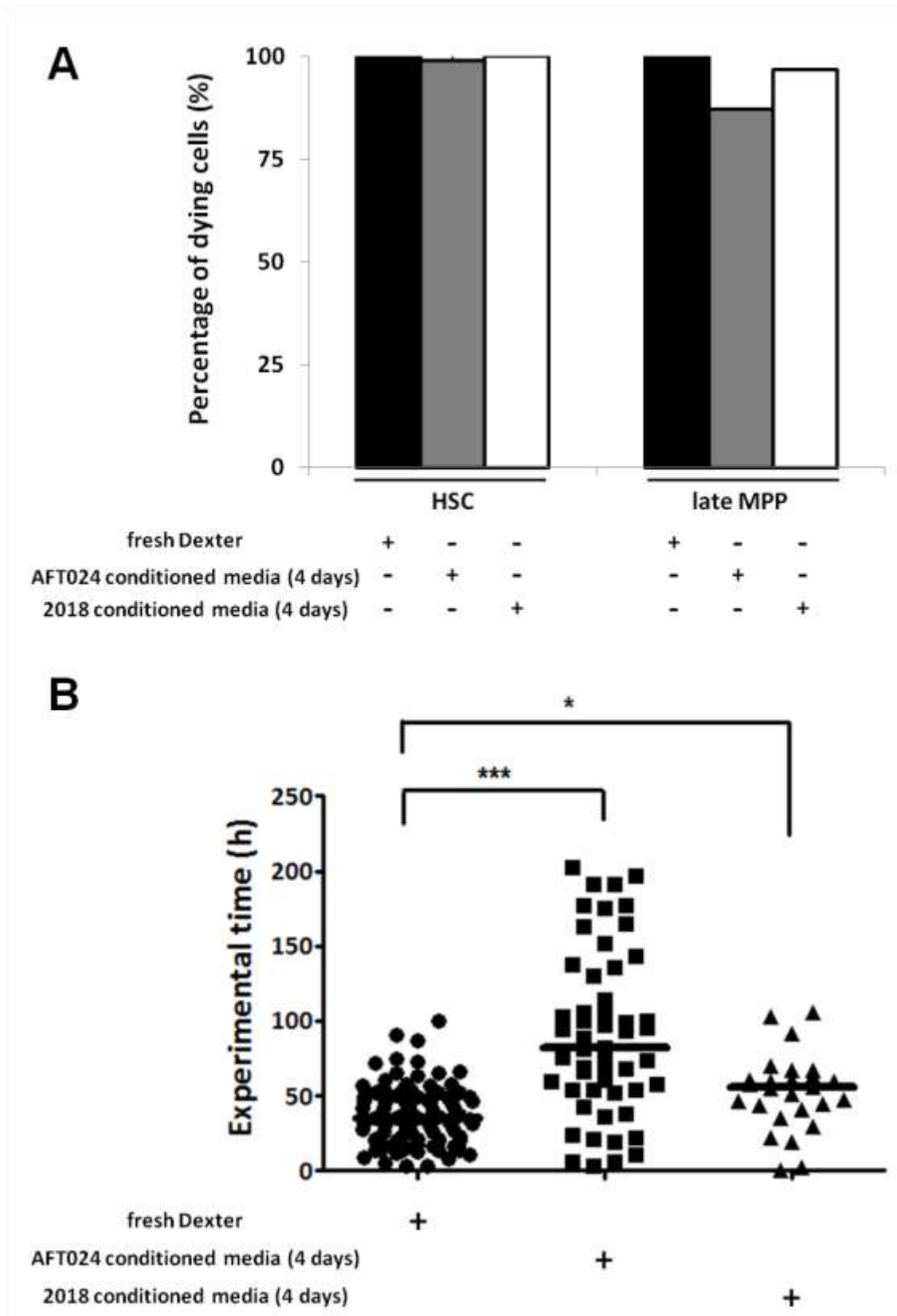
Figure 5.14. Adhesion to AFT024 stroma cells is essential for HSCs survival in Dexter-type in vitro cultures. A. Bar charts representing the percentage of dying HSCs cultured in fresh Dexter (black bars, 4 experiments, 104 trees), AFT024 conditioned media for 4 days (grey bars, 3 experiments 54 trees) or 2018 conditioned media (white bars, 1 experiment, 27 trees). **B.** Dot plots representing the number of dying HSCs cultured in stroma-free cultures supplemented either with fresh Dexter media, AFT024-conditioned media or 2018-conditioned media. Black lines represent the

median and the statistical test was one-way analysis of variance (Kruskal-Wallis test with Dunn's post-hoc test). ***p<0,001, *p<0,05

5.4 Is the differential HSC behavior a result of a positive effect from AFT024 or a negative effect from 2018 stroma?

The observed differential HSC behaviors (division on the AFT024 stroma, cell death on the 2018 stroma) could be explained either by a molecule promoting survival and proliferation expressed exclusively by the AFT024 stroma (positive effect, Figure 5.15A) or by the presence of a factor leading to cell death expressed only by the 2018 stroma (negative effect, Figure 5.15B). Alternatively, a combination of both scenarios could also be possible (Figure 5.15C). Identifying the "direction" of the observed differential HSC behavior upon co-culture with the different stroma cells (survival on AFT024, cell death on 2018) could be an additional layer for screening the published gene lists (Hackney et al., 2002; Charbord and Moore, 2005) for molecules with a profile matching our observations. Potential synergistic effects requiring the presence of more than one factors to promote an effect on co-culture HSCs' cell fates are also possible.
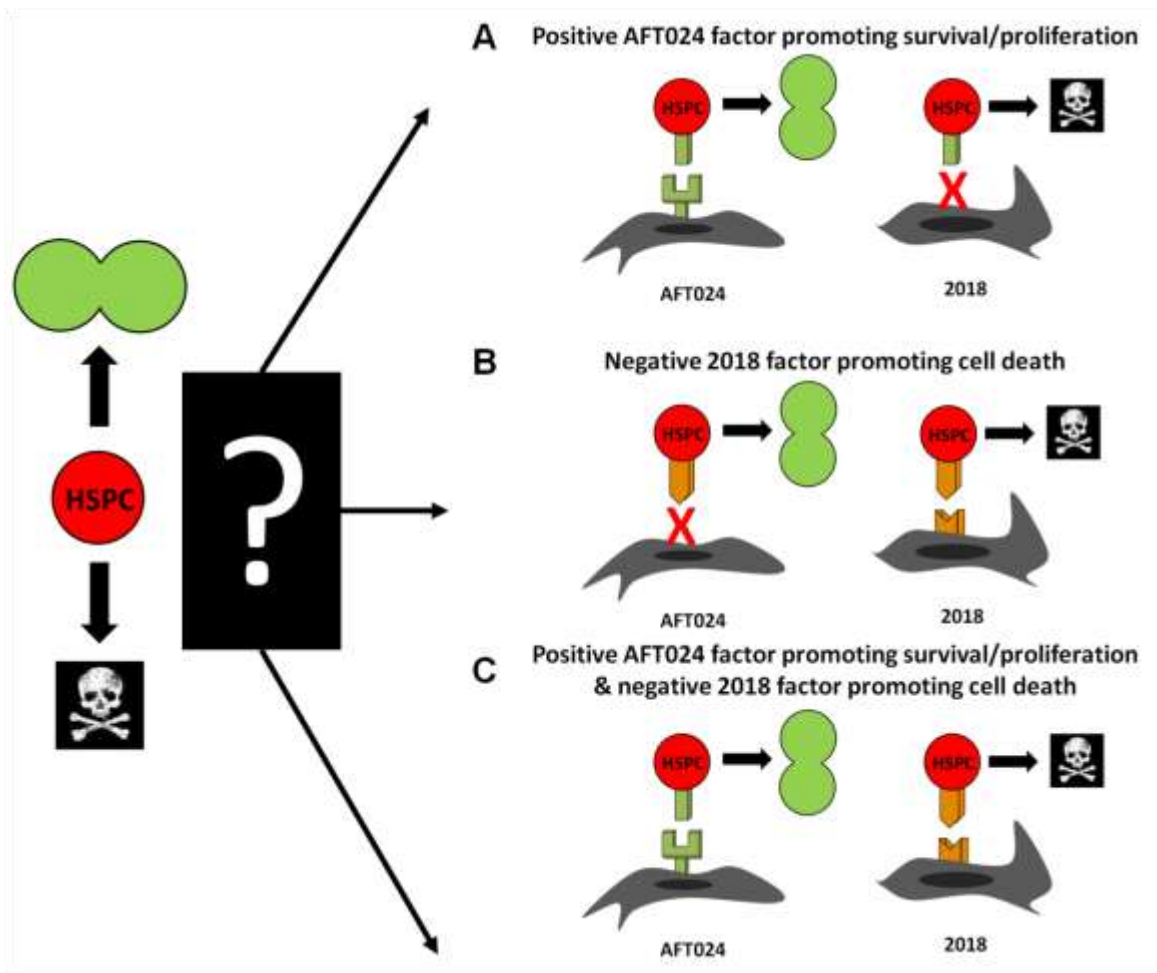
Figure 5.15. Possible scenarios explaining the differential behavior of HSCs upon co-culture with AFT024 or 2018 stroma. A. In the first scenario AFT024 stroma cells express a molecule promoting long-term survival and proliferation of co-cultured HSCs, whereas its absence from the 2018 stroma leads to the observed cell death (positive effect from AFT024). **B.** In the second scenario, 2018 stroma expresses a factor leading to HSCs cell death (negative effect from 2018). AFT024 stroma does not express this factor, thus HSCs survive. **C.** The last scenario is a combination of both previous scenarios, with both a positive pro-survival and proliferation effect from AFT024 and a negative effect leading to cell death from the 2018 stroma. Synergistic effects, in which more than one molecules/interactions are essential to lead to a cell fate are possible, but not depicted in this figure for simplicity reasons.

5.4.1 Secreted factor(s) produced by the 2018 stroma have minor negative effects upon HSC survival and proliferation

As we report in the current study, bone marrow-derived HSCs die when co-cultured with 2018 stroma in Dexter-type culture in vitro. To investigate whether the 2018 stroma promotes death of co-cultured HSCs, I first tested 2018-conditioned media for negative regulators of survival/proliferation.

To do this, I used the conditioned media assay, in which HSCs were exposed to 2018-conditioned media while having direct physical contact with AFT024. Analysis of the results revealed no statistically significant difference from the controls. In more detail, Figure 5.16A shows that 78,1%±10,6% of the HSCs co-cultured with AFT024 and exposed to 2 days 2018-conditioned media divided (versus 82,6%±3,3% in the control), 12,6%±8,8% underwent cell death (versus 11,9%±5,1% in the control) and 9,3%±6,0% survived without division (versus 5,6%±3,8% in the control). In addition, 67,6%±9,3% of HSCs exposed to 4 days 2018-conditioned media divided, 28,7%±6,0% died and 3,8%±4,0% survived without division (Figure 5.16A). These results suggest that potential factors secreted from the 2018 stroma cells have only a minor negative effect upon HSCs survival, or their influence is surpassed by a positive AFT024 factor.
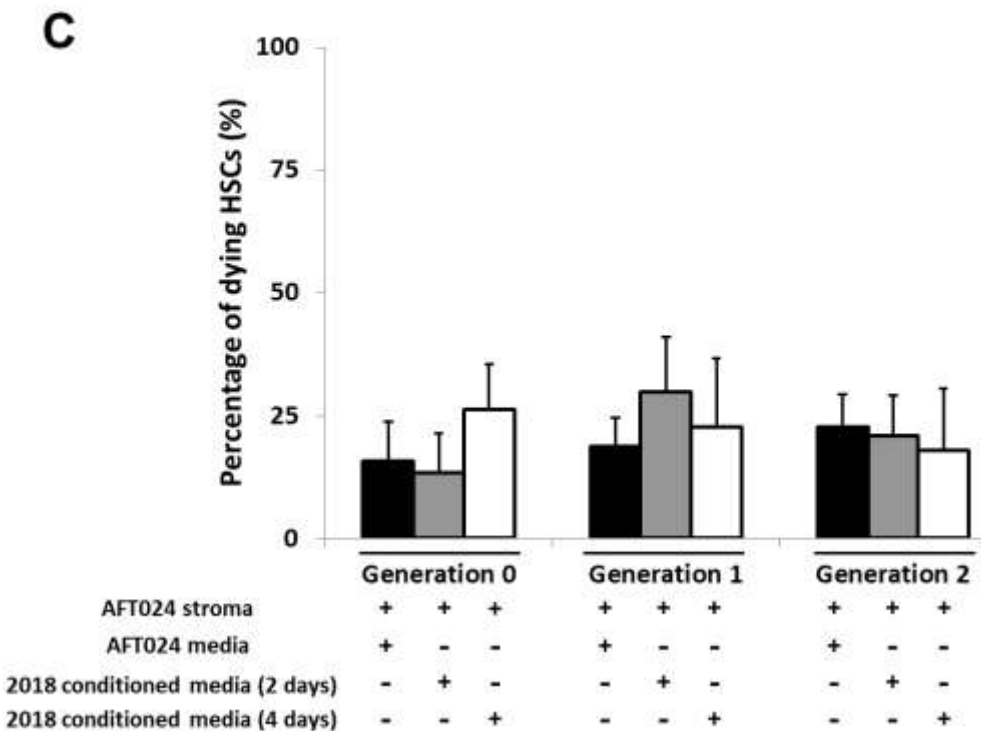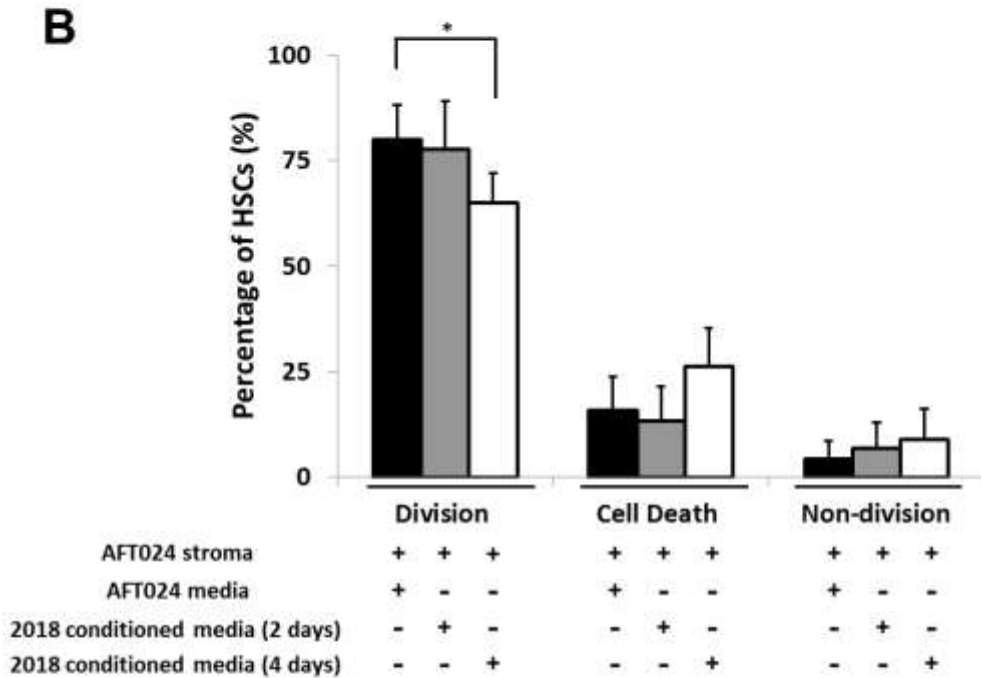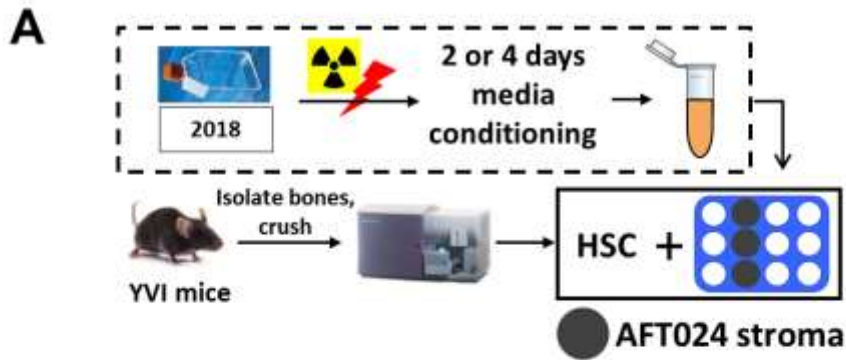
Figure 5.16. 2018-conditioned media has minor effects on the balance between proliferation and cell death of co-cultured HSCs. A. Schematic representation of the experimental approach. 2018 stroma cells were irradiated and cultured in Dexter media for two or four days. Then, conditioned media was collected and added in the cultures of freshly sorted HSCs (via flow cytometry) with AFT024 stroma cells. **B.** Bar graph representing the percentage of HSCs followed a certain fate in generation 0. HSCs were either co-cultured on AFT024 stroma i) without any conditioned media exchange (black bars, 7 experiments, 290 trees), ii) with 2018 media conditioned for two days (grey bars, 3 experiments, 186 trees) or iii) with 2018 media conditioned for four days (white bars, 3 experiments, 148 trees). **C.** Bar graphs depicting the percentage of dying cells under the conditions mentioned above (same colour-code) over different generations. Error bars are ±SD.

Additional experiments in which the culture media was continuously conditioned by 2018 stroma cells being physically separated by the AFT024 stroma, were also conducted (Figure 5.17A). In those assays, HSCs were cultured in direct contact with the AFT024 stroma and their cell-fate decisions were monitored over the first three generations. No differences in the behavior of generation 0 HSCs cultured under those conditions was observed, since 82,8%±5,0% divided (compared to 80,0%±8,0% in AFT024 conditions), 14,2%±6,9% died (compared to 15,8%±8,0%) and 2,1%±2,6% survived without divisions (compared to 4,2%±4,4%) (Figure 5.17B). Further analysis of the HSCs progeny revealed that cells cultured on AFT024 stroma while exposed to factors secreted by 2018 stroma had no difference in the cell-death rates for the first three generations, from cells cultured exclusively on AFT024 stroma and media (Figure 5.17C). In more detail, 22,4%±12,4% of generation 1 cells died (compared to 18,6%±5,9% in the control conditions), while 11,1%±9,0% of generation 2 cells also did not survive (compared to 22,8%±6,6% in the control). It is important to note that under those culture conditions, the percentage of dividing cells in generations 1 and 2 was decreased (compared to the control conditions), while the percentage of non-dividing cells increased (data not shown). However, since the levels of cell death observed in this assay were not altered, we suggest that factors secreted by 2018 do not have any effect on the balance between proliferation and cell death of cultured HSCs.
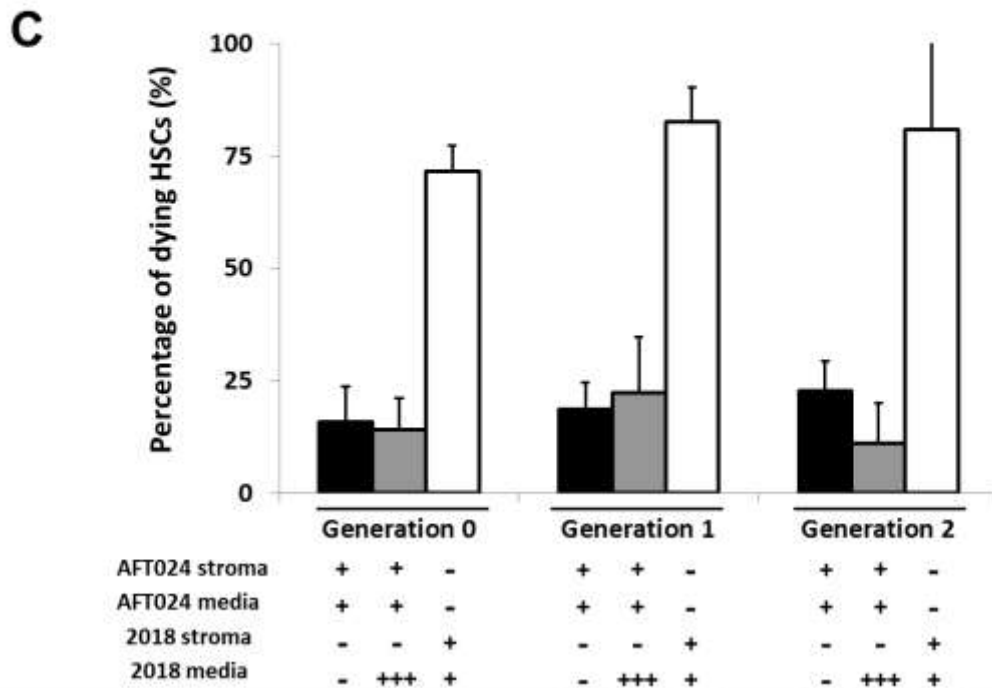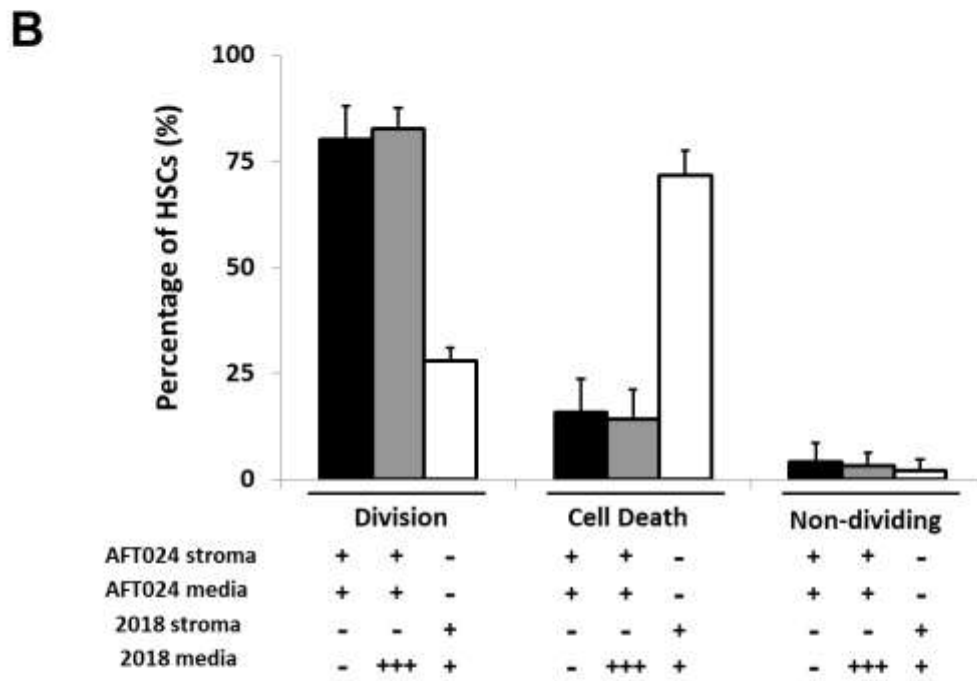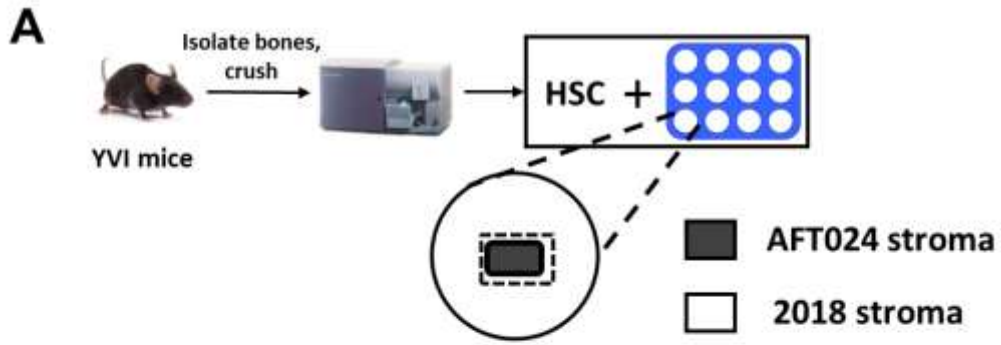
Figure 5.17. Factor(s) secreted by 2018 stroma cells does not alter the survival of co-cultured HSCs. A. Graphical representation of the experimental approach. HSCs were isolated via flow cytometry and cultivated in contact with AFT024 stroma in media constantly conditioned by spatially separated 2018 stroma cells. **B.** Bar graphs showing the percentage of HSCs following different cell fates in generation 0, under different conditions. HSCs were cultured on i) AFT024 stroma cells exclusively (black bars, 7 experiments, 290 trees), ii) on AFT024 stroma with factors mostly secreted by 2018 stroma (grey bars, 3 experiments, 141 trees) or iii) 2018 stroma exclusively (white bars, 5 experiments, 264 trees). **C.** Analysis of the percentage of dying cells over different generation in the conditions mentioned above (same colour-code). Error bars are ±SD.

5.4.2. Quantifying the cell-fate decisions of HSCs cultured in mixed stroma conditions

Since 2018-secreted factors have only minor influence in the cell death of co-cultured HSCs, I then sought to investigate the role of 2018-derived adhesion molecules. For this reason, I cultured HSCs in a mixed environment comprising of different percentages of supportive and non-supportive stroma cells. This analysis revealed that, in a mixed environment consisting of 90% AFT024 stroma and 10% 2018 stroma, the majority of the HSCs divided (75,8%±4,9%, Figure 5.18, dark grey bars), whereas some died (22,0%±7,9) and few survived without division (4,4%±6,0%), showing a slight decrease compared to the described behavior on 100% AFT024 (Figure 5.18, black bars). Altering the percentage of the mix (50% AFT024 stroma - 50% 2018 stroma) resulted in a significant decrease of the divisional rate of HSCs (57,1%±4,0%, grey bars) and in an increase of cell-death rate (20,9%±8,7%). Additional decrease in the percentage of supportive cells (10% AFT024 - 90% 2018) caused additional decrease in the levels of HSC division (23,8%±7,4%, light grey bars) and increase in cell death (72,9%±7,7%) to levels similar as HSC cultured in 100% 2018 (Figure 5.18). Notably, these experiments revealed that supportive and non-supportive cells control HSC fates in a dose-dependent manner, but they provide no information regarding the "direction" of the interaction.
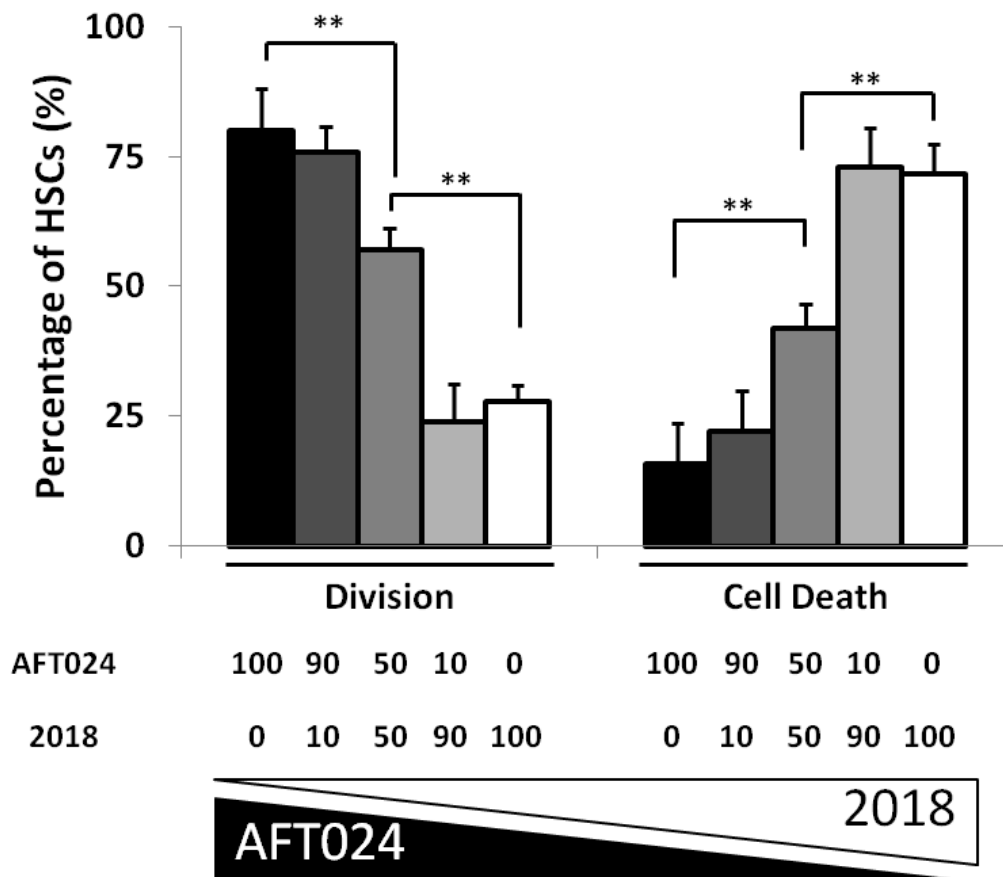
Figure 5.18. Adhesion to mixed stroma consisting of AFT024 and 2018 cells in different ratios has a dose-dependent effect upon the observed HSCs' cell-fate decisions. Bar graphs representing the percentage of dividing (left panel) or dying HSCs (right panel) upon co-culture with a mixed environment of 90% AFT024 and 10% 2018 cells (dark grey bars, 6 experiments, 231 trees), 50% AFT024 and 50% 2018 cells (grey bars, 4 experiments 122 trees) or 10% AFT024 and 90% 2018 cells (light grey bars, 4 experiments 132 trees). Co-cultures with exclusively AFT024 (black bars) or 2018 cells (white bars) were used as controls.

5.4.3. Quantifying the adhesion of HSCs to the different stromata under mixed culture conditions

In order to observe the entire cell volume, cells from the different stromata were transduced with lentiviral vectors expressing fluorescent reporters (distinct for each cell line) fused with a membrane anchoring signal (c-HA-Ras farnesylation signal). This enabled us to quantify the time for which HSCs adhere to AFT024-tdTOMATO expressing cells or 2018-mseCFP expressing cells in a 50%-50% mixed environment and correlate it with their future fate through time-lapse imaging (Figure 5.19A). This analysis revealed that dividing mother

HSC were adherent mostly to AFT024 cells (75,5% of their lifetime) and less to 2018 (17,0%) (Figure 5.19B). On the contrary, dying cells stayed longer adherent to 2018 (60,3%) and less to AFT024 (19,6%). These results directly link stroma adherence with the future fate of HSCs, but again the direction of the effect has not been clarified.
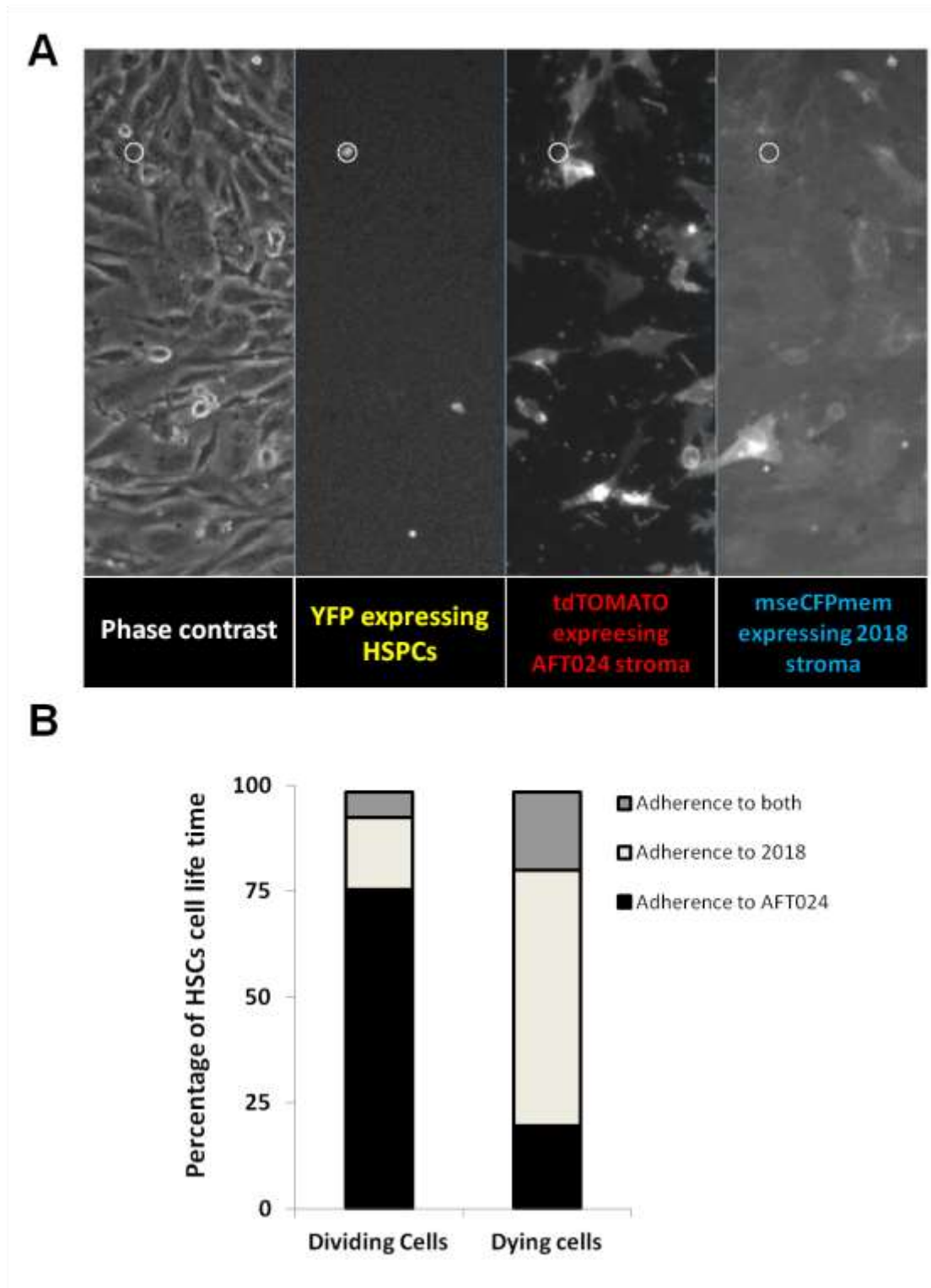
Figure 5.19. Stroma adherence determines the fate of co-cultured HSCs. A. Snapshot from time-lapse imaging experiment showing the different acquired wavelengths in addition to phase contrast.

Cells from different stromata were differentially transduced with lentiviral vectors expressing distinct fluorescent proteins fused with membrane anchoring domains. AFT024 stroma cells were transduced with constructs expressing tandem TOMATO protein, whereas 2018 cells with mseCFP protein. The membrane anchoring signal allows visualisation of the entire cell volumes (for example cell protrusions). HSCs were isolated from the B6J;129-Tg(CAG-EYFP)7AC5Nagy/J mouse strain, therefore expressing YFP **B.** Bar chart representing the percentage of the cell life time, for which dividing (left panel) or dying HSCs (right panel) were adherent to AFT024 (black bar) or 2018 stroma (white bar) or both (grey bar) (47 trees).

5.4.4. Adhesion to 2018 stroma does not result in immediate cell death of co-cultured HSCPs

We have previously shown that the observed death of co-cultured HSCs does not occur due to factors secreted by the 2018 stroma. To investigate whether adhesion molecules are responsible for the observed high cell-death rates of HSCs cultured on 2018 stroma, I further analyzed the cell-death kinetics under different conditions. A direct negative effect of 2018 stroma upon co-cultured HSCs would decrease their life time (faster occurrence of cell death) when compared to other culture conditions.

To test this, freshly sorted HSCs were cultured in medium allowing self-renewal and some survival for short culture periods (serum free media with stem cell factor and thrompbopoietin) (Ema et al., 2000) or in co-culture with different stroma cells (AFT024, 2012, 2018). Analysis of the cell-death kinetics revealed that HSCs that died in co-cultures with 2018 stroma exhibited the longest cell-life time of all groups tested, since the 50% value ($T_{50\%}^{2018-Gen0}$) was 45,6 hours after culture initiation (Figure 5.20). The respective values for dying HSCs cultured on AFT024 were 30 hours, on 2012 19,5 hours and on stroma-free conditions 35,30 hours (Figure 5.20). Notably, almost half of the HSCs cultured on 2018 stroma lived for more than 100 hours after culture initiation, whereas very few of the dying cells in the other conditions survived that long. These data allows us to propose that it is rather the absence of a positive factor promoting survival and proliferation (on e.g. AFT024 cells), rather than a cell-death promoting factor on the 2018 stroma which leads to the observed death of co-cultured HSCs. However, knock down of certain candidate molecules expressed by the AFT024 stroma which affect HSC survival and proliferation is required to further strengthen this model.
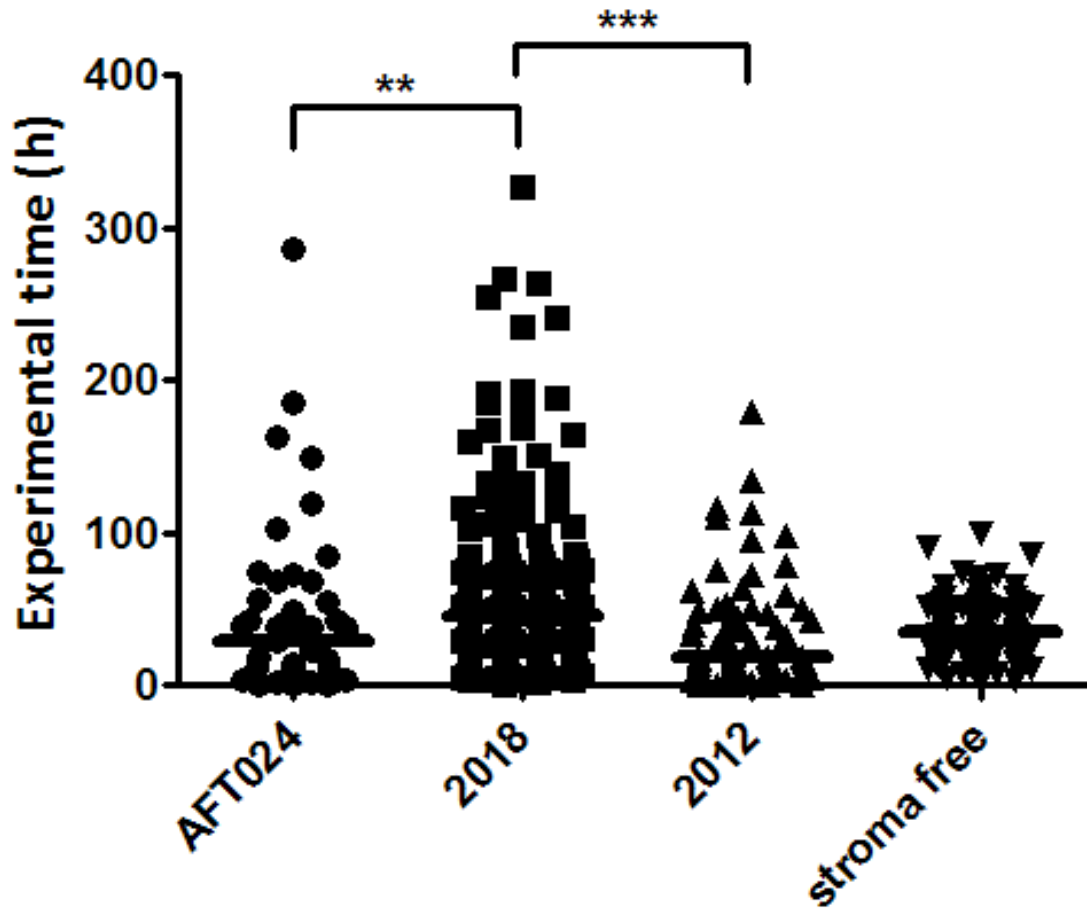
Figure 5.20. Long cell life time of HSCs dying on 2018 stroma reveals the absence of a negative, adhesion factor leading to cell death of co-cultured cells. Dot plot depicting the cell life time of dying HSCs under different culture conditions. HSCs were cultured on AFT024 (7 experiments, 49 trees), 2018 (5 experiments, 184 trees), 2012 (3 experiments, 75 trees) or under stroma-free conditions (4 experiments, 104 trees).

5.5. Identification of key molecule(s) promoting HSC survival and in vitro maintenance

Continuous, time-lapse imaging at the single-cell level enabled us to get an improved understanding of the type and kinetics of HSC behavior induced by AFT024 stroma, as well as of the cellular interactions involved. This allowed us to generate a profile of the candidate molecules governing the observed HSC behavior in Dexter-type co-cultures, with cell surface proteins promoting survival, proliferation and/or self-renewal being the most promising candidates. To test their function robust molecular manipulation of stromal cells was required.

5.5.1. Confirming the published lists of differentially expressed genes between AFT024 and 2018 stroma cells

The published lists of genes which are preferentially or exclusively expressed on the AFT024 stroma were identified using subtractive libraries (Hackney et al., 2002) and micro-array analysis (Charbord and Moore, 2005). These high-throughput approaches enable processing of large amounts of data, but lack sensitivity of complementary methods, such as the quantitative real-time PCR (qRT-PCR). Thus, confirmation of the differential expression of genes matching our time-lapse imaging observations (transmembrane, cell surface or extracellular matrix molecules promoting survival/proliferation or block apoptosis/differentiation) was performed by qRT-PCR, prior to the molecular manipulation of the AFT024 supportive stroma.

Intron-separated (if applicable) gene-specific PCR primers were designed for each gene of interest (340 primers designed, 170 genes checked in total). For this analysis, non-irradiated AFT024 cells were compared with non-irradiated 2018. Since our *in vitro*, time-lapse data illustrated the importance of adhesion molecules, I focused on genes coding for membrane-bound and extra-cellular matrix (ECM) proteins. qRT-PCR experiments confirmed the published gene lists for the Rho, GDP dissociation inhibitor (GDI) beta (Arhgdib), transmembrane 4 superfamily member 1(Tm4sf1), plasminogen activator urokinase receptor (Plaur), vascular cell adhesion molecule 1 (Vcam1), thrombospondin 2 (Thbs2), decorin (Dcn), matrix metalloprotease 9 (Mmp9), dermatopontin (Dpt), fibroblast activation protein (Fap), collagen type VI, alpha 3 (Col6a3), transforming growth factor, beta induced (Tgfbi) and lysyl oxidase-like 1 (Loxl1), which were found to be preferentially expressed by the AFT024 stroma and showed less than 30-fold difference in expression between the two stromata (Figure 5.21A). Genes showing higher fold differences were also revealed, such as the delta-like 1 homolog (Dlk1), solute carrier organic anion transporter family, member 2a1 (Slc02a1), solute carrier family 38, member 4 (Slc38a4), biglycan (Bgn), insulin-like growth factor binding protein 6 (Igfbp6) and pentraxin related gene (Ptx3) (Figure 5.21B). To better mimic the co-culture conditions, I also analyzed irradiated stroma cells cultured for two days in modified "Dexter" media. This approach further confirmed the differentially expressed genes shown before in non-irradiated stroma cells, but revealed lower fold differences between the irradiated AFT024 and 2018.

Importantly, only approximately 20% of the published genes could be confirmed by qRT-PCR experiments as being differentially expressed between the two different stroma cell lines.
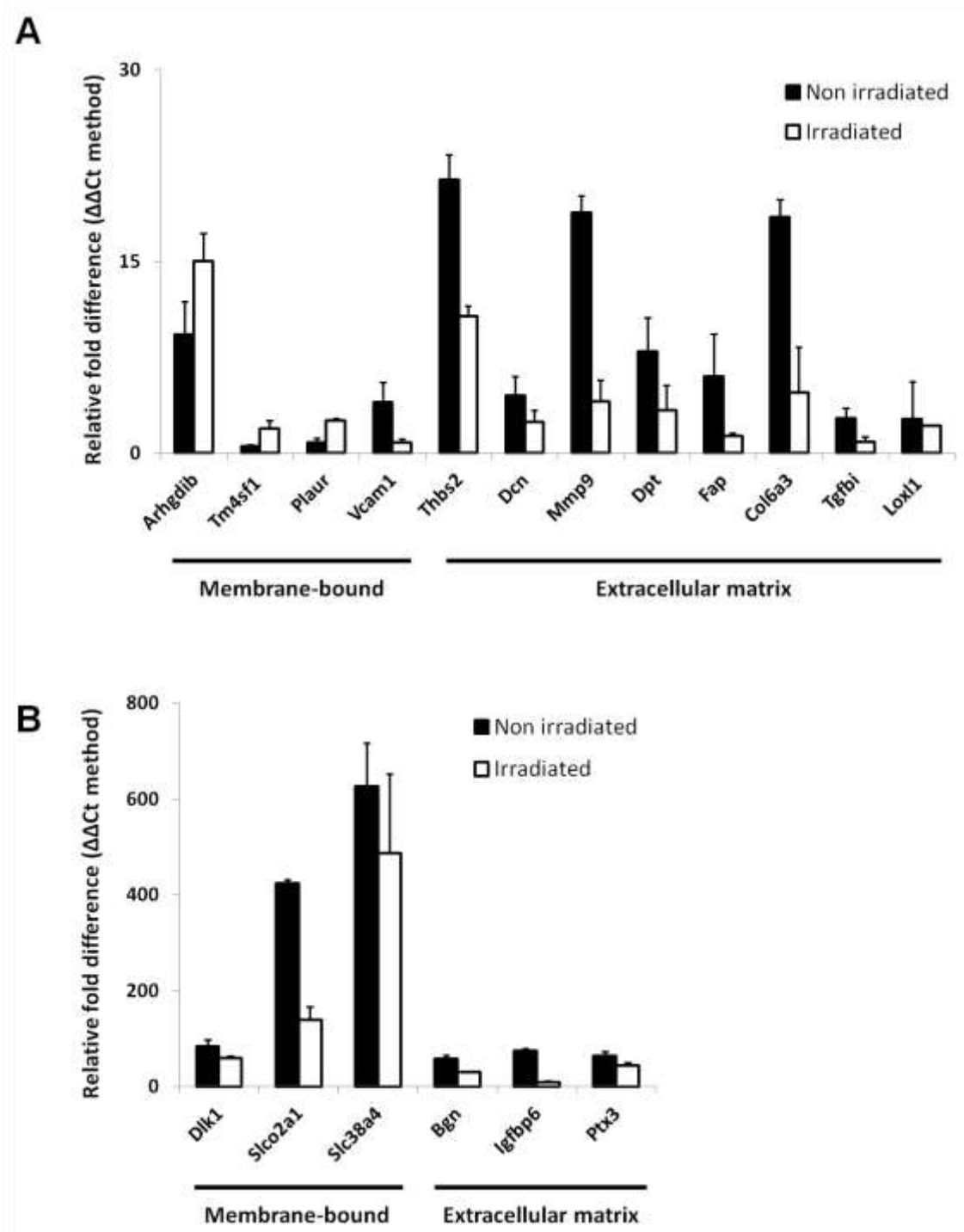
Figure 5.21. Quantitative real-time PCR analysis confirms differentially expressed genes between AFT024 and 2018 stroma. Bar graphs showing the fold difference (ΔΔCt method) in the gene expression between non-irradiated or irradiated AFT024 versus 2018 stroma, at the RNA level (n=3). Differentially expressed genes with differences between 2- and 30 fold are shown in figure A and above 30-fold in figure B. Error bars are ±S.D.

5.5.2. Gene-specific shRNAs viral constructs for stroma manipulation

The next step after confirming the differentially expressed genes, was to generate shRNA constructs targeting the relevant molecules. Since the properties of available shRNAs (knock-down efficiency, off-target effects, stability) are cell-type dependent, multiple shRNAs (four to six) were designed against each gene through the online shRNA library of the Broad Institute ("The RNAi Consortium shRNA Library"). The gene-specific shRNA sequences are provided in the Materials and Methods section. Next, shRNA oligonucleotides were introduced into lentiviral backbones and viruses expressing the shRNA of interest were generated.

5.5.3. Stroma manipulation via viral transduction with shRNA constructs

Generating stroma cells with stable expression of the viral constructs was an important step to assess the roles of selected genes on fates of co-cultured HSCs. For this reason, lentiviral vectors were implemented, in which shRNA expression was driven by the human U6 promoter (transcription via RNA polymerase III). To distinguish transduced from non-transduced stroma cells, a fluorescent reporter protein (tandem dimer TOMATO) was driven by the human phosphoglycerate kinase (PGK) promoter (Figure 5.22A). This allowed us to use flow cytometry to isolate transduced cells (co-expressing the the tdTOMATO fluorescent protein with the gene-specific shRNA). Interestingly, stroma cells were easy to transduce (Figure 5.22B), since relatively low MOIs (multiplicity of infection) of 5 to 10 already resulted in high transduction efficiency (usually higher than 75%). Importantly, stroma cells sorted for the expression of tdTOMATO maintained its expression after several passages and multiple thawing/freezing rounds (data not shown).
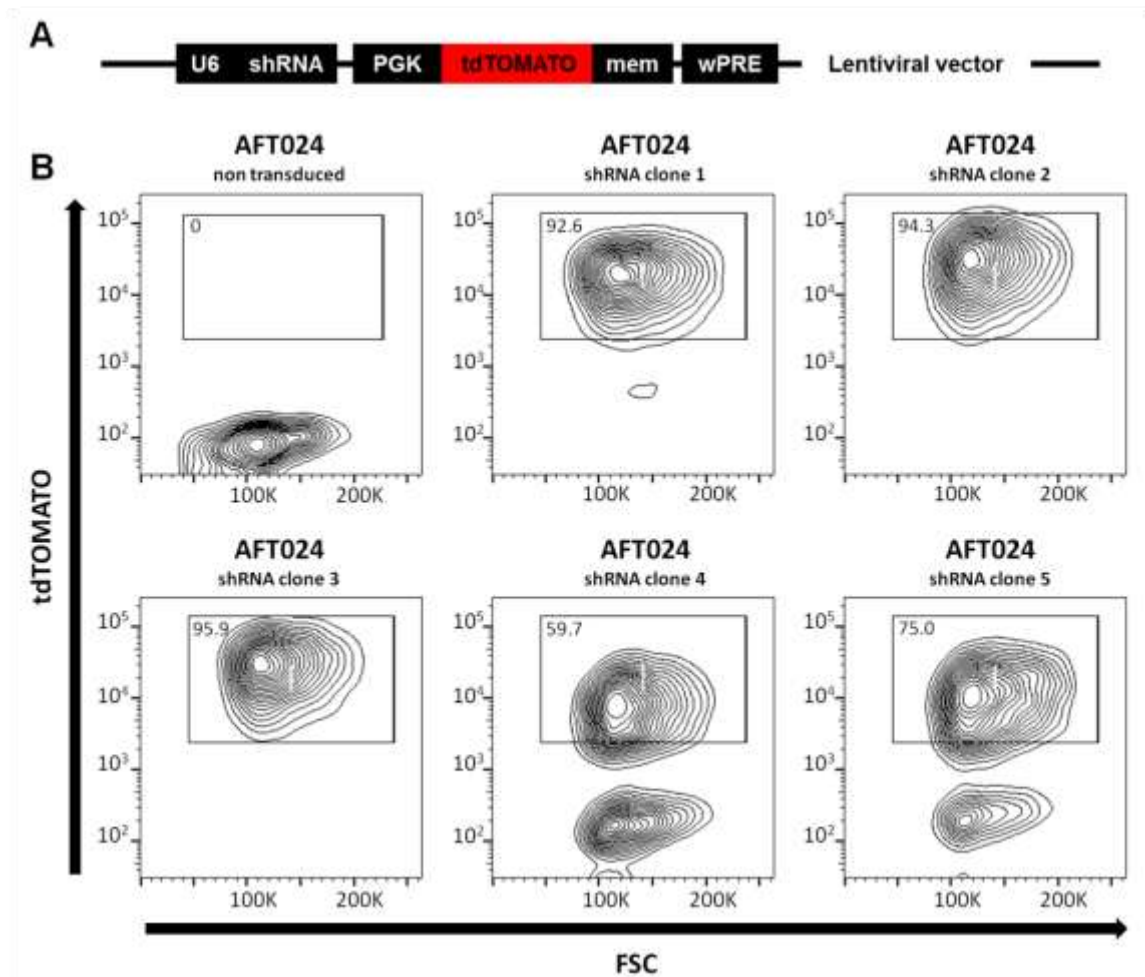
Figure 5.22. Lentiviral vectors enable robust expression of transgenes in fetal-liver derived stroma cells transduced with low MOI's. A. Schematic depiction of the viral construct used for shRNA and fluorescent-reporter expression. **B.** Flow cytometric analysis of AFT024 stroma cells transduced with different shRNA vectors at a MOI of 5. The indicated gate was used for sorting of transduced tdTOMATO positive cells.

5.5.4. Identification of the most efficient shRNA

The quantification of the knock-down efficiency of different shRNAs designed against selected genes was accomplished by flow cytometry, immunoblot or qRT-PRC analysis. Flow cytometry allows fast quantification of relative protein levels in large populations at the single-cell level. A prerequisite for such analysis is the existence of specific antibodies against the protein of interest suitable for flow cytometric analysis. Such analysis was pursued for membranes proteins (such Dlk1).

The results of the analysis of AFT024 cells transduced with shRNA constructs against DLK1 are depicted in Figure 5.23A,B. Non-transduced AFT024 and 2018 cells were used to

assess the levels of the DLK1 protein in wild-type cells. AFT024 stroma cells transduced with a scrambled shRNA control construct had no alteration in DLK1 expression. Six shRNA constructs against DLK1 were tested; the best clone reduced DLK1 expression by 11 folds (3125 versus 285 mean intensity in wild type versus transduced cells, Figure 5.23A bottom right plot and 5.23B green histogram). It is important to note that reduced DLK1 levels remained stable in the transduced stroma cells even after series of cell passages and repetitive rounds of cell freezing/thawing (data not shown).
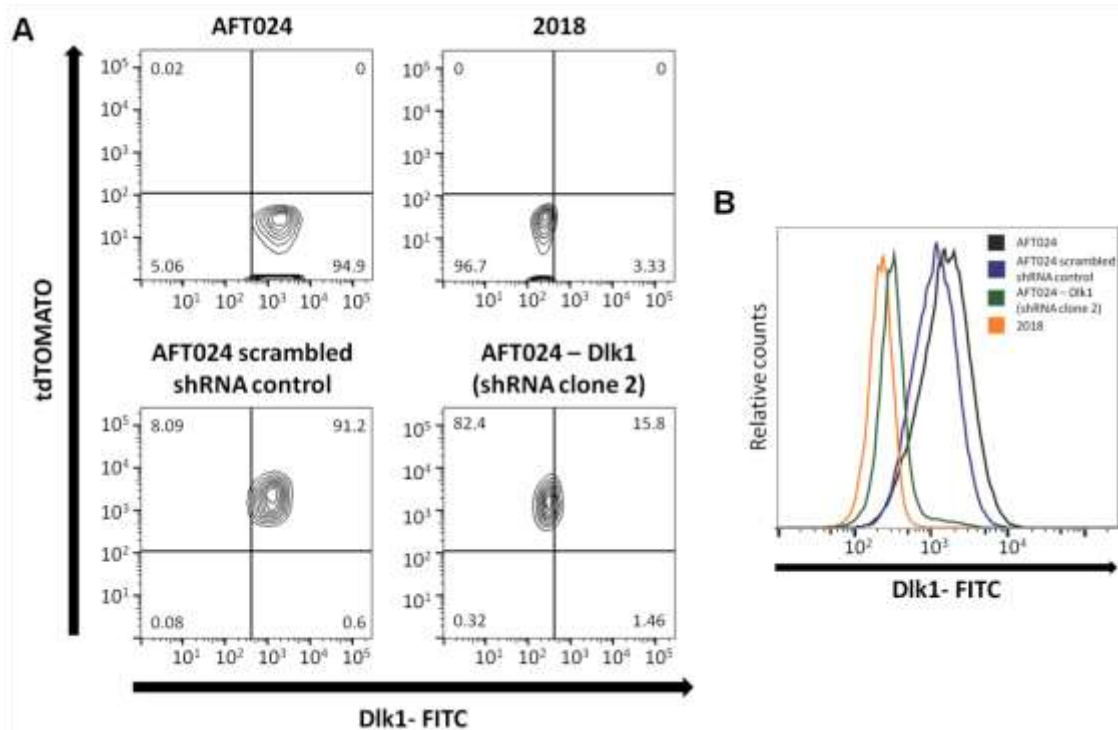
Figure 5.23. Quantification of the knock-down efficiency of different shRNA clones against delta-like homolog 1 (Dlk1). A. Density plots of wild-type, non-transduced AFT024, 2018 stroma cells as well as transduced stroma with scrambled shRNA control and one clone against DLK1 protein. Gate design was based on negative controls and the percentages of each population are shown. Thirty thousand cells were acquired for each analysis. **B.** Histogram showing DLK1 expression of the stroma shown in panel A.

In the case of DPT and FAP detection, the use of currently available FACS antibodies was problematic (minor shifts in stained sample versus unstained control, even after long incubation periods). Also, immunoblot analysis showed unspecific binding of the used antibodies (data not shown). For this reason, quantification of the knock-down efficiency of the different shRNAs against DPT and FAP was performed by qRT-PCR, in the RNA level. Such analysis has often been used to determine the efficiency of different shRNA against a gene of interest (Kim et al., 2006). In addition, qRT-PCR analysis of the shRNA clones

against DLK1 verified our previous FACS results regarding the most efficient shRNA clone (data not shown).

qRT-PCR analysis of shRNA clones against Dpt showed that stroma cells transduced with clone 3 had low relative Dpt expression (Figure 5.24A). Interestingly, clone 3 reduced Dpt expression to levels comparable to 2018 (Figure 5.24B). Similar analysis for Fap expression (Figure 5.24C) revealed that clone 2 is the most efficient leading to 95% knock down (Figure 5.24D). Further experiments were therefore conducted only with stroma cell lines transduced with the most efficient shRNA clones.
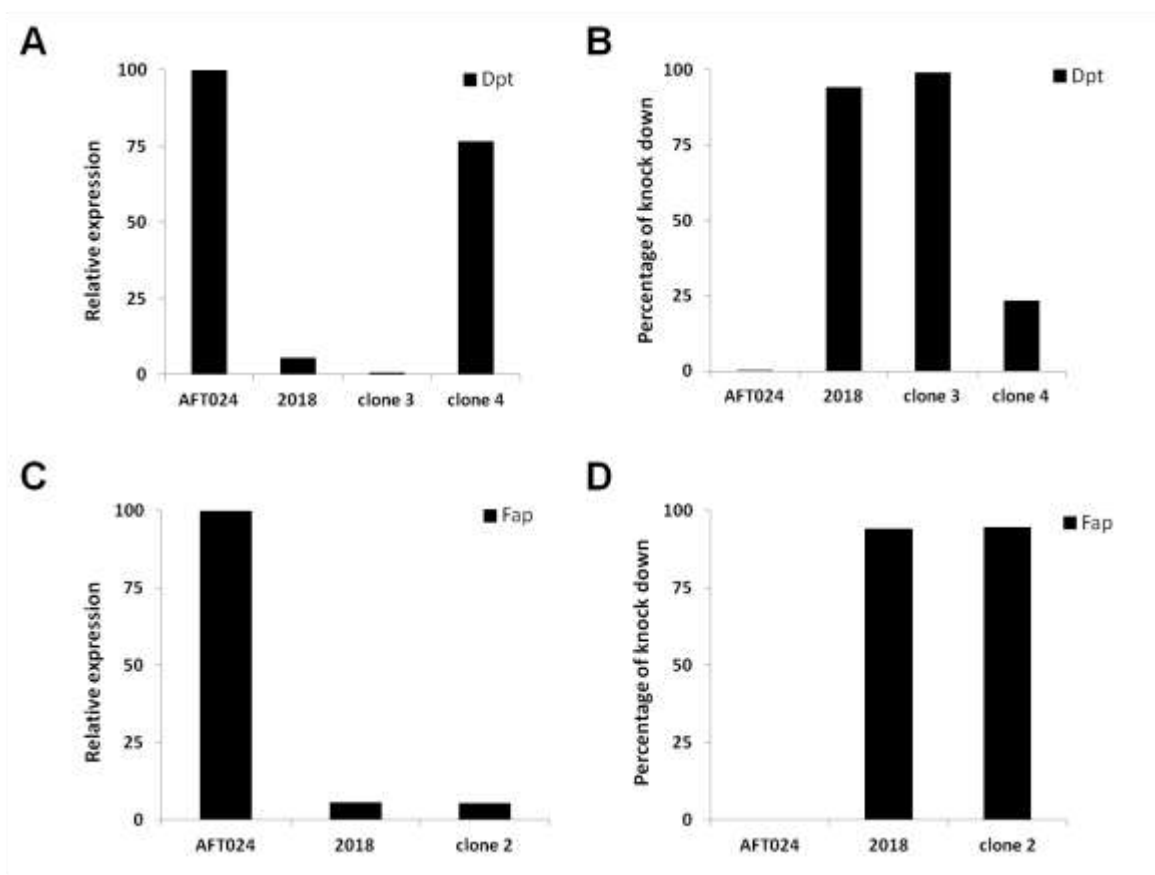
Figure 5.24. Quantification of the knock-down efficiency of different shRNA clones against dermatopontin (Dpt) and fibroblast activation protein (Fap). Bar charts showing the relative expression of Dpt (**A.**) or Fap (**C.**) and the percentage of Dpt (**B.**) or Fap knock down (**D.**) on AFT024, 2018 and AFT024 stroma transduced with virus containing different shRNA clones. Expression was normalised to GAPDH abundance. Bar graphs are the average of three technical triplicates.

5.5.5. Delta-like 1 (DLK1), dermatopontin (DPT) and fibroblast activation protein (FAP) are necessary for the AFT024-mediated survival of HSCs in Dexter-type co-cultures

Potential effects of genes found to be differentially expressed between the supportive (AFT024) and non-supportive stroma (2018) were first investigated through gene knock-down approach via gene specific shRNAs. Out of eighteen genes screened in this study, three were found important for the AFT024-mediated survival and proliferation of HSCs in Dexter type co-cultures. AFT024 stroma cells with reduced levels of delta like 1 (DLK1), dermatopontin (DPT) or fibroblast activation protein (FAP) showed reduced potential to support HSC survival in vitro. In detail, 58,6% of HSCs co-cultured with DLK1 knocked-down AFT024 stroma (DLK1^{KD}) divided compared to 82,6% in the wild type AFT024 showing a 1,4 fold reduction (Figure 5.25A). No further decrease in HSCs survival was observed upon FACS isolation of the DLK1 negative, AFT024 knocked-down cells (Figure 5.25A,"-Dlk1 sorted" column). A 1,9- and 2-fold reduction on HSCs' survival was observed upon co-culture with DPT (DPT^{KD}) and FAP knocked down AFT024 (FAP^{KD}). Interestingly, preliminary experiments revealed no additional decrease on HSC survival/proliferation upon co-culture with double knocked-down stroma (DLK1^{KD}FAP^{KD} or DLK1^{KD}DPT^{KD}). AFT024 stroma transduction with scrambled shRNA had no influence on the survival/proliferation of co-cultured HSCs (Figure 5.25A, "Scrambled shRNA" column).

Analysis of HSCs' progeny revealed that DLK1, DPT and FAP knock-down had an effect also on later generations (Figure 5.25B). These data, together with the increased levels of cell death (Figure 5.25C) suggest that knock down of specific genes in the AFT024 stroma cell line results in a non-transient impairment of HSC survival/proliferation potential.
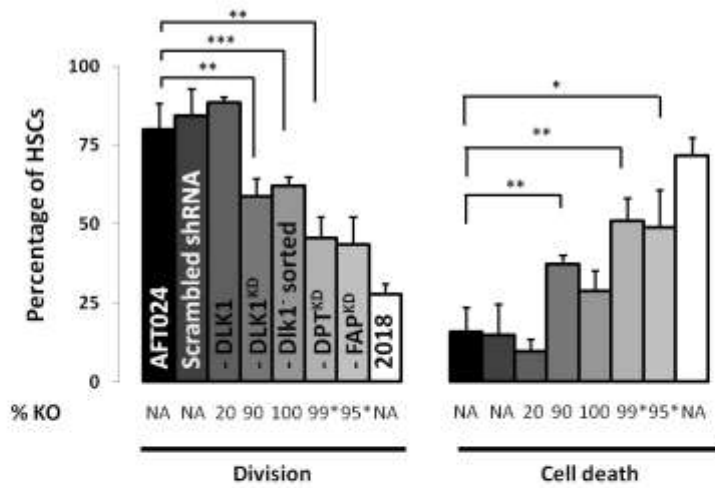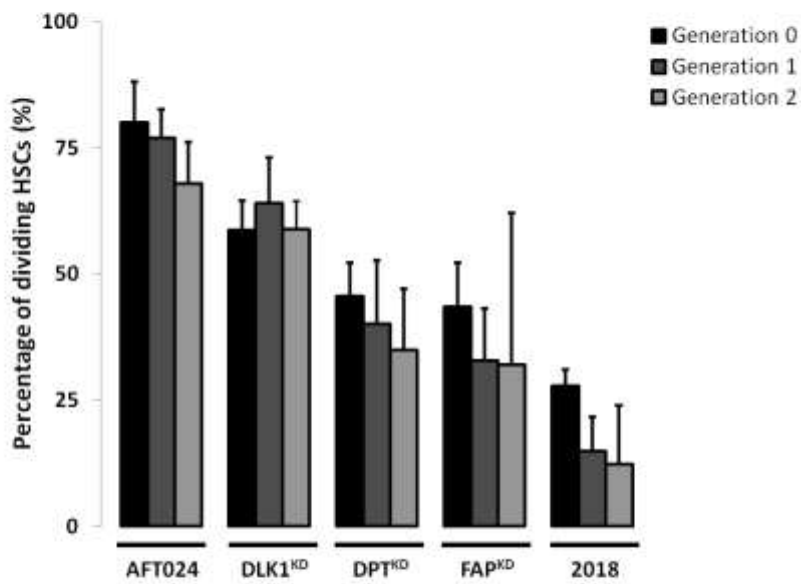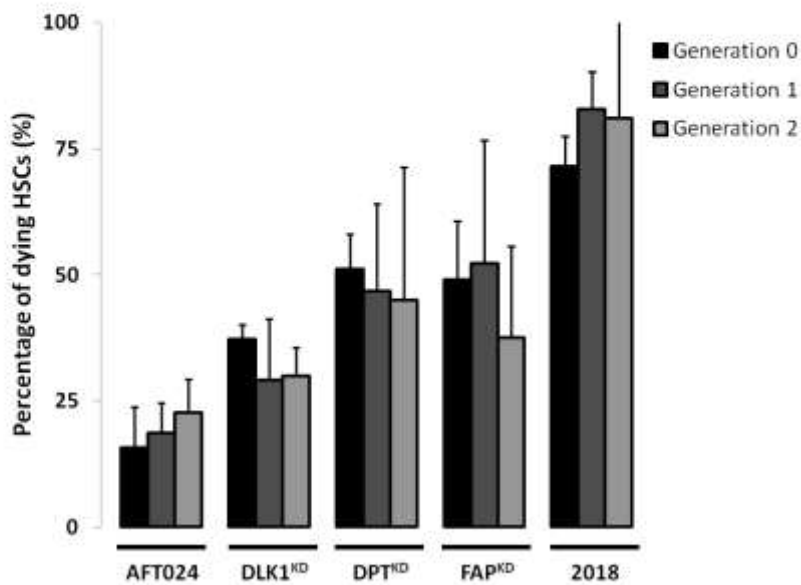
Figure 5.25. Membrane protein DLK1 and extracellular matrix proteins DPT and FAP are essential for HSC survival and proliferation in AFT024-based, Dexter-type long-term cultures. A. Bar graphs showing the percentage of dividing or dying "generation 0" HSCs upon co-culture with different stroma cell lines, such as AFT024 (7 experiments, 290 trees), AFT024 transduced with scrambled shRNA control (3 experiment, 103 trees), AFT024 transduced with shRNAaDlk1clone 1 (knock-down efficiency 20%, 3 experiments, 179 trees), AFT024 transduced with shRNAaDlk1 clone 2 (DLK1^{KD}, knock-down efficiency 90%, 4 experiments 163 trees), AFT024 transduced with shRNAaDlk1 sorted negative for DLK1 expression (knock-down efficiency 100%, 2 experiments, 55 trees), AFT024 transduced with shRNAaDpt (DPT^{KD} knock-down efficiency 99% measured by qRT-PCR in the RNA level, 6 experiments, 211 trees), AFT024 transduced with shRNAaFap (FAP^{KD} knock-down efficiency 95% measured by qRT-PCR in the RNA level, 4 experiments, 109 trees) and 2018 stroma cells (5 experiments, 264 trees). **B.** Generation-based analysis of the dividing HSCs and their progeny on co-culture with the different stroma cell lines. **C.** Similar analysis for the dying HSCs and their progeny. Error bars are ±SD.

5.5.6. Effect of stroma manipulation upon MPPs

To further investigate the specificity of the negative effect of the knocked-down AFT024 stroma upon the survival/proliferation of co-cultured HSCs, I tested the effect of manipulated stroma upon early MPPs. As mentioned in paragraph 5.2.1 (Figure 5.8A), AFT024 stroma also supports proliferation of co-cultured MPPs, since 54,5% (±6,0%) of the cells divided compared to 80,0% (±8,0%) of HSCs, in generation 0.

Comparison of the divisional rates between HSCs and early MPPs co-cultured with the DLK1^{KD} stroma (Figure 5.26) revealed a 1,4-fold decrease for HSCs (from 80,0%±8,0% to 58,6%±5,9%) and a 1,2-fold increase for MPPs (from 54,5%±6,0% to 64.1%±7,7%). Similar comparison for the DPT^{KD} stroma showed a 1,75-fold decrease for HSCs (from 80,0%±8,0% on AFT024 to 45,6%±6,5% on knocked-down AFT024) and a 4,25-fold decrease for early MPPs (from 54,5%±6,0% to 12,8%±2,6% on knocked-down AFT024). Finally, for the FAP^{KD} stroma, the divisional rates of HSCs were decreased by 1,8-fold (from 80,0%±8,0% to 43,5%±8,7%) and 1,3-fold for MPPs (from 54,5%±6,0% to 42,3%±4,3 respectively). These data suggest that DLK1^{KD} and FAP^{KD} decreased the percentage of dividing HSCs while having a minor effect upon early MPPs. In contrast, DPT^{KD} affected both HSCs and early MPPs.
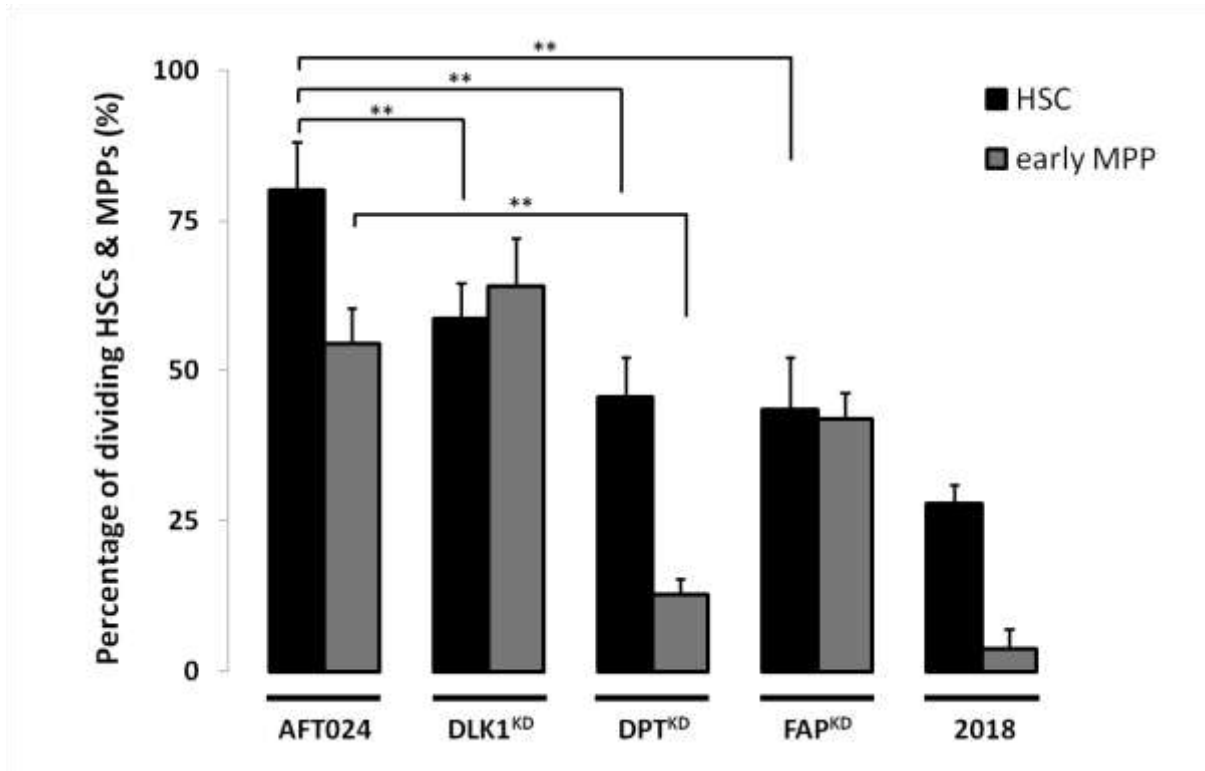
Figure 5.26. Knocked-down AFT024 stroma also reduced survival/proliferation of co-culture early progenitors (MPPs). Bar graphs showing the percentage of dividing HSCs (black bars) or early MPPs (grey bars) upon co-culture with different stroma cell lines, including knocked-down AFT024, such as DLK1[KD] (for HSCs: 4 experiments, 163 trees and for early MPPs: 3 experiments, 108 trees), DPT[KD] (for HSCs: 6 experiments, 211 trees and for early MPPs: 3 experiments, 91 trees) and FAP[KD] (for HSCs: 4 experiments, 109 trees and for early MPPs: 4 experiments, 184 trees). Error bars are ±SD. **p<0,01.

5.5.7. Over-expression or exogenous addition of recombinant DLK1, DPT or FAP robustly rescue HSC survival on 2018 stroma

Protein over-expression in non-supportive cells (2018) is a critical step to confirm the specificity of the observed effects of DLK1, DPT and FAP on HSCs survival. For this reason, 2018 cells were transduced with viral vectors containing the open reading frames of Dlk1 or Dpt (Fap is currently under construction) under the control of the human PGK promoter. Transduced stroma cells were sorted and plated in co-cultures with freshly isolated HSCs, the behavior of which was monitored over the first three generations (Figure 5.27). Viral over-expression of DLK1 ("voDLK1" column) resulted in a 1,9-fold increase of HSC survival of generation 0 cells (51,7%±7,6% versus 27,9%±3,2% on 2018). Similar results (2-fold increase) were observed from the viral over-expression of DPT upon HSC survival/proliferation (60,2%±8,9% versus 27,9%±3,2% on 2018). Interestingly, the levels of

cell divisions in the progeny of HSCs were constantly higher than the non-supporting conditions (wild type 2018), illustrating that the effect of DLK1 and DPT on HSCs survival was robust and stable over generations.

Exogenous addition of recombinant proteins was also implemented as an alternative method to investigate the role of DPT or FAP on HSC survival, without genetic manipulation of the non-supportive stroma. Addition of 5ug of recombinant mouse DPT in HSC co-cultures with 2018 ("rmDPT (5ug)" column) showed similar potential in rescuing HSC survival/proliferation (2,2-fold increase) as the viral over-expression. Interestingly, human recombinant DPT ("rhDPT (5ug)" column) was equally capable of rescuing survival/proliferation of murine HSCs (2-fold increase). Finally, preliminary experiments showed that exogenous addition of recombinant mouse FAP protein had also a positive effect of HSC proliferation ("rmFAP (5ug)" column). Importantly, the effect of recombinant proteins upon rescuing HSC survival/proliferation were maintained over future generations.
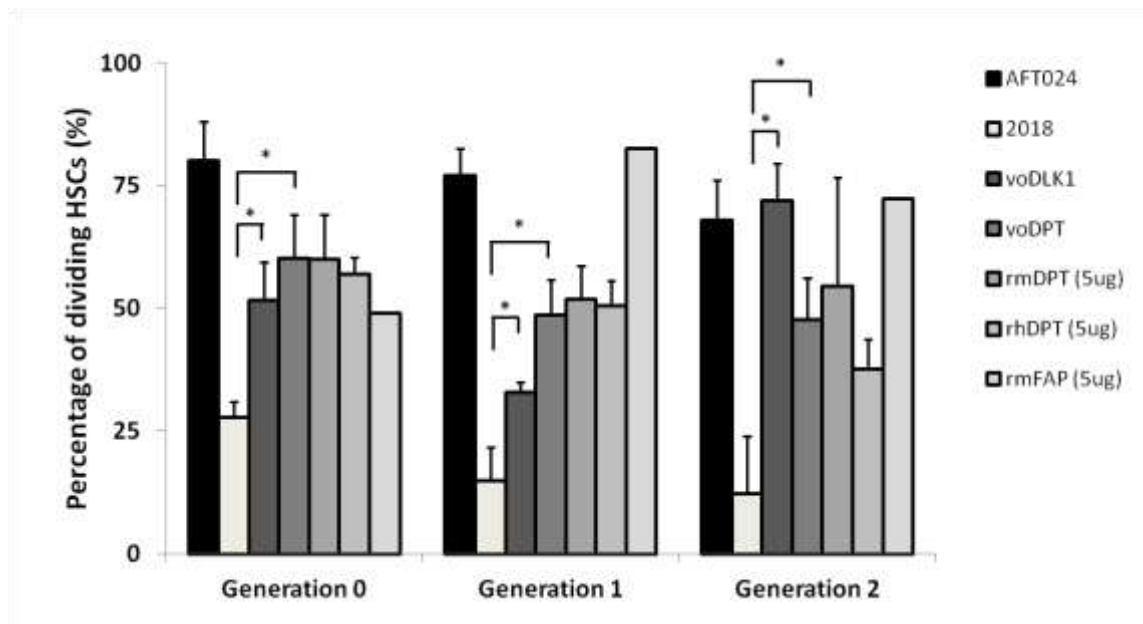
Figure 5.27. Viral over-expression or exogenous addition of DPT protein stably rescues the survival/proliferation potential of HSCs. Bar graphs representing the percentage of dividing HSCs and their progeny over different generations in co-culture with AFT024 stroma (black bars), 2018 stroma (white bars), 2018 stroma transduced with DLK1 over-expression construct (3 experiments, 69 trees), 2018 stroma transduced with DPT over-expression constructs (3 experiments, 117 trees), exogenously added mouse recombinant DPT protein (3 experiment, 115 trees), exogenously added human recombinant DPT (3 experiments, 105 trees) and exogenously added mouse recombinant FAP (1 experiment, 47 trees). Error bars are ±SD. Abbreviations are; vo: viral overexpression, rp: addition of recombinant protein.

5.5.8. Knocked down AFT024 stroma reduces the "cobblestone-area forming" and "long-term culture initiating-cell" potential of co-cultured HSCs

The data presented so far in this thesis clearly illustrate that AFT024 stroma cells with impaired expression of DLK, DPT or FAP lead to reduced levels of survival/proliferation of co-cultured HSCs. To investigate whether the reduced levels of HSCs survival leads to observable defects in HSC function/potential, I performed "cobblestone-area" and long-term culture initiating-cell (LTC-IC) in vitro assays.

The ability of HSCs to form "cobblestone-area" (CA) colonies after long-term culture is a well-established assay to retrospectively measure primitive colony forming potential (lineage and proliferation potential) as an in vitro surrogate measure for HSC potential (Ploemacher et al., 1989). Potential to form CA colonies after 4 weeks in culture correlates with in vivo repopulating potential as tested by transplantation experiments (Van der Sluijs et al., 1990; Ploemacher et al., 1991). In addition, executing CA forming-cell (CAFC) assays in a limiting-dilution mode can reveal the frequency of cells with CA-forming potential.

For these reasons, specific dilutions of HSCs were directly sorted in 96-well plates coated with different stroma cell lines and their ability to form CA colonies after six weeks in culture was monitored (Figure 5.28A). 38,9%±9,6% of the initially sorted HSCs produced CA colonies after a 6-week culture with AFT024, whereas the respective percentage for the 2018 stroma was only 5% (5,1%±0,7%) (Figure 5.28B). Interestingly, HSCs co-cultured with knocked-down stroma revealed reduced levels of CA forming potential, since only 15,9%±7,1% (2,5-fold reduction) of HSCS cultured in DLK1^{KD}, 5,1%±2,3% (7,6-fold reduction) HSCs cultured in DPT^{KD} and 15,6%±6,3% HSCs cultured on FAP^{KD} stroma showed CA potential (Figure 5.28B). These results confirm our hypothesis that the reduced survival/proliferation of HSCs in knocked-down stroma leads to impaired HSC potential.
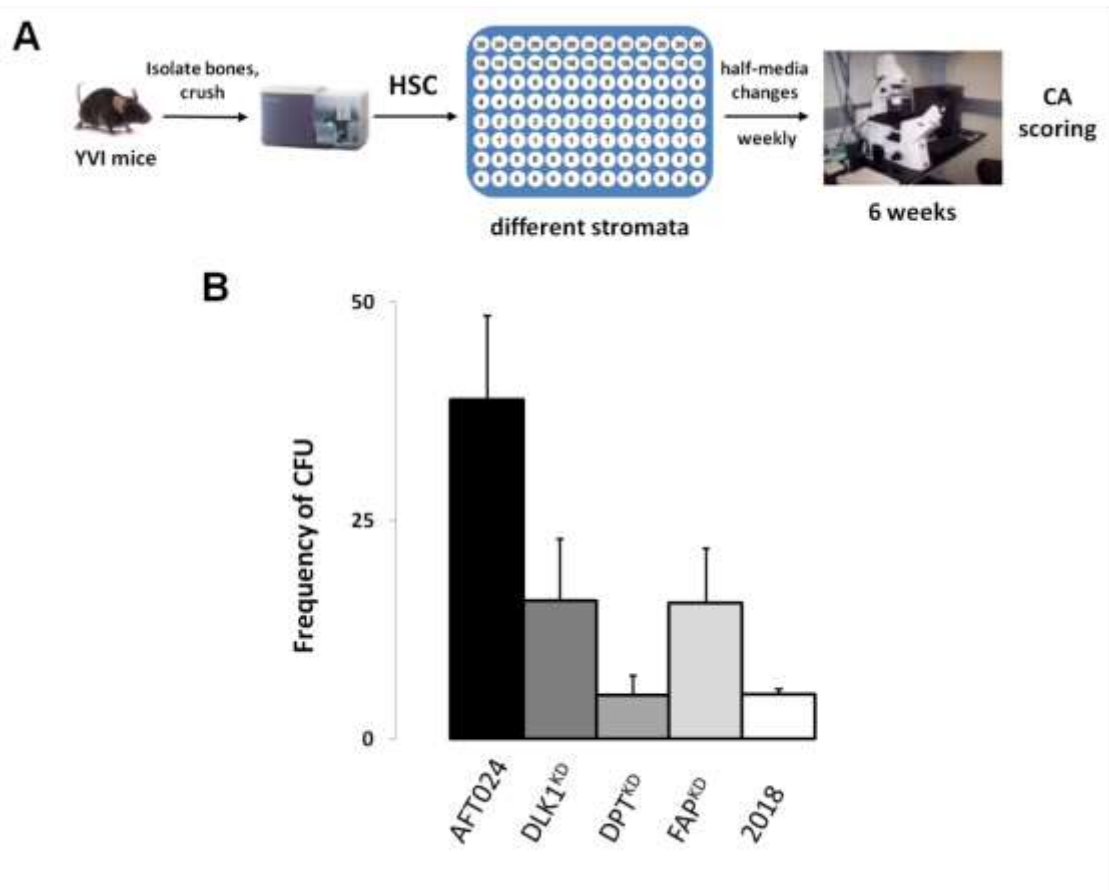
Figure 5.28. HSPs have reduced potential of forming cobblestone-area colonies after co-cultured with knocked-down AFT024 stroma. A. Schematic representation of the experimental approach for the cobblestone-area forming cell (CAFC) assay. Different doses of freshly purified HSC or early MPP cells were directly sorted into 96-well plates on top of different stroma cell lines. Co-cultures were continued for six weeks, with weekly half-media changes. At the sixth week, individual wells were scored for the presence of cobblestone areas and statistics were used to calculate the respective frequencies of cobblestone-forming units (CFU) in the initial population. **B.** Bar graphs representing the frequencies of HSCs with CAFC potential after co-culture with different stroma conditions (3 experiments). Error bars are ±SD.

To further confirm the link between HSC survival/proliferation and HSC potential, I also performed long-term culture initiating-cell (LTC-IC) assays, a more stringent assay for HSC function. Like in CAFC assays, the potential of cells to generate LTC-IC colonies correlates well with their repopulating potential in in vivo transplantation experiments (Cho and Müller-Sieburg, 2000). To do this, single HSCs were directly sorted in 96-well plates on top of different stroma cell lines. After six weeks of co-culture with weekly half-media changes, cells were placed on semi-solid, methylcellulose media and scored after an additional period of two weeks (Figure 5.29A). Approximately 50% of the HSCs cultured on AFT024 stroma (49,3%±17,7%) versus 21,1%±11,7% on 2018 stroma showed LTC-IC potential. The LTC-IC potential of HSCs co-cultured with knocked-down stroma was again

reduced, with 19,8%, 41,7% and 30,8% of HSCs scored positive upon co-culture with DLK1^{KD}, DPT^{KD} or FAP^{KD} stroma respectively (Figure 5.29B, left panel). These results further confirm that reduced DLK1, DPT or FAP expression levels in the AFT024 stroma has a negative effect upon HSC function.
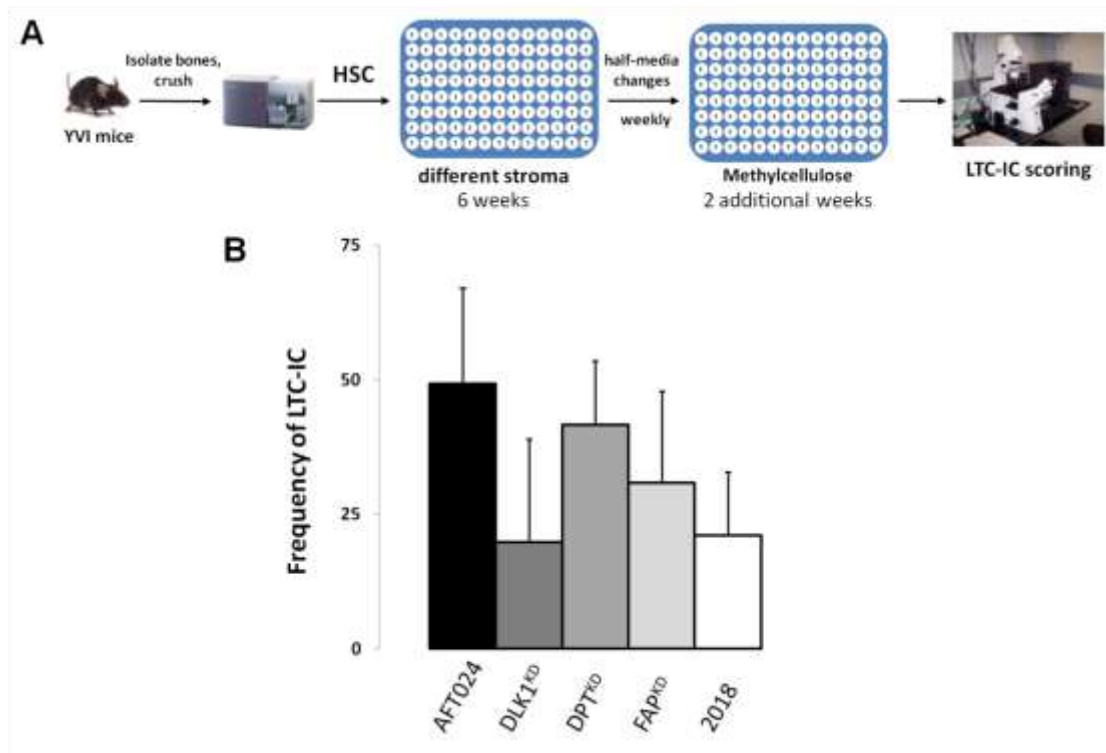
Figure 5.29 HSPs have reduced potential for forming long-term culture initiating-cell colonies after co-culture with knocked-down AFT024 stroma. A. Schematic representation of the experimental approach for the long-term culture initiating-cell (LTC-IC) assay. Single HSC cells were directly sorted into 96-well plates on top of different stroma cell lines. Co-cultures were continued for six weeks, with weekly half-media changes. After six weeks, individual wells were placed in methylcellulose semi-solid media and were scored for the presence or absence of colonies (wells with >25 cells were scored as positive) after two additional weeks. **B.** Bar graphs representing the frequencies of HSCs (left panel) or early MPPs (right panel) with LTC-IC potential after co-culture with different stroma (3 experiments). Error bars are SD.

5.5.9 DPT is essential for HSC maintenance in vitro

It is important to note, however, that the results from the CAFC and LTC-IC in vitro assays may emanate from the impaired ability of the knocked-down stroma itself to support the outgrowth of colonies, instead of a direct effect on HSC potential. In any case, the ultimate method required to show whether DLK1, DPT or FAP are essential for the in vitro

maintenance of HSCs is the in vivo transplantation experiments. For this reason, different doses of HSCs from CD45.1 mice were co-cultured with the different stroma cell lines for 7 days. Then, their progeny was transplanted (together with the surviving stroma cells) into sub-lethally irradiated CD45.2 recipient mice (Figure 5.30A).

The analysis of the peripheral blood from the CD45.2 recipient mice revealed a dose-dependent effect in their chimerism, since the progeny of 100 (CD45.1) HSCs co-cultured with AFT024 stroma led to 1% contribution, the progeny of the 350 HSCs to 24,5%±4,1% and the progeny of 1250 HSCs to 53,4%±5,9% (Figure 5.30B). Similar dose-dependent contribution effects were also observed in the other co-cultures. HSCs co-cultured with 2018 stroma gave low contribution, since the progeny of 100 HSCs gave 1,6%±1,8%, the progeny of 350 cells 1,2%±1,6% and the progeny of 1350 HSCs 9,6%±6,9%. The chimerism in recipient mice transplanted with cells co-cultured with DLK1^{KD} or FAP^{KD} stroma was slightly lower compared to the AFT024 controls. However, mice transplanted with cells co-cultured with DPT^{KD} stroma showed approximately 2,5-fold lower percentage of chimerism (10,4%±1,0% versus 24,5%±4,1% in the control for the 350 cell dose and 20,5%±11,7% versus 53,4%±5,8% in the control for the 1250 cell dose) (Figure 5.30B). These results illustrate that DLK1 and FAP have minor effects, whereas DPT is essential for the in vitro maintenance of HSCs under AFT024-based co-cultures in vitro. It is important to note that the percentage of chimerism has to be calculated also in later timepoints (16-24 weeks) in order to further support our findings.
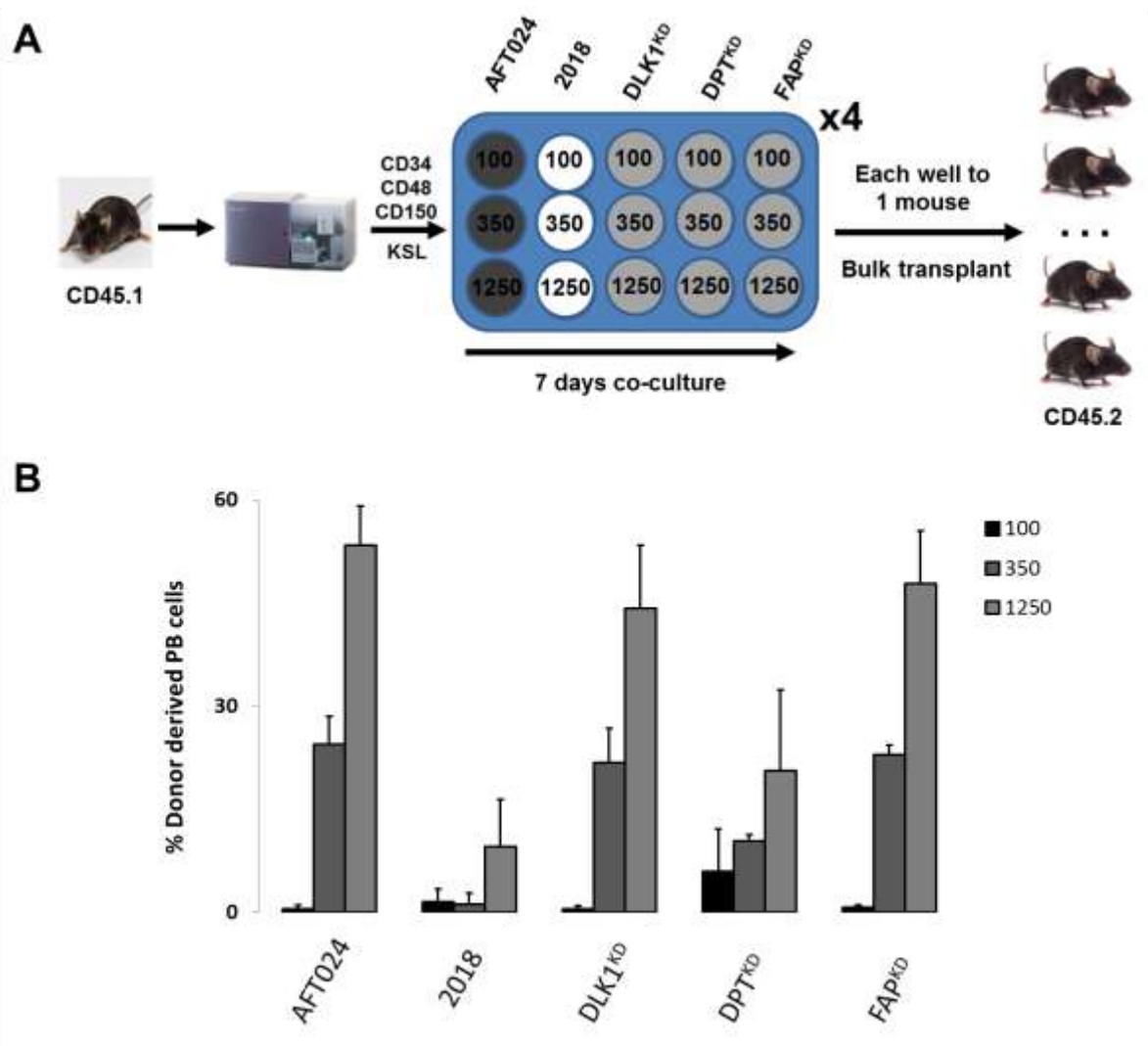
Figure 5.30 DPT is essential for the in vitro maintenance of HSCs. A. Schematic representation of the experimental approach. CD45.1 HSCs were isolated through flow cytometry and co-cultured with different stroma cell lines in different cell numbers (100, 350 and 1250 starting HSCs). After seven days of co-culture, the content of each well was transplanted into a CD45.2 sub-lethally irradiated recipient. Each dose/condition was conducted in quadruplicates. **B.** The peripheral blood (PB) of recipient mice was analyzed for the presence of CD45.1+ cells, twelve weeks after the transplantation. The bar graphs show the percentage of the PB donor contribution per condition. Error bars are ±SD.

5.5.10 DPT's expression in the bone marrow of adult mice

Despite the fact that the purpose of this study is to identify molecules promoting HSC maintenance in vitro, I sought to investigate the presence of DPT in the in vivo, bone-marrow niche. Current methodologies include cryo-sections of bone fragments which inevitably distort cell morphology and architecture. To circumvent this limitation, 100μm thick sections from decalcified femurs were isolated and bone-marrow sections were stained for DAPI,

CD150, CD31 (blood vessels), Dpt and a cocktail of lineage antibodies (a method developed in collaboration with Daniel Coutu, PhD.). The epiphysis, growth plate and metaphysis of the bone were visible in those sections. Combination of CD150 expression and lineage markers allowed us to identify CD150+Lin- cells (HSCs) (Kiel et al., 2005). Our analysis revealed that DPT expression in the adult bone marrow is localized to blood vessels, differentiated blood cells (megakaryocytes) and to bone surfaces (Figure 5.31). However, only few CD150+Lin- cells were found adjacent to DPT expressing cells.
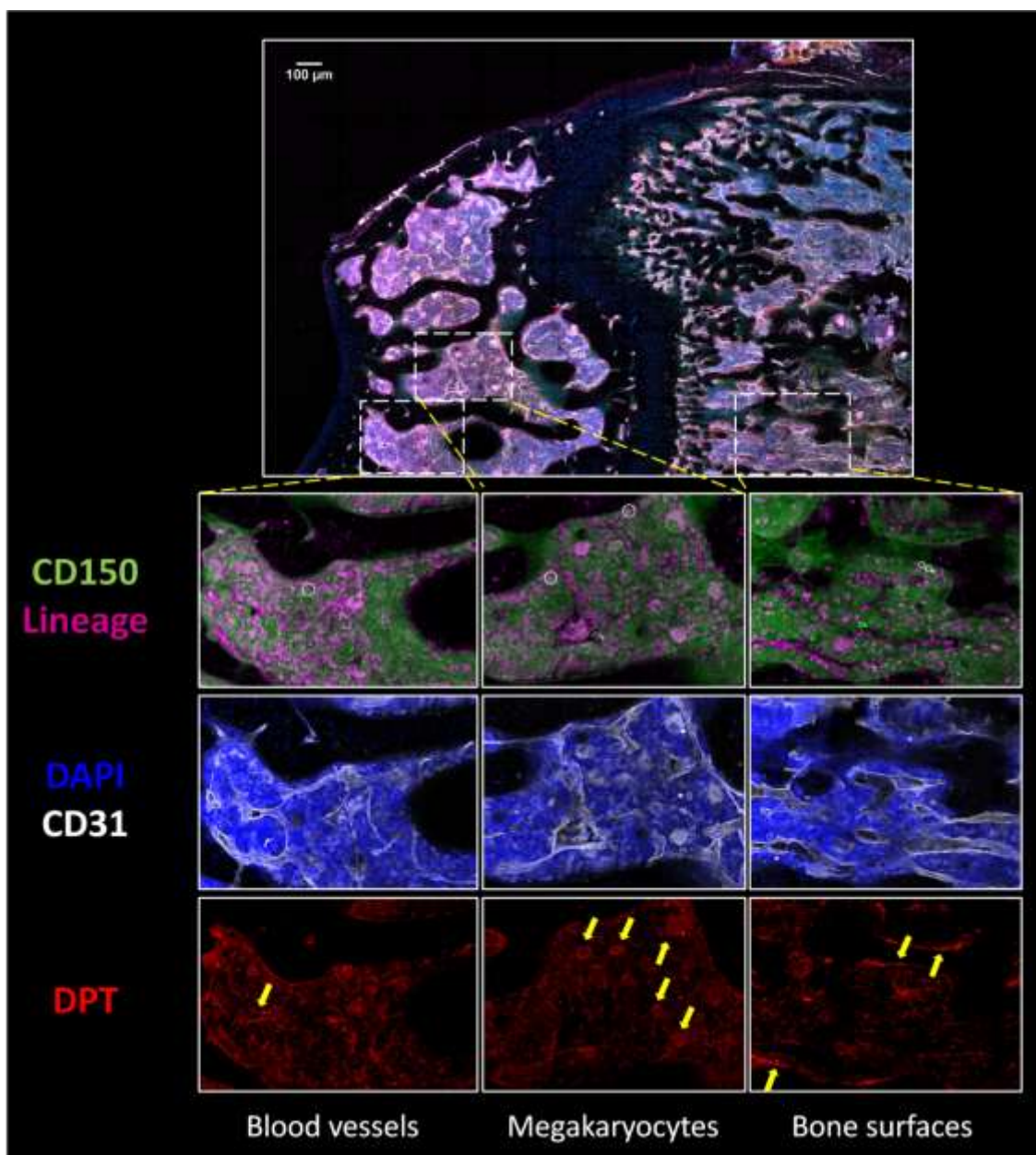
Figure 5.31 Dermatopontin's expression in the in vivo bone-marrow niche. Bone-marrow sections of murine femur (100μm) were stained for CD150 (green), DAPI (blue), CD31 (white), Dermatopontin – Dpt (red) and a cocktail of different lineage markers for HSC identification (CD4,

CD8, CD41, CD48, CD34, Mac1, Gr1 - magenta). The upper panel shows the 3D-projection of the entire imaged area. In the panels below, CD150 and lineage markers are shown together to allow identification of CD150+Lin- cells (white circles), while DAPI and CD31 show the nucleus of individual cells as well as blood vessels. In the last panel, DPT expression is observed in different parts of the bone marrow, such as in blood vessels, megakaryocytes and bone surfaces (yellow arrows).

6. Discussion

Culturing HSCs ex vivo results in loss of their potential. They fail to self-renew and repopulate the blood system of mouse recipients upon transplantation, especially when cultured in stroma-free conditions (Ema et al., 2000). The current inability to maintain stemness of HSCs ex vivo hampers their clinical application. To circumvent this limitation, many groups since decades focus on the establishment of culture conditions capable of HSC maintenance or expansion. Indeed, several culture systems have been identified to robustly maintain stemness of HSCs, upon co-culture with stroma cell lines (Moore et al., 1997a; Oostendorp et al., 2002; Shimizu et al., 2008). Among those systems, the fetal-liver derived stroma cell line AFT024 has been reported to qualitatively and quantitatively support long-term self-renewal of co-cultured HSC for culture periods of up to 6 weeks (Moore et al., 1997a). Since the molecular profile of this supportive stroma cell line has been identified through subtractive libraries and microarray analyzes (Hackney et al., 2002; Charbord and Moore, 2005), AFT024 stroma is a unique tool to investigate the key factors supporting HSC maintenance in vitro. In addition, AFT024 stroma has been used by many groups over the years for the maintenance of human HSCs (Thiemann et al., 1998; Punzel et al., 1999b, 2002; Lewis et al., 2001; Nolta et al., 2002; Hutton et al., 2006). Here, we provide new insights into the molecular mechanisms governing the maintenance of single HSC by continuous time-lapse imaging (Schroeder, 2008, Schroeder, 2011; Eilken et al., 2009; Rieger et al., 2009). This allowed to dissect the heterogeneous HSC population by analyzing single cells individually over time and to reveal key molecules responsible for the reported HSC maintenance in AFT024-based co-cultures.

6.1 Continuous time lapse imaging allows reliable long-term single-cell observation of the fates of HSCs and their progeny

Continuous observation is indispensable when studying dynamic biological processes, such as the behavior of living cells. Depending on the culture conditions and the cell type, cultured cells may follow different cell fates in vitro. Division of initially plated cells may lead to increased cell numbers and eventually single-cell identity and history will be lost. At the same time, the total number of cells may stay the same or only change slightly depending on the number of dying cells of the starting population. As an example, Moore and colleagues showed that the numbers of HSCs can be maintained when co-cultured with the AFT024 stroma, over long culture periods. Without single-cell observation, however, opposing interpretations could be used to explain the observed HSC behavior: increased levels of cell division and/or reduced levels of cell death and/or quiescent/senescent cells that survive without division could lead to the same output. Published studies are mostly snapshot analyzes conducted on the population level or time-lapse imaging with low temporal resolution (Punzel et al., 2003), thus fail to provide single-cell data. On the other hand, studies with single-cell resolution (single cells plated on different wells of multi-well dishes) often fail to follow the fates of "generation 0" cells and their progeny over long culture periods (Kent et al., 2008; Sekulovic et al., 2011). Unraveling the biology behind such events requires a live-cell imaging method with short time intervals and post-acquisitional reconstitution of cellular history and genealogy.

The imaging method established in the Schroeder group allows continuous monitoring of single cells with high temporal resolution over 2 weeks in vitro. This approach allowed to quantify the number of initially plated HSCs (generation 0 cells) and to follow their different fates (cell division, cell death, survival without any division) upon co-culture with different types of stroma cells. Fates of the HSC progeny could be monitored for two weeks of culture. In this timeframe, cells from different generations can be followed (tracked) with high resolution and low error rates (loosing identity and mixing cells coming from different "founder"). Another critical advantage of such high temporal resolution, single-cell imaging is the ability to define with high sensitivity the kinetics of the different cell fates. Thus, the exact time between the beginning of the co-culture and the fate of each single cell (division or death) could be determined. Through this approach, HSC behavior under maintenance conditions could be identified and also brings new insights into the behavior of in vitro culture of murine, bone-marrow derived HSCs cultured on AFT024 stroma.

6.2 Dexter-type AFT024-based co-cultures support HSC maintenance by preventing early cell death of murine HSCs

As mentioned above, ex vivo culture of HSCs leads to progressive loss of stemness resulting in reduced repopulation potential upon transplantation into irradiated recipients. According to the current notion in the field, cell death and/or differentiation of cultured HSCs are the main reasons for the reported loss of stemness and subsequent reduced repopulation capacity. However, currently there is no direct evidence linking early cell death with loss of stemness.

Here we report that the most striking difference between HSCs cultured under supportive (AFT024) or non-supportive (2018, BFC012) conditions in vitro was the early survival rate of HSCs. Freshly purified CD34-CD48-CD150+KSL murine cells cultured directly after isolation, showed significantly higher levels of survival/division on the AFT024 stroma (80,0%±8,0%) compared to 2018- or BFC012-based cultures (27,9%±3,2% and 20,6%±5,2% respectively). In non-supportive conditions, the majority of CD34-CD48-CD150+KSL cells died (71,6%±5.8% on 2018 and 78,8%±4,2% on BFC012), during their initial generation ("generation 0" cells). Notably, co-cultures with the 2012 stroma, a stroma supporting intermediate levels of repopulating cells, resulted in intermediate levels of HSCP survival/proliferation. These results show for the first time that the capacity of fetal-liver derived stromata to maintain repopulating cells is linked with the initial survival/proliferation rates of co-cultured HSCs. Therefore, our analysis provides evidence that cell death is a major reason for the loss of stemness of mouse HSCs cultured under non-supportive conditions.

Due to the high temporal-resolution of image acquisition, the cell-fate kinetics (experimental time until division or cell death) of HSCs and their progeny were monitored with high precision. Our data clearly demonstrate that differences in the HSC behavior appear early after the initiation of the culture; within the first 7 days of the co-culture >94% of the cells either divide or die (Figure 4.6, Results section). This is significantly shorter when compared with the conventional methods, which require 4 week of co-culture prior to the laborious/time-demanding transplantations which last for at least 16 additional weeks. Therefore, the time-lapse based, co-culture system described here constitutes a high-sensitivity and fast system to readout differences in HSC behaviors in vitro.

High temporal resolution image acquisition and subsequent single cell tracking enabled us to precisely "reconstruct" the history of single cells and their progeny by generating representative cellular pedigrees. Thus, we could expand our cell-fate analysis also to later generations. Interestingly, monitoring the fates of the HSC progeny (later cell generations) revealed that the levels of division/survival on AFT024 and cell-death rates on 2018/BFC012 stroma were constant over the first three generations. This suggests that the effect of the micro-environment is stable at least for the first three generations in vitro. To our knowledge, this is the first report providing such detailed analysis of the cell fates of murine HSCs under Dexter-type, long term culture, while highlighting the unique behavior of HSCs under self-renewing conditions.

The behavior of human HSCs co-cultured with AFT024 stroma had also been analyzed. As mentioned in paragraph 3.4.2.3, murine AFT024 stroma has also been reported to maintain human HSCs (Thiemann et al., 1998; Punzel et al., 1999b; Nolta et al., 2002). Snapshot analysis of human umbilical cord blood (UCB) CD34+CD38- cells co-cultured with murine AFT024 revealed similar levels of "generation 0" cells undergoing division (84,4% ± 4,8%), quiescence/senescence (3,1% ± 0,8%) or cell death (13,9% ± 1,8%) (Punzel et al., 2003). However, Punzel and colleagues provided no data for the behavior of human HSCs under non-supporting conditions, in order to pinpoint potential differences in the proliferation/survival rates. Also, due to the low temporal resolution of their imaging (acquisition every 12-24 hours), the kinetics of the reported behaviors could not be precisely defined. Earlier studies implementing time-lapse imaging with intermediate temporal resolution (3 to 12-hour intervals) reported that the majority of CD34+CD38- human HSCs divided within the first 36 to 38 hours after culture initiation (Huang et al., 1999). Nevertheless, those cells were cultured in stroma-free conditions and their divisional history was based on the intensity of the PKH26 dye (decreasing brightness following cell division) rather than continuous tracking at the single cell level. Again, no comparison with non-supportive conditions was performed in order to reveal the time frame when potential differences take place.

Despite the fact that no direct comparison can be made between the two systems due to different culture conditions and species variation, we report that murine HSCs have a similar behavior as human HSCs at least for the initial generation under self-renewing conditions, since the majority of cells survive and proliferate in both scenarios. These results illustrate the potential value of the results of our study for clinical applications.

6.3 AFT024-based co-cultures also support survival/proliferation of multipotent progenitor cells

Current HSC isolation approaches result in impure cell populations. Transplantation experiments revealed that the HSC purity of current sorting schemes is approximately 50-60%, meaning that only half of the cells sorted for a stem-cell immunophenotype have stem cell function (Kent et al., 2009). This suggests that the current knowledge for stem-cell markers is limited and identification of additional, more specific markers is a prerequisite for HSC isolation with higher purity. It is currently challenging to characterize the remaining 50% of the contaminating cells which are sorted as stem cells, but fail to read out as such.

Since half of the sorted 'HSCs' have to be assumed not to be stem cells, but possibly some type of early progenitors, we sought to investigate the effect of the Dexter-type, long term culture also upon MPPs. Such analysis would reveal the specificity of the observed AFT024-mediated pro-survival effect upon co-cultured hematopoietic populations. It is important to note that different types of MPP populations have been reported. Based on their reconstitution potential, cell-cycle status and immunophenotype, Wilson and colleagues reported a putative hierarchy of different populations of MPP cells within the KSL cell compartment (Wilson et al., 2008). According to that hierarchy, the most primitive population of cells with the higher repopulation potential are the CD34-CD48-CD150+CD135- KSL cells (HSCs). This is mainly the immunophenotype followed in the current study for HSC isolation, since the vast majority of CD34-CD48-CD150+ KSL are also CD135- (data not shown). In MPPs, CD34 is the first marker which turns on distinguishing them from stem cells (CD34+CD48-CD150+CD135-KSL were called MPP1) with CD48 being the next (CD34+CD48+CD150+CD135-KSL were called MPP2). Later, CD150 expression is lost (CD34+CD48+CD150-CD135-KSL were called MPP3) while CD135 finally turns on (CD34+CD48+CD150-CD135+KSL were called MPP4). In the current study, we used a slightly different combination of marker expression to isolate early MPPs (CD34+CD48-CD150-KSL) and followed Wilson's protocol for late MPPs (CD34+CD48+CD150-KSL).

Our analysis of "generation 0" cells showed a cell type-dependent support of the observed survival of hematopoietic populations, in the AFT024-based cultures. As mentioned previously (section 6.2) the majority of primitive HSCs in generation 0 divided (80,0%±8,0%). Almost half of the early MPPs divided in co-cultured with the supportive

stroma (54,4%±6,0%) compared with only one fifth of the late MPPs (18,6%±16,8%). Analysis of later generations revealed similar levels of cell division between HSCs and different MPP populations (around 75%) suggesting that after an early selection, the surviving cells are stably supported by the AFT024 stroma. This is the first demonstration, to our knowledge, that AFT024-based cultures affect cell fates based on the primitiveness of the co-cultured adult stem and progenitor cells. The positive effect of the AFT024 co-cultures upon more committed progenitors (colony forming unit-high proliferative potential mix-lineage colonies, CFU-HPP-Mix and pro-b cell progenitors) has already been reported, since both types of progenitors could be expanded under the same culture conditions (Moore et al., 1997a). However, the reported effects were observed in fetal-liver derived murine HSCs. In the human system, the reported purity of the sorted CD34+CD38-Lin- HSCs is below 1%. It is logical to assume that the majority of the surviving cells reported by Punzel and colleagues upon co-culture with the AFT024 stroma (Punzel et al., 2003), were progenitors rather than stem cells. Therefore, the positive effect of the AFT024 stroma upon progenitor cells could be also extended in the human system.

Taken together, these findings regarding the support of both murine and human stem/progenitor cell populations on AFT024-based cultures are of potential clinical relevance. From transplantations conducted in the murine system, it is known that multipotent and committed progenitors are important for the short-term reconstitution of the blood system of the recipients, due to their short cell-cycle status. On the other hand, primitive HSCs are mainly quiescent and require long periods before generating differentiated blood cells. A culture system, supporting both stem and progenitor cells can be extremely valuable for subsequent transplantation experiments (or potentially for bone marrow transplantation in case of human patients), since it facilitates both short- and long-term blood regeneration.

6.4 Direct contact is necessary for the survival of HSCs co-cultured with the AFT024 stroma

After revealing the unique behavior of HSCs under supporting conditions, we sought to investigate the relevant molecules responsible for this interaction. To efficiently filter through the published list of genes preferentially or exclusively expressed in the AFT024 stroma (Hackney et al., 2002; Charbord and Moore, 2005), I investigated whether adhesion molecules or secreted factors are responsible for the observed interaction between HSC and

stroma cells. This list (containing around 1000 genes) can be subdivided into three categories: i. genes coding for membrane, adhesion or extracellular matrix proteins (requiring cell-cell contact), ii. genes coding for secreted factors and cytokines and iii.transcription factors or proteins of the cytoskeleton. Since I was interested in the interaction of the stroma cells with co-cultured cells, the adhesion and the secreted genes were the main focus of this study. Revealing the underlying mechanism governing the interaction between the AFT024 stroma and the HSCs would allow efficient screening of molecules with desired properties from the entire gene list.

It is important to note that currently there are no available data deciphering whether direct contact or secreted factors are responsible for the maintenance of mouse HSCs by the AFT024 stroma. Interestingly, studies attempting to reveal the nature of the interaction using human HSCs led to contradictory results. Initially, work from the Crooks group showed that human bone marrow- or cord blood-derived CD34+CD38- cells could be maintained only in direct contact with the AFT024 stroma, since non-contact cultures failed to do so (Thiemann et al., 1998). This observation, based on cobblestone-area forming cell assay and immunophenotypic analysis of cultured cells, was later confirmed by transplantation experiments using a xenograft mouse model (Nolta et al., 2002). At the same time, the group of Catherine Verfaillie further confirmed that AFT024 maintain human HSCs through direct contact, while identifying large-size O-sulfated heparan sulfate as one of the molecules responsible for the observed interaction (Punzel et al., 2002). This finding contradicted earlier results from the Verfaillie group in which stroma non-contact cultures supplemented with a cytokine cocktail (FL, SCF, IL-7) were sufficient to maintain human umbilical cord blood HSCs for at least 7 days capable of engrafting in the NOD/SCID mice (Lewis et al., 2001). In the same study, they also reported a stroma-free culture system (FCS, G-CSF, MIP-1a, IL-6, MCP-1, VEGF, IL-8, N-desulfated-O-sulfated heparin, Tpo, FL) with similar performance in maintaining engrafting HSCs. These studies challenged the requirement for direct contact with the AFT024 stroma, suggesting the AFT024 maintain HSCs through secretion of cytokines. Another study from the Lewis group further supported this concept, since BMP4 was identified as one of the key molecules for the AFT024-mediated maintenance of human HSCs (Hutton et al., 2006). However, the fact that non-supportive stroma cell lines also express BMP4 in equal or higher doses than AFT024 challenged again their hypothesis. In conclusion, besides the extensive investigation, the mechanism through which AFT024 maintain mouse or human HSCs is still unknown.

In order to investigate whether the observed effect in the murine system is governed by adhesion molecules or secreted factors, I performed a series of conditioned media experiments. In the initial experiments, generation-based analysis revealed similar levels of cell division between HSCs cultured on 2018 stroma with or without AFT024-conditioned media. These results suggest that AFT024 stroma requires direct contact to fully promote survival of co-cultured HSCs, since secreted factors are redundant for HSC survival/proliferation. Conditioned media are generally sensitive and the activity of contained secreted molecules may be easily irreversibly affected. To exclude potential effects of handling in the activity of secreted factors, I also designed assays in which HSCs were in contact with 2018 cells, but the majority of the media was stably conditioned by neighboring AFT024 cells (without physical contact between the two stromata). AFT024-derived secreted factors had minor effect on the proliferation potential of HSCPs suggesting again that adhesion molecules are the main mediators of the positive interaction between HSCPs and AFT024 stroma. These results were further confirmed by the fact that HSCs did not survive in stroma-free cultures, thus highlighting the importance of the stroma in the observed interaction.

In addition, we report no migration of HSCs towards the AFT024 stroma. These data contradict previously published data showing active migration of human umbilical-cord-blood derived CD34+CD38- HSCs towards AFT024 cells shortly after co-culture initiation (Wagner et al., 2005). However, species variation may lead to the observed discrepancy.

Taken together our data illustrate that murine HSCs require direct contact to AFT024 stroma cells to proliferate/divide, since stroma-free cultures resulted in massive cell death in Dexter-type media (Figure 4.13A).

6.5 Positive effect from AFT024 or/and negative from 2018 stroma?

We report in this thesis that the majority of HSC proliferate/survive under supporting conditions (≈80%), while undergoes cell death in non-supporting conditions (72%-79%). This differential HSCs behavior may be explained by the presence of a (positive) factor promoting proliferation/survival exclusively expressed by the AFT024 stroma, which lacks from the 2018 stroma. Alternatively, the same behavior could be explained by the absence of a (negative) factor on the AFT024 leading to cell death of co-cultured cells, which is present on the 2018 stroma or by a combination of both scenarios.

To address this, I initially performed a series of conditioned media experiments showing that 2018 stroma does not secrete any factor cell-death related factor or any inhibitor of proliferation/survival promoted by the AFT024 stroma. To investigate the effect of HSC adhesion to the different stromata, I performed experiments, in which AFT024 and 2018 cells were mixed in different ratios. A similar approach has been followed by Buckley and colleagues while investigating the potential of two AGM-derived stroma cell lines (EL08-1D2 and UG26-1B6) to maintain HSC in non-contact cultures. UG26-1B6 stroma could maintain HSC in non-contact cultures, while EL08-1D2 required direct contact. Complementing the EL08-1D2 cultures with just 25% UG26-1B6 cells was sufficient to rescue HSC maintenance and multilineage reconstitution of mouse recipients in non-contact cultures (Buckley et al., 2011). Similar results were obtained in cultures with higher ratios of UG26-1B6 cells, suggesting that this stroma secretes one or more factors capable of supporting HSC maintenance, while EL08-1D2 did not.

The analysis of the results presented in the current thesis showed no effects when mixing the AFT024 stroma compartment with 10% 2018 cells or vice versa. However, cultures comprising 50% of AFT024 stroma and 50% of 2018 stroma resulted in intermediate proliferation levels of co-cultured HSCs, suggesting that HSC cell-fate decisions are strongly dependent on the continued interaction with each stroma type. Indeed, quantification of the absolute time HSCs were adherent to each stroma type revealed that dividing HSCs were mostly adherent to AFT024 (75% of their lifetime), whereas dying HSC were mostly adherent to 2018 stroma.

Interestingly, the analysis of the cell-death kinetics of HSCs cultured with AFT024, 2018 or 2012 revealed that the slower death kinetics occurred during the 2018 co-cultures (Results, section 5.4.4, Figure 5.20). This result minimizes the likelihood of a negative, cell-death promoting factor expressed by 2018 and rather suggests the absence of pro-survival factor(s) expressed by the supportive AFT024 cells. In addition, the fact that stroma-free cultures (in Dexter-type media) result in the cell death of virtually all cultured HSCs, whereas approximately 25% survived on 2018 stroma, further support that 2018 cell do not actively kill HSCs.

To conclude, our analysis suggests that the observed differences in the HSC behavior upon culture with the different stroma is mainly the result of one or more pro-survival, cell surface or matrix factors expressed by the AFT024 stroma, while they are absent from the

2018 stroma. However, an additional negative effect from the 2018 could not be entirely excluded.

6.6. Confirmation of the gene-expression differences between supportive and non-supportive stroma

The AFT024 stroma cell line has been reported to qualitatively and quantitatively maintain co-cultured murine and human HSCs over long culture periods (Moore et al., 1997a; Thiemann et al., 1998; Punzel et al., 1999; Nolta et al., 2002). Published gene lists have revealed the molecular signature of AFT024 stroma (Hackney et al., 2002) consisting of around 1000 differentially expressed genes. These can be subdivided into three categories: i) genes coding for membrane, adhesion or extracellular matrix proteins (requiring cell-cell contact), ii) genes coding for secreted factors and cytokines and iii) transcription factors or cytoskeleton-related proteins. The results presented in the current thesis reveal that adhesion molecules are at least in part responsible for the AFT024-mediated maintenance of HSCs. For this reason, I further confirmed the differential expression of adhesion-related genes by qRT-PCR experiments.

Around 170 genes predicted to be differentially expressed between AFT024 and 2018 or BFC012 stroma were further analyzed. From those, 33 were indeed found to be exclusively or preferentially expressed by the supportive stroma. This means that only 20% of the published genes could be confirmed with more sensitive methods.

It is important to note that the untreated stroma was used for the generation of the subtractive library (Hackney et al., 2002) and for the microarray analysis (Charbord and Moore, 2005). However, irradiated stroma cells were used in the Dexter-type, long-term cultures reported to support HSC self-renewal. To better simulate the culture conditions and to reveal potential differences in the gene expression occurred from the stroma irradiation, we expanded our analysis in irradiated stroma cells cultured for two days in Dexter media. Irradiation reduced the fold differences in the gene expression between the two stromata, however it did not affect the list with differentially expressed molecules.

Multiple shRNA constructs were then designed against twenty of the differentially expressed genes and a variety of knocked-down stroma cell lines was generated. Continuous time-lapse imaging of Dexter-type co-cultures was implemented to monitor potential effects of the manipulated stroma manipulation upon HSCs cell fates.

6.7 DLK1, DPT and FAP are important for early HSC survival/proliferation, but DPT alone is essential for in vitro HSC maintenance in AFT024-based co-cultures

From the panel of eighteen candidate genes screened, the knock down of three proteins resulted in reduced proliferation rates of co-cultured HSCs.

6.7.1. Delta-like 1 homolog (Dlk1)

The murine delta-like 1 homolog (Dlk1) gene encodes a transmembrane protein containing six epidermal growth factor (EGF) like repeats, a protein domain found in the extracellular part of transmembrane proteins. A soluble form of DLK1 has also been identified (upon proteolytic cleavage of the extracellular domain) and reported to inhibit adipocytic differentiation of pre-adipocytic cells (Smas et al., 1997; Garcés et al., 1999; Mei et al., 2002) or osteogenic differentiation of bone marrow mesenchymal cells (Abdallah et al., 2004; Sul, 2009).

Knock down of DLK1 resulted in intermediate levels of proliferation/survival of co-cultured HSCs (from 80,0%±8,03% on AFT024 to 58,6%±5,9% on AFT024-DLK1). It has been previously reported that over-expression of a transmembrane form of DLK1 in BFC012 non-supportive stroma led to a 4- to 6-fold increase in the number of "cobblestone area" (CA) colonies generated by co-cultured HSCs (Moore et al., 1997b). Interestingly, exogenous addition of the soluble form of DLK1 resulted in a 2-fold increase of the number of CA colonies, in Dexter-type co-cultures. However, the maintenance of those CA colonies was transient (less than two weeks) and only low levels of repopulating cells were maintained in short-term, DLK1-expressing co-cultures, as shown by competitive transplantations. These results led authors to postulate that other factors might be necessary for the AFT024-driven maintenance of co-cultured HSCs, in addition to DLK1 (Moore et al., 1997b).

In an attempt to identify the fetal liver stroma responsible for the hematopoietic maintenance and expansion occurring during fetal hematopoiesis, Chou suggested that DLK1+SCF+ fetal liver cells might play this role. According to their data, E15.5 DLK1+SCF+ cells comprise a homogeneous population of bipotent hepatic stem cells giving rise to both hepatocytes and epithelial cells. Interestingly, E15.5 DLK1+SCF+ stroma could maintain the repopulation potential of fetal liver-derived HSC after short co-culture (4 days)

in media containing SCF, IL-6 and Flt3 (Chou and Lodish, 2010). Recent data from the same group showed that DLK1+ cells could maintain co-cultured HSC for periods up to 3 weeks (Chou et al., 2013). It is important to note that direct contact was a prerequisite for the in vitro maintenance of co-cultured HSCs, a result that confirms our observations. However, DLK1 was used as a marker to isolate those bipotent stroma cells and there was no evidence for a role of DLK1 in the described in vitro HSC maintenance. It is also not clear to which extend the E15.5 fetal liver-derived DLK+SCF+ cells described in those studies are related with the immortalized AFT024 stroma cells (isolated from the same organ at E14).

Herein, we report that HSCs co-cultured on DLK1^{KD} stroma exhibit reduced levels of proliferation in generation 0. The levels of proliferation/survival of HSCs progeny (generations 1 and 2) are also reduced, while cell-death levels are slightly increased compared to the wild-type AFT024 stroma (Results, section 5.5.5, Figure 5.25). On the contrary, DLK1^{KD} stroma had no detectable influence on the survival/proliferation of early progenitors. Interestingly viral over-expression of Dlk1 partially rescued HSC survival/proliferation (1,9-fold increase compared to 2018 conditions), a result coinciding with Moore's data (Moore et al., 1997b). Long-term in vitro assays (CAFC and LTC-IC) showed an impaired potential of DLK1^{KD} stroma to support HSC potential. However, in vivo transplantation experiments (the gold-standard method to show HSC function) revealed that co-cultures on DLK1^{KD} stroma had minor influence upon HSC numbers. Taken together these data suggest that DLK1 is in part responsible for the AFT024-driven survival/proliferation of HSCs in vitro, but it is not required for HSC maintenance as shown by the in vivo transplantations. Finally, the fact that the cleaved/soluble form of the protein has biological activity lead us to hypothesize that the cleaved domain of DLK1 might account for the minor positive effect of AFT024 conditioned media upon HSC proliferation.

6.7.2. Dermatopontin (Dpt)

Another candidate molecule that I identified as essential for HSC proliferation/survival upon co-culture with the AFT024 stroma is dermatopontin (Dpt), an extracellular matrix protein facilitating cellular adhesion to the matrix as well as matrix assembly (Superti-Furga et al., 1993; Forbes et al., 1994). Takeda and colleagues generated the Dpt knockout mice, in order to identify its biological role. Dpt-null mice had increase skin elasticity, a significant decrease in the dermis layer and irregularities in collagen fibril formation (Takeda et al., 2002). Dpt was initially purified in a complex with decorin (Dcn), a

matrix proteoglycan, from bovine dermis (Neame et al., 1989). It has been reported that Dpt forms a complex with Dcn augmenting the binding and the availability of transforming growth factor β1 (TGF-β1) to cells (Okamoto et al., 1999). The role of Dpt has been mainly studied in lung epithelial (Okamoto et al., 1999), human epidermal keratinocytic (Okamoto et al., 2010) or human fibroblastic cell lines (Kato et al., 2011).

In the current thesis, I presented data of DPT^{KD} stroma showing impaired potential to support survival/proliferation of co-cultured HSCs and their progeny. DPT knock down also affected early progenitors, suggesting that DPT is important in the early stages of hematopoiesis. Furthermore, HSCs cultured on DPT^{KD} stroma showed reduced potential to form colonies in long-term in vitro assays (CAFC and LTC-IC). Most importantly, HSCs co-cultured with DPT^{KD} stroma showed reduced levels of repopulation in recipient mice. Therefore, we provide the first evidence for a novel role of Dpt in hematopoiesis, as a key molecule for HSC survival/proliferation and most importantly for HSC maintenance in vitro.

Next, I sought to investigate whether DPT is present in the in vivo bone marrow niche. DPT's expression in the bone and cartilage has been previously reported by immunoblotting and northern analysis in porcine tissues (Forbes et al., 1994). In the current thesis, we provide a more detail expression profile of DPT in the different regions of murine bone marrow. To do this, we developed and implemented confocal imaging of bone marrow section from murine femurs preserving bone morphology and tissue architecture, which revealed that DPT is expressed by cell types functioning as HSC niches, such as bone surfaces, blood vessels and mature blood cells (megakaryocytes).

6.7.3. Fibroblast activation protein (Fap)

Finally, I also presented evidence for fibroblast activation protein (Fap) being another molecule involved in HSC proliferation and survival in vitro. FAP is a type II transmembrane glycoprotein (single-pass molecule with its C-terminal domain anchoring to the endoplasmic reticulum). It was first identified in cultured fibroblasts and named as F16 cell surface antigen, due to its reactivity with the respective monoclonal antibody (Rettig et al., 1986). Four years later, Fap was independently isolated from a melanoma cell line (LOX) and named "seprase" after its protease activity (surface expressed protease) (Aoyama and Chen, 1990). Cloning of the two molecules (F16 and seprase) revealed that seprase was the

dimerized form of F16 (Scanlan et al., 1994) and the protein was finally designated fibroblast activation protein (FAP) (Rettig et al., 1994).

FAP has reported dipeptidyl peptidase activity (removes dipeptides from the N-terminus of substrate proteins) and endopeptidase activity (break peptide bonds between amino-acids localized away from the terminal protein domains) (Niedermeyer et al., 1998). It plays a functional role in matrix architecture and remodeling, due to its ability to degrade type I collagen (Cheng et al., 2005). Like DLK1, FAP has also a soluble form originating from cleavage of the extracellular protein domain (Lee et al., 2006). The soluble form of FAP is often called antiplasmin-cleaving enzyme (APCE), although soluble FAP (sFAP) is lately more preferable (Jacob et al., 2012). Interestingly, the FAP null mice have no obvious abnormalities (Niedermeyer et al., 2000).

FAP's expression has been detected in activated stroma cells, such as fibroblastic cells associated with different types of cancer (Kidd et al., 2012; Liu et al., 2012). It is also expressed in normal tissues during development, such as the human uterus and placenta (Dolznig et al., 2005) as well as in the adult bone marrow, where it can be used as a marker for mesenchymal stem cells (Bae et al., 2008). It is currently believed that FAP expression in healthy tissues is transient compared to its stable expression pattern in cells associated with wound healing or diseases (Jacob et al., 2012). However, a recent study using a transgenic mouse line allowing visualization of all FAP expressing cells reported expression in almost all adult tissues (Roberts et al., 2013). Deletion of FAP expressing cells using the diphtheria toxin system (administration of diphtheria toxin - DTX selectively kills cells expressing the diphtheria toxin receptor - DTR) resulted in a hematopoietic phenotype, since the numbers of committed progenitor populations were decreased in the bone marrow compartment (granulocyte-macrophage progenitor GMP, common lymphoid progenitor CLP, megakaryocyte-erythroid progenitor MEP, pro-erythoblasts and pro-B- cell progenitors) (Roberts et al., 2013). Interestingly, the number of MPPs was slightly increased, whereas HSCs remained unaffected by this manipulation. Another striking result of that study was the identification of FAP+, osteocalcin+ and osteopondin + bone-lining cells which also express Cxcl12 and KitL; two cytokines with key roles in HSC homing and normal hematopoiesis (Roberts et al., 2013). These data suggest a novel role of the FAP expressing stroma in in vivo hematopoiesis and especially in survival of committed progenitor cells. It is important to note that such manipulations are always limited by the specificity and off-target effects of the administered compounds (in this case DTX). The absence of an effect on the HSC

compartment might be related with the short time between DTX administration and bone-marrow isolation (3 days). On the contrary, our data revealed a role of FAP in survival and proliferation but not maintenance of HSC under in vitro culture with AFT024 stroma. Comparing the effect of FAP knock down between HSCs and early progenitors, we found that FAP mainly affects HSCs. The different experimental approach (in vitro versus in vivo) may account for the observed discrepancies regarding the role of FAP in the different hematopoietic populations.

7. Experimental Procedures

7.1 Molecular biology

7.1.1. Restriction Digest – Dephosphorylation

For restriction digests, 1-5μg of backbone plasmid were digested with either one or a combination of different restriction enzymes in the suggested buffer for 1 hour or overnight in some cases. Heat inactivation of the different enzymes was performed as suggested in the manufacturer's instructions.

If the two ends of the digested backbone are compatible (blunt ends or sticky, complementary ends), de-phosphorylation is required to inhibit self-ligation or concatamers (two or more linear plasmids ligated together). During this reaction, alkaline phosphatase is added to remove the 5' phosphate groups of the backbone DNA fragment, which are required by ligases to form the phosphodiesteric bond between the nucleotides of the backbone and insert DNA. The insert DNA fragment will not be treated and it will still be able to ligate to the vector through its 5' phosphate group. Notably, the 3' end of each insert will not ligate to the 5' end of the backbone (due to the de-phosphorylation) and one break will be created on each strand of the recombinant DNA plasmid. This break will be later repaired enzymatically in the bacterial cell.

7.1.2. Design shRNA oligonucleotides

Gene-specific shRNA oligonucleotides were designed using the online library of the Broad Institute ("The RNAi Consortium shRNA Library") following the pattern below (listed in table 7.1):

5' – CCGG – XXXXXXXXXXXXXXXXXXXXX – CTCGAG - XXXXXXXXXXXXXXXXXXXXX – TTTTT - G 3'

3' -   YYYYYYYYYYYYYYYYYYYYY – GAGCTC – YYYYYYYYYYYYYYYYYYYYY – AAAAA – CTTAA 5'

Gene	Clone	Sequence
scrambled	1	CAACAAGATGAAGAGCACCAACTCGAGTTGGTGCTCTTCATCTTGTTG
	2	CTTACGCTGAGTACTTCGACTCGAGTCGAAGTACTCAGCGTAAG
	3	TGGTTTACATGTTTTCTGACTCGAGTCAGAAAACATGTAAACCA
	4	CCTAAGGTTAAGTCGCCCTCGCTCGAGCGAGGGCGACTTAACCTTAGG
Thbs2	1	GCCCTATTGATGGGTGCTTATCTCGAGATAAGCACCCATCAATAGGGC
	2	GCTGTAGGTTTCGACGAGTTTCTCGAGAAACTCGTCGAAACCTACAGC
	3	CCATTCTATGAGCAGCTAGAACTCGAGTTCTAGCTGCTCATAGAATGG
	4	CCAAGACAACTGCCCATACATCTCGAGATGTATGGGCAGTTGTCTTGG
	5	CCACGTCAAGGACACTTCATTCTCGAGAATGAAGTGTCCTTGACGTGG
	6	GATTCGTGCTGTTCTATAATGCTCGAGCATTATAGAACAGCACGAATC
Dlk1	1	CTCAGGCAACTTCTGTGAGATCTCGAGATCTCACAGAAGTTGCCTGAG
	2	GCTGGTGATGAGGAGATCTAACTCGAGTTAGATCTCCTCATCACCAGC
	3	GACGGGAAATTCTGCGAAATACTCGAGTATTTCGCAGAATTTCCCGTC
	4	CCATCGTCTTTCTCAACAAGTCTCGAGACTTGTTGAGAAAGACGATGG
	5	CATCCTGAAGGTGTCCATGAACTCGAGTTCATGGACACCTTCAGGATG
	6	CCACATGCTTCGCAAGAAGAACTCGAGTTCTTCTTGCGAAGCATGTGG
Bgn	1	CCACTCAGAGACTCCCTATAACTCGAGTTATAGGGAGTCTCTGAGTGG
	2	GCCATCCAATTTGGAAATTATCTCGAGATAATTTCCAAATTGGATGGC
	3	GCCCTGGTCTTGGTAAACAATCTCGAGATTGTTTACCAAGACCAGGGC
	4	GCTATTGAGTTGGAGGACCTACTCGAGTAGGTCCTCCAACTCAATAGC
	5	CTCCCTGGTAGAACTACGAATCTCGAGATTCGTAGTTCTACCAGGGAG
Mmp9	1	CCCTCTGAATAAAGACGACATCTCGAGATGTCGTCTTTATTCAGAGGG
	2	CCAGGATAAACTGTATGGCTTCTCGAGAAGCCATACAGTTTATCCTGG

	3	GAGGCATACTTGTACCGCTATCTCGAGATAGCGGTACAAGTATGCCTC
	4	CCACTTACTATGGAAACTCAACTCGAGTTGAGTTTCCATAGTAAGTGG
	5	CAGTACCAAGACAAAGCCTATCTCGAGATAGGCTTTGTCTTGGTACTG
Vcam1	1	CCAGATCCTTAATACTGTTTACTCGAGTAAACAGTATTAAGGATCTGG
	2	CCCTTTGACCATCTGGAGATTCTCGAGAATCTCCAGATGGTCAAAGGG
	3	CCAAATTGATTCTACACTCAACTCGAGTTGAGTGTAGAATCAATTTGG
	4	CGAGGCTGGAATTAGCAGAAACTCGAGTTTCTGCTAATTCCAGCCTCG
	5	CCAGATAGACAGCCCACTAAACTCGAGTTTAGTGGGCTGTCTATCTGG
Dpt	1	CGTCCTCTATTCAAAGATATACTCGAGTATATCTTTGAATAGAGGACG
	2	GAGGAGCATCTTTAGCAAGAACTCGAGTTCTTGCTAAAGATGCTCCTC
	3	GCGAGGAGCAACAACCACTTTCTCGAGAAAGTGGTTGTTGCTCCTCGC
	4	CTATAGCAAGAGGTGTCCATACTCGAGTATGGACACCTCTTGCTATAG
	5	CTGGATCGTGAGTGGCAATTTCTCGAGAAATTGCCACTCACGATCCAG
Tgfbi	1	GCCTTGGCATGGTTCTGTAAACTCGAGTTTACAGAACCATGCCAAGGC
	2	CGAGTCTTTGTTTATCGAAATCTCGAGATTTCGATAAACAAAGACTCG
	3	CCCAATGGGATTGTAACTGTTCTCGAGAACAGTTACAATCCCATTGGG
	4	CCTCCAGAAGAACTGAACAAACTCGAGTTTGTTCAGTTCTTCTGGAGG
	5	GCCATTGACATCCTCAAACAACTCGAGTTGTTTGAGGATGTCAATGGC
Fap	1	GCCACTTCATATAGGACTTAACTCGAGTTAAGTCCTATATGAAGTGGC
	2	GCACATTATGAAGCAGAAATTCTCGAGAATTTCTGCTTCATAATGTGC
	3	GCCTATTCTTATTATGGTGATCTCGAGATCACCATAATAAGAATAGGC
	4	CCCTTTGCTAATTCAAGTGTACTCGAGTACACTTGAATTAGCAAAGGG
Col6a3	1	GCCATCAACAAAGTCGTCTATCTCGAGATAGACGACTTTGTTGATGGC
	2	CCAAGGAAGTTTCAATACGAACTCGAGTTCGTATTGAAACTTCCTTGG

	3	CCCTCAGGTTATCATAGTATTCTCGAGAATACTATGATAACCTGAGGG
	4	CCTTTCTCATATTGTGAACATCTCGAGATGTTCACAATATGAGAAAGG
Dcn	1	CCTGTCTAAGAACCAACTAAACTCGAGTTTAGTTGGTTCTTAGACAGG
	2	CGACTTCAATGGACTGAACAACTCGAGTTGTTCAGTCCATTGAAGTCG
	3	GCCTGAAAGGACTGATTAATTCTCGAGAATTAATCAGTCCTTTCAGGC
	4	GTCCGGTATTGGGAAATCTTTCTCGAGAAAGATTTCCCAATACCGGAC
	5	CCTGAAGGACTTGCATACCTTCTCGAGAAGGTATGCAAGTCCTTCAGG
Slc38a4	1	GACGCCATGAACAGCCAATTTCTCGAGAAATTGGCTGTTCATGGCGTC
	2	GACGCCATGAACAGCCAATTTCTCGAGAAATTGGCTGTTCATGGCGTC
	3	CGGAAATCTGACGTTCAACAACTCGAGTTGTTGAACGTCAGATTTCCG
	4	CGTGCCTACCATCAAATACATCTCGAGATGTATTTGATGGTAGGCACG
Slco2a1	1	CCACCACTTTGGGAAGTATAACTCGAGTTATACTTCCCAAAGTGGTGG
	2	GCCTATGCCAACTTACTCATTCTCGAGAATGAGTAAGTTGGCATAGGC
	3	GCTCGGTCTTCAACAACATTACTCGAGTAATGTTGTTGAAGACCGAG
	4	ACAGGTAATCTACAAGGTCTTCTCGAGAAGACCTTGTAGATTACCTG
Arhgdib	1	CACACATTTCATCACCAATATCTCGAGATATTGGTGATGAAATGTGTG
	2	CGAGAGTCTAACCAAGTACAACTCGAGTTGTACTTGGTTAGACTCTCG
	3	GACTGGCATGAGAGTGGATAACTCGAGTTATCCACTCTCATGCCAGTC
	4	AGTGGATAAAGCCACATTCATCTCGAGATGAATGTGGCTTTATCCACT
Igfbp6	1	GCTGTATGTGAAGCAATGAATCTCGAGATTCATTGCTTCACATACAGC
	2	CGGCCCAATCCTGTTCAAGATCTCGAGATCTTGAACAGGATTGGGCCG
	3	CGCAGACACTTGGATTCAGTACTCGAGTACTGAATCCAAGTGTCTGCG
	4	AGATGGTCAAGGAAGCACTCACTCGAGTGAGTGCTTCCTTGACCATCT
Ptx3	1	CGAGCTCATGTATGTGAATTTCTCGAGAAATTCACATACATGAGCTCG

	2	CTTTGACGAATCATTAGCATTCTCGAGAATGCTAATGATTCGTCAAAG
	3	CCAATGTTCCATTTGGGAGAACTCGAGTTCTCCCAAATGGAACATTGG
	4	GCATCCTGTGAGACCAATGAACTCGAGTTCATTGGTCTCACAGGATGC
Serpinb2	1	GCAGTTATGGTATCACCACAACTCGAGTTGTGGTGATACCATAACTGC
	2	GCTTTATCCTTTCCGTGTGAACTCGAGTTCACACGGAAAGGATAAAGC
	3	CCACAGTTTGTGGCCGATCATCTCGAGATGATCGGCCACAAACTGTGG
	4	ATTACCCACACGATACTATTTCTCGAGAAATAGTATCGTGTGGGTAAT
	5	TGCTTACAGTATAACTCTATTCTCGAGAATAGAGTTATACTGTAAGCA
Loxl1	1	CTATGACCTCCGAGTGCTATTCTCGAGAATAGCACTCGGAGGTCATAG
	2	ACTGCCAGTGGATCGACATAACTCGAGTTATGTCGATCCACTGGCAGT
	3	TCGCTACGTTTCTACAACAAACTCGAGTTTGTTGTAGAAACGTAGCGA
	4	CTTCGTAAACCAGTATGAGAACTCGAGTTCTCATACTGGTTTACGAAG
Tm4sf1	1	CTTGTGTCTCATTCAAGTAATCTCGAGATTACTTGAATGAGACACAAG
	2	GCTTCCTGTATTTCACTGTAACTCGAGTTACAGTGAAATACAGGAAGC
	3	CATTGTGGCATCACTGGGTTTCTCGAGAAACCCAGTGATGCCACAATG
	4	GCTTTGCTCTACTTTCCTAATCTCGAGATTAGGAAAGTAGAGCAAAGC

Table 7.1. List of shRNA sequences designed against candidate genes.

7.1.3. Agarose Gel Electrophoresis

Agarose gels were made by adding 1g agarose in 100ml 1xTAE buffer. The solution was heated in a regular microwave, until agarose crystals were completely dissolved. The solution was subsequently cooled down and 2ul of Ethidium Bromide (EtBr) were added at 100mL solution. The last step was to pour the solution in the appropriate gel cassette including the comb(s) with the desired number of wells.

7.1.4. DNA extraction from Agarose Gel

The DNA extraction was performed according to the "QIAquick Gel Extraction Kit" protocol (Qiagen, Cat No 28704).This protocol involves weighting the band extracted from the agarose gel, adding 3 gel volumes of buffer QG and incubating at 50oC (heating block) to dissolve the agarose. After it was completely dissolved, 1 volume of isopropanol was added and then 700μl of this solution were placed in a QIAquick spin column with a collecting tube and centrifuged for 1 minute at 13000 rpm. After discarding the flow-through, 750μl of buffer PE were added to the spin column and incubated for 5 minutes at room temperature. The next step was to centrifuge the spin column for 1 minute at 13000 rpm and discard the flow-through again. Then, this washing step with the buffer PE was repeat followed by an additional centrifugation without additional buffer PE, in order to remove the residual ethanol. The spin column was then placed in a new 1,5ml ependorf and 30μl of H2O were directly added on the membrane, incubated for 2-5 minutes at room temperature and then were centrifuge for 1 minute at 13000 rpm to elute DNA. The final step was to measure the DNA concentration in the spectrophotometer (NanoDrop ND-1000).

7.1.5. Annealing of oligonucleotides (protocol from NEB)

First, a tube with the following was prepared:

Top strand DNA oligo (100μM)	10 μl
Bottom strand DNA oligo (100μM)	10 μl
10x NEB Buffer 2	2,2 μl
TOTAL	**22,2 μl**

The tube(s) were heated at 95oC for 5 minutes and then placed on water with temperature of 70°C which was cooling down over night.

7.1.6. Phosphorylation of oligonucleotides

A tube with the following reagents was prepared:

1x buffer A (10x)	2 µl
ATP 10mM	2 µl
DNA (annealed oligos)	0,4 µl
T4 PNK (Fermentas 10u/ul)	1 µl
H$_2$0	14,6 µl
TOTAL	**20 µl**

The tube(s) were then placed at 37°C for 20-60 minutes (heating block). The PNK enzyme was then heat inactivated by putting the tube(s) at 75°C for 10 minutes.

7.1.7. Ligation

During ligation, a double-stranded fragment of DNA (insert) is ligated to another double-stranded DNA molecule which contains an origin of replication (backbone plasmid). Ligation requires compatible ends between the two DNA fragments. This insertion is feasible by the generation of a phosphodiester bond between the 5' phosphate and the 3' hydroxyl group of the adjacent nucleotides of the two DNA fragments. This endergonic (requires energy) biochemical reaction is catalyzed by T4 DNA ligase, an enzyme which derives from the phage T4.

To ensure that there is sufficient insert DNA to produce recombinant DNA molecules, the molar ratio of the insert has to be 3-4 times more than the backbone plasmid's. To calculate the amount of insert to be used in a ligation, the following equation is used:

$ng\ of\ insert\ DNA =$

$$\frac{(ng\ of\ vector)(size\ of\ insert\ in\ kb)}{size\ of\ vector\ in\ kb}(desired\ molar\ ratio\ of\ insert:vector)$$

For the ligation, a tube containing the following reagents was prepared:

Vector (≈150 ng)	x µl
Insert	y µl
Rapid ligation buffer	1 µl
T4 ligase	1 µl
H$_2$0	(13-x-y) µl
TOTAL	**15µl**

The tube was left at room temperature for 60 minutes (or 4oC over night) and then the enzyme was heat inactivated at 65°C for 10 minutes.

7.1.8. Transformation of DH5α *E.Coli*

For transformation, the competent DH5α strain of E. coli was used. After thawing the bacteria for 5 minutes on ice, 50µl of the bacterial solution were mixed with the ligated DNA. The solution was incubated on ice for 15 minutes, then was heated for exactly 90 seconds at 42°C and finally was placed on ice for another 2 minutes. Since Ampicilin is a bacterio-static antibiotic (competitive inhibitor of transpeptidase, an enzyme needed by bacteria to build their cell wall – ultimately this leads to cell lysis), the bacterial solution can be plated directly on the LB plates (containing Ampicilin) and incubated overnight at 37°C. Only the transformed bacteria containing the desired plasmid, which also includes the gene giving resistance to Ampicilin, will survive and grow as independent colonies in the plate. Single colonies were then picked, placed in a tube containing 3ml LB medium containing ampicilin and incubated over night on a shaker at 37°C.

7.1.9. DNA preparation (mini)

DNA from single colonies was isolated by transferring 2ml from the bacterial culture (incubated overnight) in a 2.0ml tube and centrifuging at 13000 rpm for 1 minute, at room temperature (RT). The supernatant was discarded and the pellet was re-suspended in 250μl of buffer P1. 250μl of buffer P2 were then added and the solution was mixed by inverting the tube few times (bacterial lysis). In the next step, 350μl of buffer P3 were added to neutralize the reaction, the tube was inverted again for several times to ensure mixing and was centrifuged at 13000 rpm for 1 minute (RT). The supernatant was transferred in a new 1.5ml tube, 700μl isopropanol were added and the solution was again centrifuged at 13000 rpm for 1 minute (RT). The supernatant was discarded this time, the pellet was washed with 250μl of 70% ethanol and centrifuged at 13000 rpm for 1 minute (RT). The supernatant was discarded carefully, the pellet was air-dried before it was re-suspended in 30μl of H_2O.

7.1.10. DNA preparation (maxi)

If higher DNA yield (amount and concentration) was necessary (i.e. for virus production), the bacteria were placed on 200-250 ml of LB medium supplemented with Ampicilin and incubated overnight on a shaker at 37°C. After 15-16 hours, the plasmid DNA was isolated using the QIAprep Plasmid Maxiprep Kit (Qiagen, Cat No 12362). The bacterial cells were harvested by centrifugation at 4600 rpm for 15 minutes at 4°C. The pellet was re-suspended in 10ml of buffer P1, in which RNase (to degrade RNA) and LyseBlue (for visual confirmation of optimum buffer mixing preventing inefficient cell lysis and incomplete precipitation of genomic DNA, sodium dodecyl sulfate and cell debris in next steps) were added. Then, 10 ml of buffer P2 were added and the tube was mixed thoroughly by inverting the tube 6 times until a homogeneously blue-colored solution was achieved (cell lysis). Buffer P2 contains sodium dodecyl sulfate (SDS), a detergent which will dissolve the phospholipid membranes and cause the lysis of the bacterial cell wall. It also contains sodium hydroxide (NaOH), which will raise the pH causing the denaturation of cell proteins, DNA and high-molecular-weight RNA. However, the plasmid DNA remains supercoiled and remains in the solution. Important precautions in this step are to: 1. not vortex the tube

(shearing of genomic DNA) 2. not allow the lysis reaction to proceed for more than 5 minutes and 3. to close immediately the lid of the bottle containing buffer P2 to avoid acidification from the CO_2 of the air. Subsequently, 10ml of chilled buffer P3 (contains potassium acetate - CH_3CO_2K) were added and the solution was mixed immediately again by inverting the tubes 6 times (neutralization). In this step, the SDS will precipitate together with proteins, lipids and chromosomal DNA, since it is attached to cell membrane proteins. It is important to get a homogeneous colorless solution after the addition of buffer P3, which indicates the successful precipitation of SDS, genomic DNA and cell debris. If the solution still appears viscous the neutralization was not completed and additional mixing is required. In the next steps the tubes were places on ice for 20 minutes and then were centrifuged at 20000xg for 30 minutes to separate the precipitated solution from the solved plasmid DNA. An additional centrifugation step followed (15 minutes) if the solution was not separated. During this time, the QIAGEN-tip 500 was equilibrated by applying 10ml of buffer QBT and allowing the column to empty by gravity flow. Then, the supernatant from the previous centrifugation step was transferred in the column and was allowed to pass by gravity flow (as in all following steps). The QIAGEN-tip was washed two times by adding 30ml of buffer QC. Then, 15ml of buffer QF were added to elute the DNA, which was later precipitated by the addition of 10.5ml room-temperature isopropanol. After centrifuging at 4600 rpm for 45 minutes and discarding the supernatant, the pellet was washed with 5ml of 70% ethanol (EtOH). After a 10-minute centrifugation, the supernatant was decanted and the pellet was left to air dry. The last step was to re-suspend the pellet in the appropriate volume of H_2O (50-100μl) and to determine the DNA concentration by using the spectrophotometer (NanoDrop ND-1000).

7.1.11. Glycerol stocks

Positive clones (identified by screen digests) were stored at -80°C, after the addition of 700μl of bacterial over-night culture in 300μl 50% glycerin solution.

7.1.12. Sequencing

Positive clones, screened by a digest and gel electrophoresis, were then sequenced to validate the DNA sequence. The first step was a PCR to amplify the DNA sequence to be confirmed. The following reagents were added in a well of a multi-well sequencing plate:

BigDye (contains dNTP, Polymerase)	0,5 µl
BigDye buffer (5x)	1 µl
template *	x µl
DMSO	0,1µl
Primer (5µM stock)	1 µl
Water	(5-x) µl
TOTAL	5 µl

*The table below shows the amount of template to use in a cycle sequencing reaction (recommendation of the original protocol of Applied Biosystems)

Template	Quantity
Single stranded	25 – 50 ng
Double stranded	150 – 300 ng
Cosmid, BAC	0,5 – 1 µg

Then, a PCR was performed according to the following program:

Step	Temperature	Duration	Number of cycles
Initialisation	96°C	1 minute	1
Denaturation	96°C	10 seconds	
Annealing	50°C	5 seconds	35
Elongation	60°C	4 minutes	
Stanby	12°C	∞	

The next step after the PCR reaction was to precipitate the DNA with ethanol. For this reason, 0.5μl of 125mM EDTA, 2.0μl of 3M Na-Acetate and 50μl 100% EtOH were mixed with each PCR product and the plate was incubated for 15 minutes at room temperature in the absence of light. The plate was then centrifuged at 2000xg for 30 minutes at 4°C and the supernatant was discarded. A second brief centrifugation step followed (180xg), 70μl 70% EtOH were added in each well and the plate was centrifuged again (2000xg, 15 minutes at 4°C). The plate was inverted to remove the ethanol, centrifuged briefly (180xg) and rested for 2 minutes in the dark to allow evaporation of residual EtOH. After this step, 20μl of HPLC H_2O were added in every well and the plate was sealed. The plate was sequenced by an ABI 3730 DNA analyzer.

7.1.13. RNA extraction

For RNA isolation from AFT024, 2018 and other cell lines the RNeasy Mini Kit for Qiagen (Qiagen, Cat No 74106) was used. This kit allows isolation of up to 100μg RNA from 100 to 10^7 cells. It enables isolation of RNA molecules longer than 200 nucleotides, which results in an enrichment of mRNA molecules over most other RNAs which are sorter (i.e. 5.8S rRNA, 5S rRNA, tRNA etc). Cells were harvested after a PBS wash, trypsinization, transfer to a polypropylene (RNase-free) tube, centrifugation at 1000 rpm for 5 minutes and re-suspension to buffer RLT (350μl for $<5\text{x}10^6$ cells or 600μl for $>5\text{x}10^6$ cells) supplemented with β-Mercaproethanol. After mixing the solution by pipeting, the sample was either frozen at -80°C or placed in QIshredder spin column (Qiagen, Cat No 79654) and centrifuged at full

speed for 2 minutes (lysate homogenisation). One volume of 70% EtOH was then added to the homogenized lysate and up to 700μl were transferred to the RNeasy spin column which was centrifuged at >10.000 rpm for 15 seconds. The flow through was discarded and the previous step was repeated until all the lysate was added to the column and centrifuged. Next, 350μl of buffer RW1 were added to the spin column and the tube was centrifuged at >10.000 rpm for 15 seconds (washing step). To digest the residual DNA, 80μl of DNase solution (10μl of DNase stock solution in 70μl of buffer RDD) were added directly on the silica membrane of the spin column and were incubated for 15 minutes at room temperature. Another washing step with addition of 350μl of buffer RW1 and centrifugation followed. After discarding the flow through, 500μl of buffer RPE were added. The sample was centrifuged and additional 500μl of buffer RPE were added to the column and centrifuged for 2 minutes. Then, the RNeasy spin column was placed in a new collection tube and they were centrifuged for an additional 1 minute to completely remove the residual ethanol contained in the RPE buffer. The RNeasy spin column was placed in a new 1,5ml tube and 30μl of RNase-free H_2O were added to elute the RNA bound in the silica membrane upon centrifugation. The concentration of the eluted RNA was determined in a spectrophotometer (NanoDrop ND-1000). In addition, the quality of the eluted RNA was accessed by running few microliters of individual samples in a 1% agarose gel.

7.1.14. cDNA synthesis

For the reverse transcription of the mRNA produced during the RNA extraction method described above, the following reagents were added in a tube:

Reagent	Company	Cat No	Quantity
Oligo(dT)$_{12-18}$ (500 μg /ml)	Promega	C1101	1 μl
total RNA (2μg)			x μl
dNTP mix (10mM each)			1 μl
Sterile DNase- and RNase-free H_2O			(12-x) μl
TOTAL			12 μl

The mixture was heated at 65°C for 5 minutes and then quickly chilled on ice. The samples were briefly centrifuged and then the following reagents were added:

Reagent	Quantity
5x first strand buffer	4 µl
0.1M DTT	2 µl
RNase OUT^{TM} (40units/µl)	1 µl

The tubes were incubated at 42°C for 2 minutes and then chilled on ice. Finally, 1µl of SuperScript II RT (Invitrogen, Cat No 18064-014, 200 units) was added to each tube (except from the control samples without reverse transcriptase, "-RT"), the solution was gently mixed by pipeting and then incubated at 42°C for 50 minutes. The reaction was inactivated by heating at 70°C for 15 minutes.

7.1.15. Quantitative real time PCR (qRT-PCR)

All samples in the quantitative real time PCRs described in this study were performed in technical triplicates. First, 5µl of the primer mix containing the forward and reverse primer for every gene of interest (5mM) were added in each of the three wells of the 384-well plate (ABgene, TF-0384) designated for this gene (Figure7.1). Then, 5µl from the diluted cDNA (1/50) synthesized from RNA isolated from the different cell lines were also added to the respective wells. Finally, 10µl of 2xSybrGreen Mix (Applied Biosystems, Cat No 4367659) were added in every well. The plate was covered with the optical adhesive, transparent cover (Applied Biosystems , Cat No 4311971), centrifuged and placed in the Abi Prism 7500HT machine (Serial No 100252). The different steps of the PCR are described below:

Temperature	time	Cycles
95°C	10min	1
95°C	15sec	
60°C	1min	40

   As a standard procedure, the dissociation (melting) curves illustrating the specificity of the different primer sets were also analyzed in every qRT-PCR. The normalization was done based on the GAPDH expression of the cell lines used.
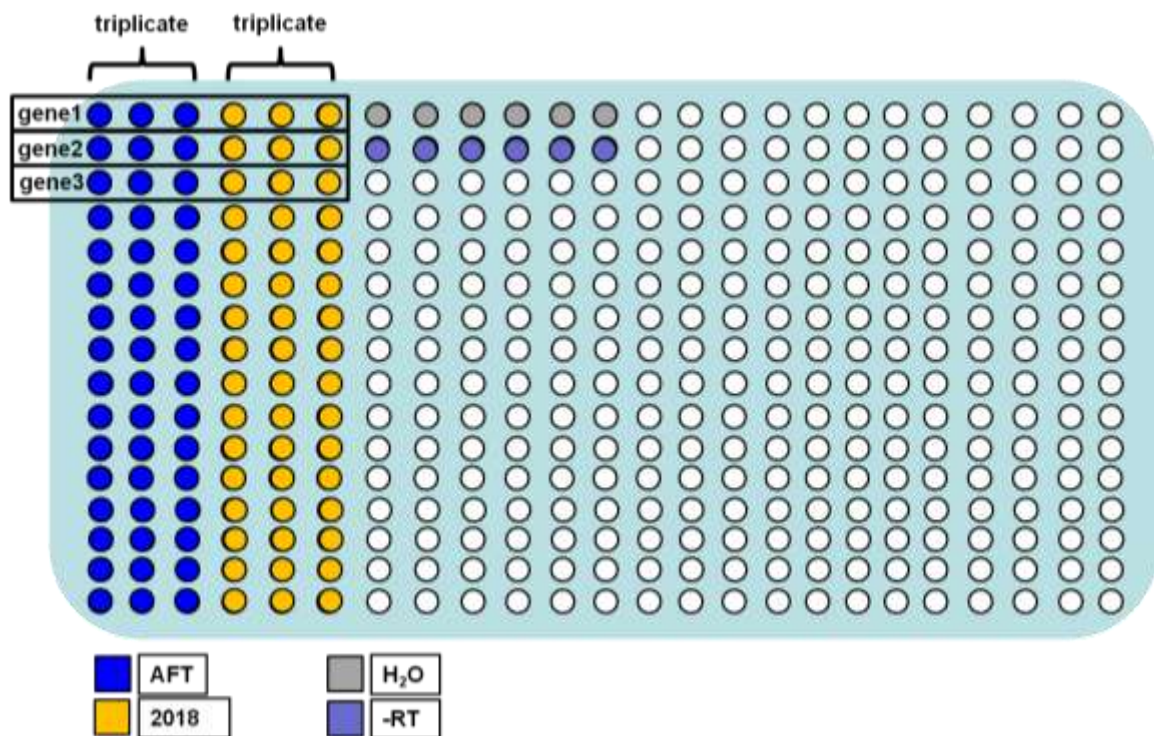
Figure 7.1. Experimental design of the qRT-PCR experiments used to compare gene expression in the AFT024 and 2018 stroma cell lines.

7.1.16. Primer design for qRT-PCR

   The gene-specific primers for qRT-PCR were designed using the online tool from IDT-DNA (http://eu.idtdna.com/scitools/Applications/RealTimePCR/). Primers are intron-separated when feasible and are presented in the table 7.2 below:

Gene	ID	Protein Type	Orientation	Sequence
Dlk1	13386	membrane	forward	GGCCATCGTCTTTCTCAACAAGTGC
			reverse	CCTCGCCGCTGTTATACTGCAAC
Ly6a	17067		forward	TCTTCTTGTGGCCCTACTGTGTG
			reverse	GGGCAGGTAATTGATGGGCAAG
Trfc	22042		forward	TTCTTGTGGCCCTACTGTGTGC
			reverse	ACTGCTGCCTCCTGAGTAACAC
Slc8a1	20541		forward	GCAAAGAAGAGGAGGAGAGGCGCATTG
			reverse	ACCACAAGGGCCAGGTTCGTCT
Npc1	18145		forward	CACGCCTCCGAAAGCTACCTGTTTC
			reverse	CCCGATGTCTACTTTGTTCACCACCG
Enpp1	18605		forward	TATGGACCTGCTGCTCGGTTGAGAC
			reverse	GGTAAGGCCGGAAATGCTGGTTTGG
Enpp2	18606		forward	AGGGTTTGTCCGCCCTCCGTTAATC
			reverse	GCCACAGGACCGCAGTTTCTCAATG
Enpp3	209558		forward	CAGGGTGATGCAGAAGAACGGAGAC
			reverse	CTCCCGGCTTGAGAACGGTGTATGA
Ly6c	17067		forward	GCTACGAGTGCTATGGAGTGCCAAT
			reverse	ACACCAGCAGGGCAGAAAGAAAGG
Ly6e	17069		forward	CCCTTCTGGGCATGGAGCAAGTTCAT
			reverse	CAGGGTGTAGCCAAGGTTGACATTCC
Dpt	56429	Extracellular	forward	CGAGGAGCAACAACCACTTTCTCTGC
			reverse	GTCGTAGTCAGTCATCCGGCACA

		matrix		
Col1a2	**12843**		**forward**	GGATGAGGAGACGGGCAGCTTGAA
			reverse	GAACGGCAGGCGAGATGGCTTATTTG
Col5a3	**53867**		**forward**	TCCAAGGGACCAACTGGGAAGAGT
			reverse	CACAGAGGCAGGAAACCCACAGAAG
Col6a3	**12835**		**Forward**	GCCCATCACCACTCTAACCTCACAG
			reverse	TTGAGTCTGCGAACGATCCTGCTG
Col7a1	**12836**		**forward**	TGGGATGGTGAAGCCGAGATTAAGG
			reverse	CAGCGCAGGGTATAGGCAGTACA
Col8a1	**12837**		**forward**	CCTATGAGATGCCTGCGTTTACTGCC
			reverse	GGTGAAGATGCCTGTCTGCGGATTG
Col13a1	**12817**		**forward**	CCAAAGGGAGAAGCTGGTGTTGAT
			reverse	CGCCTCGTTGATGCTGCCATTA
Tgfbi	**21810**		**forward**	GAAATCCTGGTTAGCGGAGGCATCG
			reverse	CGGCAACAGGCTCCTTATTGACACTC
Matn2	**17181**		**forward**	GCAGTATTCCACACAGGTCCGAA
			reverse	TGGGTCACGGCTTTCTTCATTTCC
Fn1	**14268**		**forward**	GCTGTGAAAGGGAACCAGCAGAGTC
			reverse	CGGTGTTGTAAGGTGGAATGGAGCG
Thbs2	**21826**		**forward**	GTGCTACTAATGCCACCTACCACTGC
			reverse	CGTCACAAGCATCTCCGATTCCATCC
Svep1	**64817**		**forward**	CAAATGCTTGCTCATGCCCAGACGG
			reverse	CACACAGCGCCCACCATTCAAACAG

Gene	ID	Category	Direction	Sequence
Bgn	12111		forward	CTTCAGTGCCATGTGTCCTTTCGG
			reverse	GTCTAGCAGTGTGGTGTCAGGTGAG
Dcn	13179		forward	CCAGTGTCATCTTCGAGTGGTGCAGT
			reverse	GTCTAGCAAGGTTGTGTCGGGTGGAA
Mmp9	17395		forward	GCAAACCCTGTGTGTTCCCGTTCATC
			reverse	GTAACCATCCGAGCGGCCTTTAGTG
Ogn	18295		forward	CGACCTGGAATCTGTGCCTCCTAA
			reverse	CGCTCCCGAATGTAACGAGTGTCA
Ecm1	13601		forward	CCTTGATCTTGGCCTGCTTGGCTCT
			reverse	TGGCGTCATCTCTCGCTGGTCTGAA
Ctsb	13030		forward	ACTTGCTGTGGTATCCAGTGTGGG
			reverse	GGAGGGATGGTGTATGGTAAGCAGC
Sparcl	13602		forward	CCGATCCACAAGGGAAACCTCACTG
			reverse	GTAGCAAACAGGTGACAGGAGCTGG
Fap	14089		forward	TTGACACCACCTACCCTCACCAC
			reverse	CACTGCAAGCATACTCGTTCACTGG
Adam9	11502		forward	AGGATATGGAGGAAGCGTGGACAGC
			reverse	GGAAGAAGAAGACCAGAAGCCCGTC
Itgb1	16412	Cell adhesion	forward	GTAGCAGGCGTGGTTGCTGGAATTG
			reverse	TTCACCCGTGTCCCACTTGGCATTC
Itga5	16402		forward	CTACTTGGGATACTCTGTGGCTGTGG
			reverse	CGTTGTAGAGGGAGTGGATGTCTGAG
Itga6	16403		forward	GCTTCCATAGATGTCACCGCTGCTG

			reverse	GCATCAGAATCCCGGCAAGAACAGC
Shc	**20416**		**forward**	GGAGGTCTTACAGTCAATGCGAGCC
			reverse	CAGGCACAGCTTCACACACCAAAC
Abl1	**11350**		**Forward**	TTAGTGCGGGAGAGTGAGAGTAGCC
			reverse	GTAGTGGAGTGTGGTGATGAGGCCA
Pik3r1	**18708**		**forward**	CTGAGTACCGAGAGATCGACAAACGCA
			reverse	CCAGCCACTCGTTCAGCTTCTTCTG
Map3k1	**26401**		**forward**	GGGACTGGGACTTTAATGGCTGTGA
			reverse	GATCTCTTCCCTCAACGCTTCCACC
Jnk2	**26420**		**forward**	GGGAGAGCTGGTGAAAGGTTGTGTG
			reverse	GAACTCTGCGGATGGTGTTCCTAGC
Pea-15	**18611**		**forward**	GGAGAGCCACAACAAGCTGGACAA
			reverse	GCACACGGGTTCTGTAGTCAACCA
Vcam1	**22329**		**forward**	GTGACAATGACCTGTTCCAGCGAGG
			reverse	AAGGTGAGGGTGGCATTTCCTGAGAG
NCcam	**17967**		**forward**	CAGGCCAGACAGAGCATCGTGAATG
			reverse	GCTTCTCGTCATCTTCCTCCTCGTTC
Dd	**16847**		**forward**	CTGTGTAGTGTGAGGAGGTACGTGG
			reverse	AAGCGCCGAGGGAATTGACAG
Mapre2	**212307**		**forward**	CCAAGAACATGGGCAGGAGAACGA
			reverse	CCTCTGCTTCTGGCTCTTCCGTTTG
LgalsS3	**16854**		**forward**	TATCCTGCTGCTGGCCCTTATGGTG
			reverse	CCTGTTTGCGTTGGGTTTCACTGTGCC
Lgals8	**56048**		**forward**	CTCCATCGGGTTCAGATTCAGCTCG

			reverse	GCTTCGGGCATTGGTGTTCACTTCC
Lgals9	**16859**		**forward**	TTGCTTCCTGGTGCAGAGGTCAGAG
			reverse	TGGTAGGGTACGCGGTGTTGGTACT
Nov	**18133**		**forward**	CTCTGCATCGTTCGGCCTTGTGAA
			reverse	GCTTTCAGGGATTTCTTGGTGCGG
Eda	**13607**		**forward**	AGCCTTTGGAACCGGGAGAAGATCCAC
			reverse	CTTATTGCGGCGAACACGCCTACTTTCC
Spn	**46194**		**forward**	CCTGATGAAGAGGCCACAACCACATC
			reverse	GTACTAAAGAGCCCTGGCGAGACTTCC
Cdh11	**12552**		**forward**	GGAGAGTACATGCCAAAGACCCAGAT
			reverse	TGAGCCAGGCAGTTTCTTCCCTAT
Cdh22	**104010**		**forward**	TGGCCTCTCAGGTTCCACTACAGTC
			reverse	TCATGTCCGTGTTCTCGCCCACATC
Fzd1	**14362**		**forward**	GGACATCGCGTACAACCAGACCATC
			reverse	CGCGTACATGGAGCACAGGAAGAACTTG
Lrp6	**16974**		**forward**	GCCCACTACTCCCTGAATGCTGACAAC
			reverse	CCGAAGGCTGTGGATAGGAAGGATGATG
Bsg	**12215**		**forward**	CGAAGTACATAGTGGACGCAGATGAC
			reverse	GACCAGTTTCGCAAGCTCTCC
CD82	**12521**		**forward**	GTCCTACAAACCTCATCCAGCTCGC
			reverse	GACAAAGTACAGACCCAGCAAGCAGC
Tspan 5	**56224**		**forward**	TCCAATGCAAGCCGAGAGCGATG
			reverse	TGGTCAACTTCTGGTTTCTGCCTGG

Tspan 6	56496		forward	CTGGAGGGCTGTTATCCACAGAGAGATG
			reverse	CACGAGACAGGCAGTAGGCAAGAAAG
Gapdh	14433		forward	CCCACTGAAGGGCATCTTGGGCTAC
			reverse	GGGTGGGTGGTCCAGGGTTTCTTAC

Table 7.2. List with the gene-specific primers used for the qRT-PCR analysis.

7.2. Cell Biology (Cell Culture and Viral transduction)

7.2.1. Culture of AFT024, 2012, BFC012, 2018, knocked down AFT024

Cell lines AFT024, 2012, BFC012 and 2018 were obtained from Kateri Moore, Mount Sinai School of Medicine, New York, USA. These cell lines were isolated from the fetal liver of E14.5 mice and were immortalized by the expression of large T antigen (Wineman et al., 1996). Cells were cultured in high glucose DMEM (Gibco, Cat No 11960-085) supplemented with 10% FCS 14 (PAA, Cat No A15-101, Lot No. A10108-2429), 0,1mM non-essential aminoacids 100x (Gibco, Cat No 11140-035), 1mM sodium pyruvate (Sigma, Cat No S8636), 2mM L-glutamine (Gibco, Cat No 25030-024), 5×10^{-5}M β-Mercaptoethanol (Sigma, Cat No M3142-25ML) and penicillin/streptomycin (Gibco, Cat No 15140-122), which was called "stroma media". Cells were cultured on 33°C with 100% humidity and 5% CO_2. They were passaged 1:5 to 1:6 every 3 days in 6 cm dishes with 2-3 ml of media. Cells were trypsinized by adding 0.05% trypsin-EDTA (Gibco, Cat No 25300-096) for 2-3 minutes which was then quenched by media containing serum.

7.2.2. Thawing & Freezing

When thawed, the plates were coated with 0.1% gelatin for 20 minutes prior to the addition of the cells. Frozen cells were thawed in the water bath (37°C) and then placed directly in the plate (media would have to be changed the next day to remove the DMSO). Alternatively, 9ml of media were added to the thawed cell solution and were centrifuged at 1000rpm for 5 minutes at 4°C. The supernatant was decanted and the cell pellet was re-suspended in 2-3 ml of stroma media (described above) prior to plating.

Cells were frozen in 10% DMSO in FCS 14 (PAA, Cat No A15-101, Lot No. A10108-2429), by first placed in cryo-containers (Nalgene Cryo, Cat No 5100-0001) containing isopropanol at -80°C and then in the liquid nitrogen tank.

7.2.3. Lentiviral constructs

To deliver the desired shRNA constructs (or open reading frames of genes of interest) and ensure their expression in the stroma cells, we used 3rd generation lentiviruses. Generally, lentiviruses are a sub-class of retroviruses that have the unique ability to integrate their genome also in non-dividing cells, whereas retroviruses fail to do so. Lentiviruses are RNA viruses that generate their DNA by reverse transcription upon entering the cell. Their DNA is then randomly integrated in the genome of the host cell by the enzyme integrase (pro-virus stage) and it is inherited to the cell progeny. The 1st generation of lentiviral vectors contained all the HIV genes besides the gene of the envelope (Naldini et al., 1996). In the 2nd generation of vectors, only the reading frames of the *gag*, *pol* (encoding for the structural and enzymatic components of the virion respectively), *tat* and *rev* (for transcriptional and post-transcriptional functions) were kept. Finally, in the 3rd generation, the *tat* reading frame was additionally removed and an engineered 5' LTR was used to ensure *tat*-independent transcription.

The original lentiviral construct used in this study to generate the final lentiviral backbone constructs was a kind gift from C Baum. Briefly, the pLKO.1 vectors used in this study (Figure 7.2) contain the following domains:
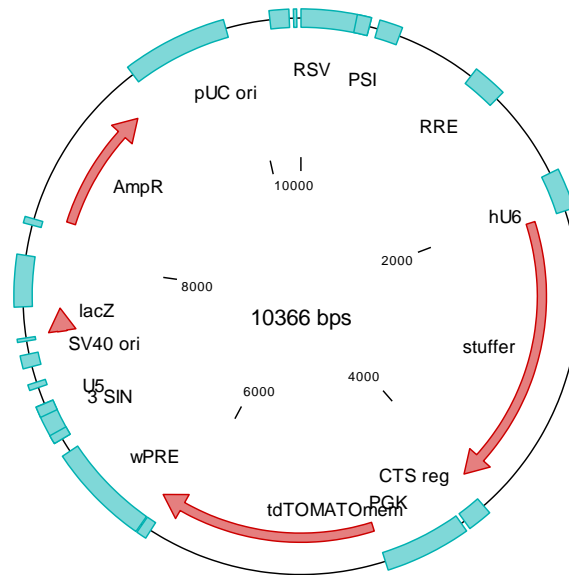
Figure 7.2. depiction of the lentiviral constructs used in this study for stroma manipulation.

- a human U6 promoter driving the transcription of the downstream shRNA by the RNA polymerase III,

- a human phosphoglycerate kinase promoter (PGK) driving the expression of the tandem fluorescent protein tdTOMATO fused with the c-HA-Ras farnesylation signal for membrane anchoring of the fluorescent protein,

- the ampicilin resistance gene (AmpR) for selection of the transformed DH5α bacteria driven by a bacterial promoter

- the pUC origin of replication, which allows DNA replication of the plasmid independently of the replication of the genomic DNA (this origin of replication is derived from *E.coli* plasmid pBR322 and originally contained a mutation (in the Rop/Rom gene) that removes the regulatory constraints on the plasmid replication – bacteria can then produced not just 30-40 plasmids per cell, but up to 500)

- the f1 origin of replication which allows DNA replication in the phage f1

- an engineered 3' self-inactivating long terminal repeat (3' SIN LTR) without the U3 region which is essential for the replication of the lentivirus (contains the viral promoter in its RNA genome), therefore increasing the bio-safety of such vectors

- U5

- SV40 ori

- LacZ

- the woodchuck hepatitis virus (WPRE) for enhancing the stability and increase the level of transcripts both in producer and target cells (Zufferey et al., 1999)

- a central termination sequence (CTS) region

- Rous sarcoma virus (RSV) U3 sequence

- PSI

- Rev response element (RRE)

Since the promoter choice is a very important factor for robust shRNA expression, we chose the human U6 (RNA polymerase III, class III) promoter because: 1. of the relative simple promoter structure, 2. of the well-defined transcriptional starting site, 3. it lacks sequences that can lead to transcription beyond the initial transcription starting site, which can lead to creation of long dsRNA and can trigger interferon response and 4. this class naturally drive the transcription of small RNAs.

7.2.3. Virus production

For the purpose of this study, 3rd generation lentiviral vectors with eco tropism (laboratory safety level S1) were used. HEK293 cells were used as the producer cell line, which plated in $60cm^2$ dishes ($5x10^6$ cells per dish). The next day, the following plasmids and reagents were used for the transfection of HEK cells (table 7.3):

Plasmid no	Reagent	Function	Quantity
391		Tropism (eco)	2ug
392		gag gene (essential for viral structure), pol gene (integration of provirus)	5ug

393		rev gene (reverse transcriptase)	10ug
plasmid of interest			5ug
	$CaCl_2$		50µl
	H_2O		to 500µl

Table 7.3. List with DNA constructs used for the production of ectropic lentiviruses.

After this, 500µl of 2xHBS were added to the mix while the sample was vortexed. HEK cells were placed in 10ml of "transfection media" (DMEM containing L-glutamine and 110mg/ml Sodium Pyruvate (Sigma, Cat No S8636) and supplemented with 10% FCS, 1% penicillin/streptomycin (Gibco, Cat No 15140-122) and 20mM Hepes buffer (Gibco, Cat No 15630-056), just before the addition of the mix mentioned above. After 12 to 24 hours, the media was changed to "stroma media" (which briefly consisted of high Glucose DMEM (Gibco, Cat No 11960-085) supplemented with FCS, non-essential aminoacids, L-glutamine, sodium pyruvate, β-mercaptoethanol and penicillin/streptomycin. One day later, the supernatant from every plate was first filtered through a 0.22μm filter, aliquoted and finally directly frozen at -80°C.

7.2.4. Viral Transduction of stroma cells

For efficient expression of shRNA constructs or open reading frames from selected genes, we used 3rd generation lentiviral vectors for transduction of the stroma cell lines (for construct details see section 7.2.3). Briefly, 15000 stroma cells were plated on a well of a 24-well plate in 2ml of "stroma media" containing viral particles from the engineered virus expressing the construct of. The media was exchanged the next day by fresh "stroma media". Cells were then passaged on 24-well, 6-well plate and finally in a 6-cm dish, before they were analyzed by FACS. Using FACS, the transduced cells, which were expressing tdTOMATO, were distinguished from the non-transduced ones, were sorted and re-plated in gelatinized 6-cm dishes (250000-350000 events per plate). Later, a small number of vials from each genetically-modified stroma cell line was frozen at -80°C and liquid nitrogen.

7.3. Primary Cell Isolation

7.3.1. Mouse strains

Fluorescent reporter transgenic mice (B6J;129-Tg(CAG-EYFP)7AC5Nagy/J), which express a construct (pCX::EYFP) containing the yellow fluorescent protein (YFP) under the control of the chicken beta actin promoter coupled with the cytomegalovirus (CMV) immediate early enhancer (Hadjantonakis et al., 2002). The construct was introduced into (129X1/SvJ x 129S1/Sv)F1-derived R1 embryonic stem cells. The transgenic offspring mice were then backcrossed with C57Bl/6J mice for at least 10 matings and used in the current study. These mice enabled me to distinguish the isolated bone marrow cells from the co-cultured stroma cells. In addition, mT/mG fluorescent reporter mice were also used. These mice express tandem Tomato protein fused with a membrane localization signal under the control of the pCAG promoter. The background of the mT/mG mice is also C57Bl/6J. It is important to note that previous results of the lab regarding the behavior of HSCs and MPPs on different stromata (Erin Drew, personal communication), were generated using YVI mice of mixed background and not C57Bl/6, which is the classical mouse strain used in hematopoietic research. Using mixed background mice can be problematic and introduce variation during experimentation, therefore these data were not used in the current thesis.

7.3.2. HSC isolation – Mouse preparation

The femur, tibia, pelvis and potentially the front legs of mice with the desired genotype were isolated and transferred to Dulbecco's phosphate buffer saline DPBS (Gibco, Cat No 14190-169). The isolated bones were cleaned from residual tissue and muscle and then were mortared. The cell suspension was transferred to a 50ml falcon by filtering through a 100μm cell strainer (Schubert und Weiss, Cat No FALC352360) and then was centrifuged at 1000rpm for 5 minutes at 4°C. The supernatant was decanted and the cell pellet was re-suspended in (2,5ml per mouse) FACS buffer (1mM EDTA, 5% FCS in PBS). Biotinylated lineage antibodies (table 7.4) were added (25μl each per mouse) and incubated for 20 minutes on ice. After a washing step with PBS, the cell solution was centrifuged again and re-suspended as mentioned above. Streptavidin-labeled magnetic beads (Roth, Cat No HP571)

were centrifuged, re-suspended in FACS buffer and then added (25μl per mouse) to the cell solution which was incubated for 20 minutes on ice.

Antibody	Clone	Company	Target cell type
CD3	145-2C11	13-0031-85	T-cells
B220	RA3-6B2	13-0452-86	B-cells
CD19	eBio1D3	13-0193-85	B-cell progenitors
CD41	eBioMWRag30	13-0411-85	Thrombocytes
Terr119	TER-119	13-5291-85	Erythrocytes
Gr1	RB6-8C5	13-5931-85	Granulocytes
Mac1	M1/70	13-0112-85	Macrophages

Table 7.4. List of antibodies used in the lineage depletion of bone marrow cells.

Additional FACS buffer was added to the solution (up to 10ml) and cells were transferred to a polypropylene round bottom (PP) tube (BD Falcon, product no 352063) and then placed in pre-chilled magnet (BigEasy EasySep magnet, Stem Cell Technologies, Cat No 18001) for 7 minutes. Lineage low (Lin^{low}) and negative (Lin^{neg}) cells were then transferred to a new PP tube in which they were centrifuged. The supernatant was decanted and the cell pellet was re-suspended in 200μl of FACS buffer. Finally, the antibodies for the HSC staining were added (table 7.5) based on the cell number (0,2μl Ab per 10^6 cells, except for CD34 for which 25μl were added per mouse, but not more than 50μl in total) and incubated for 30-45 minutes on ice. The cell solution was washed with PBS, centrifuged at 1000rpm for 5 minutes at 4^oC and re-suspended in FACS buffer (≈250μl per mouse). The cells were filtered through a cap of a polystyrene tube (BD Falcon, product no 352235) before analyzed with FACS. For the compensation samples, FACS buffer was added in the lineage positive cells (Lin^+), cells were filtered through the cell strainer to independent tubes and then a single conjugated antibody was added per tube (one tube for each flurochrome). After 30 minutes incubation, cells were washed with PBS, centrifuged and re-suspended in FACS buffer.

Antibody	Flurochrome	Clone	Company
CD34	e450	RAM34	48-0341-82
Sca1	PerCP Cy5.5	D7	45-5981-82
CD150	PE	TC15-12F12.2	115904
CD48	APC	HM48-1	17-0481-82
cKit	PE Cy7	2B8	25-1171-82
Streptavidin	APC e780		47-4317-82

Table 7.5. List of antibodies used for HSC and MPP isolation from murine bone marrow.

7.3.3. Flow cytometry

The flow cytometry analysis was conducted in a FACS Aria I and later in a FACS Aria III (Beckton & Dickinson, Cat No 648282) equipped with a 405nm violet laser, a 488nm blue laser, 561nm yellow/green laser and a 633nm red laser. The 70mm nozzle was used for FACSorting of bone marrow cells and the 100mm nozzle for stroma cells. For multicolor, flow cytometrical analysis and sorting, single-stained samples were used to calculate the bleed-through of each flurochrome to all other channels. Using a specialized algorithm incorporated in the BD software, the percentage of bleed through was then subtracted for each fluorescent channel individually. HSCs and MPP populations were isolated followed the sorting scheme depicted in Figure 7.3.
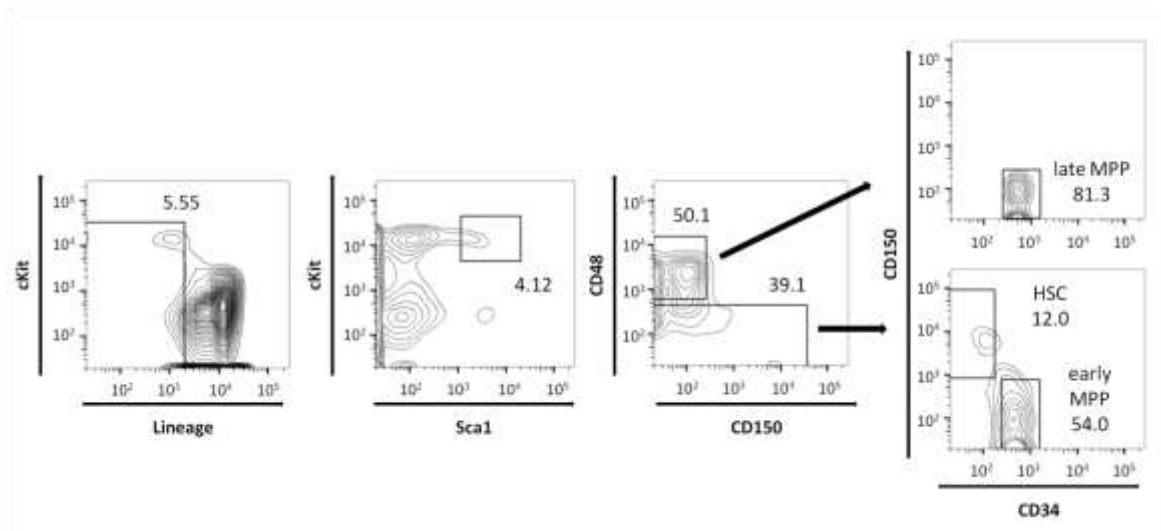
Figure 7.3. Depiction of the gating scheme for isolation of HSCs and MPPs by flow cytometry.

7.4. Time lapse imaging experiments

7.4.1. Preparation of stroma cell monolayers

Before the co-culture of freshly purified hematopoietic cells the with stroma, stroma cells were irradiated with 20Gy from a Co source (Gammacell II, Model GC 220 Type B, Cat No CDN-U13). A specific number of stroma cells (150000 AFT024 or 2012 and 125000 2018) were plated on a well of a 12-well plate (Thermo Scientific, Cat No 150628) containing an ibidi insert (Ibidi, Cat No80209) 18 hours prior to irradiation. The day of the co-culture, the "stroma media" was exchanged with "modified Dexter media" (high glucose DMEM (Gibco, Cat No 11960-085), 10%ml FCS 14 (PAA, Cat No A15-101, Lot No. A10108-2429), 10% Horse serum (Gibco, Cat No 16050-122, Lot No 460470), 5×10^{-5}mM β-mercaptoethanol, 10^{-6}mM Hydrocortisone (Stem Cell Technologies, Cat No 07904) and penicillin/strepromycin (Gibco, Cat No 15140-122).

7.4.2. Time-lapse imaging

For the acquisition of the time-lapse movies, the Zeiss Axiovert 200M or AxioObserver.Z1 microscopes were used. Endogenous YFP signal was detected using the Zeiss Filter 46HE filter (Zeiss, Excitation BP500/25 DMR 25, Beam Splitter FT 515HE, Emission 535/30 DMR 25, Cat No 489046-9901-000). Motorized stages were utilized to

enable image acquisition in different positions and self-made incubators to ensure stable temperature of $37^{o}C$. Phase-contrast or brightfield pictures were acquired every 6 to 12 minutes and fluorescent pictures every 15 minutes using a 5xPlan NeoFluar (numerical aperture 0,3), and recorded by an AxioCamHRm camera (at 1388 x 1040 or 692 x 520 pixel resolution) using the Zeiss AxioVision 4.8 software or later. Mercury lamps (HXP or HBO, both Osram) or light-emitting diode based systems (LEDs, Lumencore, Laser 2000, Cat No 1303749) were used for fluorescent illumination.

7.4.3. Single-cell tracking

Single cell tracking and reconstruction of cells genealogy into trees was performed manually using Timm's Tracking Tool (TTT).

7.4.4. Statistical analysis

Results were analyzed using the non-parametric Mann-Whitney test (one-tailed) for data not following the Gaussian distribution, unless otherwise mentioned. Error bars are standard deviation (SD).

7.5. Protein Detection

7.5.1. Western Blotting (Immunoblot)

Cultured cells were harvested, centrifuged at 12000rpm for 5 minutes, re-suspended in 20μl lysis buffer (4x LDS Sample) and placed at $95^{o}C$ for 5 minutes. Self-prepared gels were used to run cell lysates and protein ladder (Amersham, Full range rainbow molecular weight marker 12000-225000 Da, GE Healthcare, Cat No RPN800E) in running buffer (20x NUPAGE MES SDS Running Buffer, Novex, Ref NP0002) at 200 Volts for 60-90 minutes, depending on the protein bands. Then, the protein bands were transfer into PVDF membrane and run at 30 Volts for 90 minutes in transfer buffer supplemented with 10% methanol (20x

NUPAGE Transfer buffer, Invitrogen, Cat No NP0006-1) Upon successful transfer, the membrane(s) was placed in 10% TBST (0.1M Tris HCl, 1.5M NaCl, 0.5% Tween-20) supplemented with 5% milk (blocking buffer) for 60 minutes at room temperature. Membranes were stained overnight at 4^oC in blocking buffer containing the primary antibodies against dermatopondin (1:1000, rabbit anti-Dpt, Proteintech, Cat No 10537-1-AP), fibroblast activation protein (1:1000, CalbioChem, anti-Fap, Cat No OP188) or γ-Tubulin (1:1000, mouse anti γ -Tubulin, Sigma, Cat No T5326-200ul). Membranes were then washed three times for 5 minutes and subsequently stained in blocking buffer containing secondary antibodies conjugated with horseradish peroxidase HRP (1:15000, anti-rabbit or anti-mouse HRP) for 60 minutes at room temperature. After three washing steps (5 minutes each), ECL chemiluminescent substrate (Lumigen PS-3, Cat No RPN2132V1) was prepared for the detection of HRP in the membranes, by mixing solution A (RPN2132V1) with solution B (RPN2132V2) at 40:1 ratio. Membranes were then developed in a dark room using an X-ray film (FujiFilm Super RX, Cat No 47410 19230). Bands of each sample were quantified and their intensity was normalized against the band corresponding to the house keeping gene with ImageJ.

7.5.2. Immunostaining of bone sections

Femurs from 8-week old female C57Bl/6J mice were isolated and fixed with 10% formaldehyde for 2 days, at 4^oC. The fixed bones were decalcified in 10% cold EDTA for 2 weeks (EDTA was replaced every 3 days), at 4^0C. Then, they were embedded in 4% low-melting agarose and were cut with a vibrotome (Microm HM 650V, Cat No 920120), generating 100υm thick sections. The sections were placed in a microscope slide and blocking buffer was added (1% BSA, 0.1% Triton-X, 5-10% normal donkey serum in PBS) for 60 minutes, at room temperature. Slides were washed with PBDs and Avidin/Biotin block (Vector Labs, Cat No SP-2001) was added. The primary antibodies were added in blocking buffer and incubated overnight at 4^oC in a humidified chamber. Slides were then washed with PBS+0.1% Triton-X and the primary antibodies were added for 2 hours at room temperature. Slides were washed with PBS+0.1% Triton-X, then with PBS-DAPI (1:1000 dilution) and finally with PBS alone and were mounted with Vectashield mounting media (Vector Labs, Cat NoH-1000) in microscope slides for imaging.

7.6. Assays to assess HSC potential

7.6.1. Cobblestone-area forming cell (CAFC) and long-term culture initiating cell (LTC-IC) assays

Freshly purified cells (HSCs or different MPP populations) were sorted from YFP-expressing transgenic mice (mice (B6J;129-Tg(CAG-EYFP)7AC5Nagy/J) as described in the "HSC isolation – Mouse preparation" chapter of the "Materials and Methods" section. A certain number of cells (starting population) was sorted directly in 96-well plates containing different pre-irradiated stroma. The cultures were maintained in Dexter media in the case of CAFC assays or 200μl Myelocult M5300 (StemCell Technologies, Cat. No 05350) supplemented with 10^{-6}M hydrocortisone (StemCell Technologies, Cat. No 07904) and 1% penicillin/streptomycin (Gibco, Cat No 15140-122) per well for the LTC-IC assays, with weekly half-media changes. After 6 weeks of co-culture, the plates for CAFC were screened for cobblestone colonies. On the contrary, the wells of the plates for the LTC-IC assays were trypsinized and cells were transferred into new plates containing 200μl methylcellulose Methocult M3434 (StemCell Technologies, Cat. No 03434). Plates were screened by fluorescent microscopy for the presence of colonies after 2 additional weeks (8 weeks in total).

7.6.2. In vivo transplantation experiments

In vivo transplantations were performed using the CD45.1/CD45.2 congenic mouse system. In more detail, HSCs from CD45.1 were sorted according to the method described before. Different doses of HSCs (100, 350 or 1250 cells) were co-cultured with AFT024, 2018, DLK1KD, DPTKD or FAPKD stroma for 7 days in Dexter media. Then, individual wells were washed and trypsinised before the contents of each well (including the co-culture media and PBS from the washing step) were transplanted into one sub-lethally irradiated CD45.2 recipient. All conditions were performed in quadruplicates. Peripheral blood was collected after 4 and 12 weeks to assess the percentage of chimerism in the recipient mice. Peripheral blood was first washed with PBS and erythrocytes were later lysed by ACK

(Ammonium-Chloride-Potassium) buffer (Life Technologies, Cat No A10492-01). Then, samples were stained with CD45.1-biotin, CD45.2-APC, Ter119-APC e780, B220-PE, Mac1-PE Cy7 and Gr1-PE Cy7. Addition of streptavidin-PB was done as a secondary step. Samples were then washed and analyzed by flow cytometry.

8. References

Abdallah, B.M., Jensen, C.H., Gutierrez, G., Leslie, R.G.Q., Jensen, T.G., and Kassem, M. (2004). Regulation of human skeletal stem cells differentiation by Dlk1/Pref-1. J Bone Miner Res. *19*, 841–852.

Anisimov, S. (2009). Cell therapy for Parkinson's disease: II. Somatic stem cell-based applications]. Adv Gerontol. *22*, 150–166.

Anisimov, S. V, Morizane, A., and Correia, A.S. (2010). Risks and mechanisms of oncological disease following stem cell transplantation. Stem Cell Rev. *6*, 411–424.

Antonchuk, J., Sauvageau, G., and Humphries, R.K. (2002). HOXB4-induced expansion of adult hematopoietic stem cells ex vivo. Cell *109*, 39–45.

Aoyama, A., and Chen, W. (1990). A 170-kDa membrane-bound protease is associated with the expression of invasiveness by human malignant melanoma cells. Proc Natl Acad Sci U S A. *87*, 8296–8300.

Arai, F., Hirao, A., Ohmura, M., Sato, H., Matsuoka, S., Takubo, K., Ito, K., Koh, G.Y., and Suda, T. (2004). Tie2/angiopoietin-1 signaling regulates hematopoietic stem cell quiescence in the bone marrow niche. Cell *118*, 149–161.

Bae, S., Park, C., Son, H., and Ju, H. (2008). Fibroblast activation protein α identifies mesenchymal stromal cells from human bone marrow. Br J Haematol. *142*, 827–830.

Barker, J. (1994). Sl/Sld hematopoietic progenitors are deficient in situ. Exp Hematol. *22*, 174–177.

Barnes, DWH and Loutit, J. (1954). What is the recovery factor in spleen? Nucleonics *12*, 68–71.

Becker, AJ, McCulloch, EA, T.J. (1963). Cytological Demonstration of the clonal nature of Spleen Colonies Derived from Transplanted Mouse Marrow Cells. Nature *197*, 452–454.

Benveniste, P., Frelin, C., Janmohamed, S., Barbara, M., Herrington, R., Hyam, D., and Iscove, N.N. (2010). Intermediate-term hematopoietic stem cells with extended but time-limited reconstitution potential. Cell Stem Cell *6*, 48–58.

Buckley, S.M., Ulloa-montoya, F., Abts, D., Oostendorp, R.A.J., Dzierzak, E., Ekker, S.C., and Verfaillie, C.M. (2011). Maintenance of HSC by Wnt5a secreting AGM-derived stromal cell line. Exp Hematol. *39*, 114–123.e5.

Burton, a L. (1962). Time-lapse phase-contrast cinephotomicrography: a new method in biological research. Can Med Assoc J. *87*, 20–26.

Calvi, L.M., Adams, G.B., Weibrecht, K.W., Weber, J.M., Olson, D.P., Knight, M.C., Martin, R.P., Schipani, E., Divieti, P., Bringhurst, F.R., et al. (2003). Osteoblastic cells regulate the haematopoietic stem cell niche. Nature 841–846.

Challen, G. a, Boles, N.C., Chambers, S.M., and Goodell, M. a (2010). Distinct hematopoietic stem cell subtypes are differentially regulated by TGF-beta1. Cell Stem Cell *6*, 265–278.

Charbord, P., and Moore, K. (2005). Gene Expression in Stem Cell – Supporting Stroma Cell Lines. Ann. N.Y. Acad. Sci. *167*, 159–167.

Cheng, J., Valianou, M., Canutescu, A., Jaffe, E., Lee, H., Wang, H., Lai, J., Bachovchin, W., and Weiner, L. (2005). Abrogation of fibroblast activation protein enzymatic activity attenuates tumor growth. Mol Cancer Ther. *4*, 351–360.

Cho, R.H., and Müller-Sieburg, C.E. (2000). High frequency of long-term culture-initiating cells retain in vivo repopulation and self-renewal capacity. Exp Hematol. *28*, 1080–1086.

Chou, S., Flygare, J., and Lodish, H. (2013). Fetal hepatic progenitors support long-term expansion of hematopoietic stem cells. Exp Hematol. *41*, 479–490.

Chou, S., and Lodish, H. (2010). Fetal liver hepatic progenitors are supportive stromal cells for hematopoietic stem cells. Proc Natl Acad Sci U S A. *107*, 7799–7804.

Chow, A., Lucas, D., Hidalgo, A., Méndez-Ferrer, S., Hashimoto, D., Scheiermann, C., Battista, M., Leboeuf, M., Prophete, C., Van Rooijen, N., et al. (2011). Bone marrow CD169+ macrophages promote the retention of hematopoietic stem and progenitor cells in the mesenchymal stem cell niche. J Exp Med. *208*, 261–271.

Claycombe, K., King, L., and Fraker, P. (2008). A role for leptin in sustaining lymphopoiesis and myelopoiesis. Proc Natl Acad Sci USA2 *105*, 2017–2021.

Curry, B.Y.J.L., Trentin, J., Ph, D., and Wolf, N. (1967). Hemopoietic Spleen Colony Studies. II Erythropoiesis. J. Exp. Med *125*, 703–720.

Curry, JL, and Trentin, J. (1967). Hemopoietic Spleen Colony Studies. 1. Growth and differentiation. Dev Biol. *15*, 395–413.

Dexter, T., Allen, T., Lajtha, L., Schofield, R., and Lord, B. (1973). Stimulation of differentiation and proliferation of haemopoietic cells in vitro. J Cell Physiol. *82*, 461–473.

Dexter, T., Spooncer, E., Simmons, P., and Allen, T. (1984). Long-term marrow culture: an overview of techniques and experience. Kroc Found Ser. *18*, 57–96.

Dexter, T.M., Allen, T.D., and Lajtha, L.G. (1977). Conditions controlling the proliferation of haemopoietic stem cells in vitro. J Cell Physiol. *91*, 335–344.

Ding, L., and Morrison, S.J. (2013). Haematopoietic stem cells and early lymphoid progenitors occupy distinct bone marrow niches. Nature *495*, 231–235.

Dolznig, H., Schweifer, N., Puri, C., Kraut, N., Rettig, W., Kerjaschki, D., and Garin-Chesa, P. (2005). Characterization of cancer stroma markers: in silico analysis of an mRNA expression database for fibroblast activation protein and endosialin. Cancer Immun. *3*, 5–10.

Doulatov, S., Notta, F., Laurenti, E., and Dick, J.E. (2012). Hematopoiesis: a human perspective. Cell Stem Cell *10*, 120–136.

Dunn, G., and Jones, G. (2004). Cell motility under the microscope: Vorsprung durch Technik. Nat Rev Mol Cell Biol. *5*, 667–672.

Dykstra, B., Kent, D., Bowie, M., McCaffrey, L., Hamilton, M., Lyons, K., Lee, S.-J., Brinkman, R., and Eaves, C. (2007b). Long-term propagation of distinct hematopoietic differentiation programs in vivo. Cell Stem Cell *1*, 218–229.

Ehrlich, P. (1879). Ueber die specifischen granulationen des Blutes. Arch Anat Physiol *3*, 571–579.

Eilken, H.M., Nishikawa, S.-I., and Schroeder, T. (2009). Continuous single-cell imaging of blood generation from haemogenic endothelium. Nature *457*, 896–900.

Ellis, S.L., and Nilsson, S.K. (2012). The location and cellular composition of the hemopoietic stem cell niche. Cytotherapy *14*, 135–143.

Ema, H., Takano, H., Sudo, K., and Nakauchi, H. (2000). In vitro self-renewal division of hematopoietic stem cells. J Exp Med. *192*, 1281–1288.

Fliedner, T.M., Graessle, D., Paulsen, C., and Reimers, K. (2002). Structure and function of bone marrow hemopoiesis: mechanisms of response to ionizing radiation exposure. Cancer Biother Radiopharm. *17*, 405–426.

Forbes, E.G., Cronshaw, a D., MacBeath, J.R., and Hulmes, D.J. (1994). Tyrosine-rich acidic matrix protein (TRAMP) is a tyrosine-sulphated and widely distributed protein of the extracellular matrix. FEBS Lett. *351*, 433–436.

Forsberg, E.C., and Smith-Berdan, S. (2009). Parsing the niche code: the molecular mechanisms governing hematopoietic stem cell adhesion and differentiation. Haematologica *94*, 1477–1481.

Garcés, C., Ruiz-Hidalgo, M., and Bonvini, E. (1999). Adipocyte differentiation is modulated by secreted delta-like (dlk) variants and requires the expression of membrane-associated dlk. Differentiation *64*, 103–114.

Gastou, P., and Comandon, J. (1909). L'ultramicroscope et son role essentiel dans le diagnostic de la syphilis. J Med Franc *4*,.

Gekas, C., Dieterlen-Lièvre, F., Orkin, S.H., and Mikkola, H.K. a (2005). The placenta is a niche for hematopoietic stem cells. Dev Cell. *8*, 365–375.

Godin, I., Dieterlen-Lièvre, F., and Cumano, A. (1995). Emergence of multipotent hemopoietic cells in the yolk sac and paraaortic splanchnopleura in mouse embryos, beginning at 8.5 days postcoitus. Proc Natl Acad Sci U S A. *92*, 773–777.

Gong, J. (1978). Endosteal marrow: a rich source of hematopoietic stem cells. Science *199*, 1443–1445.

Goodell, B.M.A., Brose, K., Paradis, G., Conner, A.S., and Mulligan, R.C. (1996). Isolation and Functional Properties of Murine Hematopoietic Stem Cells that are Replicating In Vivo. J. Exp. Med *183*, 1797–1806.

De Graaf, C. a, Kauppi, M., Baldwin, T., Hyland, C.D., Metcalf, D., Willson, T. a, Carpinelli, M.R., Smyth, G.K., Alexander, W.S., and Hilton, D.J. (2010). Regulation of hematopoietic stem cells by their mature progeny. Proc Natl Acad Sci U S A. *107*, 21689–21694.

Hackney, J. a, Charbord, P., Brunk, B.P., Stoeckert, C.J., Lemischka, I.R., and Moore, K. a (2002). A molecular profile of a hematopoietic stem cell niche. Proc Natl Acad Sci U S A. *99*, 13061–13066.

Hadjantonakis, A.-K., Macmaster, S., and Nagy, A. (2002). Embryonic stem cells and mice expressing different GFP variants for multiple non-invasive reporter usage within a single animal. BMC Biotechnology *2*, 11.

Hamrick, M., Pennington, C., Newton, D., Xie, D., and Isales, C. (2004). Leptin deficiency produces contrasting phenotypes in bones of the limb and spine. Bone *34*, 376–383.

Huang, S., Law, P., Francis, K., Palsson, B.O., and Ho, a D. (1999). Symmetry of initial cell divisions among primitive hematopoietic progenitors is independent of ontogenic age and regulatory molecules. Blood *94*, 2595–2604.

Hulett, HR, Bonner, WA, Barrett, J, Herzenberg, L. (1969). Cell sorting: automated separation of mammalian cells as a function of intracellular fluorescence. Science *166*, 747–749.

Hutton, J.F., Rozenkov, V., Khor, F.S.L., Andrea, R.J.D., and Lewis, I.A.N.D. (2006). Bone Morphogenetic Protein 4 Contributes to the Maintenance Ex Vivo Stroma-Noncontact Co-Culture System. Stem Cells Dev. *813*, 805–813.

Ingalls, A., Dickie, M., and Snell, G. (1950). Obese , A New Mutation in the House Mouse. J Hered. *41*, 317–318.

Isern, J., and Méndez-Ferrer, S. (2011). Stem cell interactions in a bone marrow niche. Curr Osteoporos Rep *9*, 210–218.

Issaad, C., Croisille, L., Katz, a, Vainchenker, W., and Coulombel, L. (1993). A murine stromal cell line allows the proliferation of very primitive human CD34++/CD38- progenitor cells in long-term cultures and semisolid assays. Blood *81*, 2916–2924.

Itoh, K., Tezuka, H., and Sakoda, H. (1989). Reproducible establishment of hemopoietic supportive stromal cell lines from murine bone marrow. Exp Hematol. *17*, 145–153.

Jacob, M., Chang, L., and Pure, E. (2012). Fibroblast activation protein in remodeling tissues. Curr Mol Med. *12*, 1220–1243.

Jacobson, LO, Marks, EK, Robson, MJ, Gaston, EO and Zirkle, R. (1949). Effect of spleen protection on mortality following X-irradiation. J. Lab. Clin. Med. *34*, 1538–1543.

Jordan, C.T., and Lemischka, I.R. (1990). Clonal and systemic analysis of long-term hematopoiesis in the mouse. Genes Dev. *4*, 220–232.

Karsenty, G., Kronenberg, H.M., and Settembre, C. (2009). Genetic control of bone formation. Annu Rev Cell Dev Biol. *25*, 629–648.

Kato, A., Okamoto, O., Ishikawa, K., Sumiyoshi, H., Matsuo, N., Yoshioka, H., Nomizu, M., Shimada, T., and Fujiwara, S. (2011). Dermatopontin interacts with fibronectin, promotes fibronectin fibril formation, and enhances cell adhesion. J Biol Chem. *286*, 14861–14869.

Kennedy, M., Firpo, M., Choi, K., Wall, C., Robertson, S., Kabrun, N., and Keller, G. (1997). A common precursor for primitive erythropoiesis and definitive haematopoiesis. Nature *386*, 488–493.

Kent, D.G., Dykstra, B.J., Cheyne, J., Ma, E., and Eaves, C.J. (2008). Steel factor coordinately regulates the molecular signature and biologic function of hematopoietic stem cells. Blood *112*, 560–567.

Kent, D.G., Copley, M.R., Benz, C., Wöhrer, S., Dykstra, B.J., Ma, E., Cheyne, J., Zhao, Y., Bowie, M.B., Zhao, Y., et al. (2009). Prospective isolation and molecular characterization of hematopoietic stem cells with durable self-renewal potential. Blood *113*, 6342–6350.

Kidd, S., Spaeth, E., Watson, K., Burks, J., Lu, H., Klopp, A., Andreeff, M., and Marini, F.C. (2012). Origins of the Tumor Microenvironment: Quantitative Assessment of Adipose-Derived and Bone Marrow – Derived Stroma. PLos One *7*, 1–12.

Kiel, M.J., Yilmaz, O.H., Iwashita, T., Yilmaz, O.H., Terhorst, C., and Morrison, S.J. (2005). SLAM family receptors distinguish hematopoietic stem and progenitor cells and reveal endothelial niches for stem cells. Cell *121*, 1109–1121.

Kiel, M.J., Radice, G.L., and Morrison, S.J. (2007). Lack of evidence that hematopoietic stem cells depend on N-cadherin-mediated adhesion to osteoblasts for their maintenance. Cell Stem Cell *1*, 204–217.

Kiel, M.J., and Morrison, S.J. (2008). Uncertainty in the niches that maintain haematopoietic stem cells. Nature *8*, 290–301.

Kieslinger, M., Hiechinger, S., and Dobreva, G. (2010). Early B cell factor 2 regulates hematopoietic stem cell homeostasis in a cell-nonautonomous manner. Cell Stem Cell *7*, 496–507.

Kim, D.H., Villeneuve, L.M., Morris, K.V., and Rossi, J.J. (2006) Argonaute-1 directs siRNA-mediated transcriptional gene silencing in human cells. Nat Struct Mol Biol. *13(9):* 793-7.

Kodama, H., Amagai, Y., Koyama, H., and Kasai, S. (1982a). Hormonal responsiveness of a preadipose cell line derived from newborn mouse calvaria. J Cell Physiol. *112*, 83–88.

Kodama, H., Amagai, Y., Koyama, H., and Kasai, S. (1982b). A new preadipose cell line derived from newborn mouse calvaria can promote the proliferation of pluripotent hemopoietic stem cells in vitro. J Cell Physiol. *112*, 89–95.

Kodama, H., Nose, M., Yuji Yamaguchi, S., Tsunoda, J., Suda, T., and Nishikawa, S. (1992). In Vitro Proliferation of Primitive Hemopoietic Stem Cells Supported by Stromal Cells: Evidence for the Presence of a Mechanism(s) Other Than That Involving c-kdt Receptor and Its Ligand. J Exp Med. *176*, 351–361.

Kodama, H., Nose, M., Niida, S., and Nishikawa, S. (1994). Involvement of the c-kit receptor in the adhesion of hematopoietic stem cells to stromal cells. Exp Hematol. *22*, 979–984.

Kokkaliaris, K., Loeffler, D., and Schroder, T. (2012). Advances in tracking hematopoiesis at the single-cell level. Curr Opin Hematol. *19*, 243–249.

Kronenberg, H.M. (2003). Developmental regulation of the growth plate. Nature *423*, 332–336.

Köhler, G, Milstein, C. (1975). Continuous cultures of fused cells secreting antibody of predefined specificity. Nature *256*, 495–497.

Landecker, H. (2009). Seeing things: from microcinematography to live cell imaging. Nat Methods. *6*, 707–709.

Lee, K., Jackson, K., Christiansen, V., Lee, C., Chun, J., and McKee, P. (2006). Antiplasmin-cleaving enzyme is a soluble form of fibroblast activation protein. Blood *107*, 1397–1404.

Lewis, I., Almeida-Porada, G., Du, J., Lemischka, I., Moore, K., Zanjani, E., and Verfaillie, C. (2001). Umbilical cord blood cells capable of engrafting in primary, secondary, and tertiary xenogeneic hosts are preserved after ex vivo culture in a noncontact system. Blood *97*, 3441–3449.

Little, M.-T., and Storb, R. (2002). History of haematopoietic stem-cell transplantation. Nat Rev Cancer. *2*, 231–238.

Liu, R., Li, H., Liu, L., Yu, J., and Ren, X. (2012). Fibroblast activation protein: a potential therapeutic target in cancer. Cancer Biol Ther. *13*, 123–129.

Long, F., and Ornitz, D.M. (2013). Development of the Endochondrial Skeleton. Cold Spring Harb Perspect Biol. *5*, 1–20.

Lord, B.I., Testa, N.G., and Hendry, J.H. (1975). The relative spatial distributions of CFUs and CFUc in the normal mouse femur. Blood *46*, 65–72.

Lorenz E, Uphoff D, Reid TR, S.E. (1951). Modification of irradiation injury in mice and guinea pigs by bone marrow injections. J Natl Cancer Inst. *12*, 197–201.

Lymperi, S., Ersek, A., Ferraro, F., Dazzi, F., and Horwood, N.J. (2011). Inhibition of osteoclast function reduces hematopoietic stem cell numbers in vivo. Blood *117*, 1540–1549.

Main, JM and Prehn, R. (1955). Successful skin homografts after the administration of high dosage X radiation and homologous bone marrow. J. Natl Cancer Inst. *15*, 1023–1029.

Mancini, S.J.C., Mantei, N., Dumortier, A., Suter, U., MacDonald, H.R., and Radtke, F. (2005). Jagged1-dependent Notch signaling is dispensable for hematopoietic stem cell self-renewal and differentiation. Blood *105*, 2340–2342.

Mansour, A., Abou-Ezzi, G., Sitnicka, E., Jacobsen, S.E.W., Wakkach, A., and Blin-Wakkach, C. (2012). Osteoclasts promote the formation of hematopoietic stem cell niches in the bone marrow. J Exp Med. *209*, 537–549.

Maximov, A. (1909). Der Lymphozyt als gemeinsame Stammzelle des verschiedenen Blutelemente in der embryonalen Entwicklung und im postfetalen Leben der Säugetiere. Folia Haematologica *8*, 125–134.

Medvinsky, a, and Dzierzak, E. (1996). Definitive hematopoiesis is autonomously initiated by the AGM region. Cell *86*, 897–906.

Mei, B., Zhao, L., Chen, L., and SUL, H. (2002). the large soluble form of preadipocyte factor-1 (Pref-1), but not the small soluble and membrane forms, inhibits adipocyte differentiation: role of alternative splicing. Biochem. J *364*, 137–144.

Metchnikoff, E. (1887). Ueber den Kampf der Zellen gegen Erysipelkokken, ein Beitrag zur Phagocytenlehre. Arch. Pathol. Anat. [Virchow's Archiv.] *107*, 209–249.

Moore, K., Ema, H., and Lemischka, I. (1997a). In vitro maintenance of highly purified, transplantable hematopoietic stem cells. Blood *89*, 4337–4347.

Moore, K., Pytowski, B., Witte, L., Hicklin, D., and Lemischka, I.R. (1997b). Hematopoietic activity of a stromal cell transmembrane protein containing epidermal growth factor-like repeat motifs. Proc Natl Acad Sci U S A. *94*, 4011–4016.

Muller-Sieburg, CE, Whitlock, CA, Weissman, I. (1986). Isolation of Two Early B Lymphocyte Progenitors from mouse marrow. Cell *44*, 653–662.

Muller-Sieburg, C.E., Cho, R.H., Karlsson, L., Huang, J.-F., and Sieburg, H.B. (2004). Myeloid-biased hematopoietic stem cells have extensive self-renewal capacity but generate diminished lymphoid progeny with impaired IL-7 responsiveness. Blood *103*, 4111–4118.

Murayama, E., Kissa, K., Zapata, A., and Mordelet, E. (2006). Tracing hematopoietic precursor migration to successive hematopoietic organs during zebrafish development. Immunity *25*, 963–975.

Méndez-Ferrer, S., Lucas, D., Battista, M., and Frenette, P.S. (2008). Haematopoietic stem cell release is regulated by circadian oscillations. Nature *452*, 442–447.

Méndez-Ferrer, S., Michurina, T. V, Ferraro, F., Mazloom, A.R., Macarthur, B.D., Lira, S. a, Scadden, D.T., Ma'ayan, A., Enikolopov, G.N., and Frenette, P.S. (2010). Mesenchymal and haematopoietic stem cells form a unique bone marrow niche. Nature *466*, 829–834.

Nakano, T., Kodama, H., and Honjo, T. (1994). Generation of lymphohematopoietic cells from embryonic stem cells in culture. Science (New York, NY) *265*, 1098–1101.

Naldini, L., Blömer, U., Gallay, P., and Ory, D. (1996). In vivo gene delivery and stable transduction of nondividing cells by a lentiviral vector. Science *272*, 263–267.

Naveiras, O., Nardi, V., Wenzel, P.L., Hauschka, P. V, Fahey, F., and Daley, G.Q. (2009). Bone-marrow adipocytes as negative regulators of the haematopoietic microenvironment. Nature *460*, 259–263.

Neame, P.J., Choi, H.U., and Rosenberg, L.C. (1989). The isolation and primary structure of a 22-kDa extracellular matrix protein from bovine skin. J Biol Chem. *264*, 5474–5479.

Neumann, E. (1882). Das Gesetz Verbreitung des gelben und rotten Markes in den Extremitätenknochen. Zentbl. Med. Wiss. *18*, 321–323.

Niedermeyer, J., Enenkel, B., Park, J., Lenter, M., Rettig, W., Damm, K., and Schnapp, A. (1998). Mouse fibroblast-activation protein--conserved Fap gene organization and biochemical function as a serine protease. Eur J Biochem. *254*, 650–654.

Niedermeyer, J., Kriz, M., Hilberg, F., Garin-Chesa, P., Bamberger, U., Lenter, M., Park, J., Viertel, B., Püschner, H., Mauz, M., et al. (2000). Targeted disruption of mouse fibroblast activation protein. Mol Cell Biol. *20*, 1089–1094.

Nilsson, S.K., Johnston, H.M., Whitty, G. a, Williams, B., Webb, R.J., Denhardt, D.T., Bertoncello, I., Bendall, L.J., Simmons, P.J., and Haylock, D.N. (2005). Osteopontin, a key component of the hematopoietic stem cell niche and regulator of primitive hematopoietic progenitor cells. Blood *106*, 1232–1239.

Nishikawa, S.I., Nishikawa, S., Hirashima, M., Matsuyoshi, N., and Kodama, H. (1998). Progressive lineage analysis by cell sorting and culture identifies FLK1+VE-cadherin+ cells at a diverging point of endothelial and hemopoietic lineages. Development *125*, 1747–1757.

Nolta, J.A., Thiemann, F.T., Dao, M.A., Barsky, L.W., Moore, K.A., Lemischka, I.R., and Crooks, G.M. (2002). The AFT024 stromal cell line supports long-term ex vivo maintenance of engrafting multipotent human hematopoietic progenitors. Leukemia *16*, 352–361.

Oguro, H., Ding, L., and Morrison, S. (2013). SLAM Family Markers Resolve Functionally Distinct Subpopulations of Hematopoietic Stem Cells and Multipotent Progenitors. Cell Stem Cell *13*, 102–116.

Ohneda, O., Fennie, C., Zheng, Z., Donahue, C., La, H., Villacorta, R., Cairns, B., and Lasky, L. a (1998). Hematopoietic stem cell maintenance and differentiation are supported by embryonic aorta-gonad-mesonephros region-derived endothelium. Blood *92*, 908–919.

Ohta, H., Sekulovic, S., Bakovic, S., Eaves, C.J., Pineault, N., Gasparetto, M., Smith, C., Sauvageau, G., and Humphries, R.K. (2007). Near-maximal expansions of hematopoietic stem cells in culture using NUP98-HOX fusions. Exp Hematol. *35*, 817–830.

Okada, S., Nakauchi, H., Nagayoshi, K., Nishikawa, S., Miura, Y., and Suda, T. (1991). Enrichment and characterization of murine hematopoietic stem cells that express c-kit molecule. Blood *78*, 1706–1712.

Okamoto, O., Fujiwara, S., Abe, M., and Sato, Y. (1999). Dermatopontin interacts with transforming growth factor beta and enhances its biological activity. Biochem J. *337*, 537–541.

Okamoto, O., Hozumi, K., Katagiri, F., Takahashi, N., Sumiyoshi, H., Matsuo, N., Yoshioka, H., Nomizu, M., and Fujiwara, S. (2010). Dermatopontin promotes epidermal keratinocyte adhesion via alpha3beta1 integrin and a proteoglycan receptor. Biochemistry *49*, 147–155.

Omatsu, Y., Sugiyama, T., Kohara, H., Kondoh, G., Fujii, N., Kohno, K., and Nagasawa, T. (2010). The essential functions of adipo-osteogenic progenitors as the hematopoietic stem and progenitor cell niche. Immunity *33*, 387–399.

Oostendorp, R. a J., Harvey, K.N., Kusadasi, N., De Bruijn, M.F.T.R., Saris, C., Ploemacher, R.E., Medvinsky, A.L., and Dzierzak, E. (2002). Stromal cell lines from mouse aorta-gonads-mesonephros subregions are potent supporters of hematopoietic stem cell activity. Blood *99*, 1183–1189.

Orkin, S.H., and Zon, L.I. (2008). Review Hematopoiesis: An Evolving Paradigm for Stem Cell Biology. Cell 631–644.

Van Os, R., Dethmers-Ausema, B., and Haan, G. De (2008). In vitro assays for Cobblestone Area-Forming Cells, LTC-IC and CFU-C. Methods Mol Biol. *430*, 143–157.

Osawa, M., Hanada, K., Hamada, H., and Nakauchi, H. (1996). Long-term lymphohematopoietic reconstitution by a single CD34-low/negative hematopoietic stem cell. Science *273*, 242–245.

Ottersbach, K., and Dzierzak, E. (2005). The murine placenta contains hematopoietic stem cells within the vascular labyrinth region. Dev Cell. *8*, 377–387.

Pappenheim, A. (1896). eber Entwickelung und Ausbildung der Erythroblasten. Archiv Für Pathologische Anatomie Und Physiologie Und Für Klinische Medicin *145*, 587–643.

Petit, I., Szyper-Kravitz, M., Nagler, A., Lahav, M., Peled, A., Habler, L., Ponomaryov, T., Taichman, R.S., Arenzana-Seisdedos, F., Fujii, N., et al. (2002). G-CSF induces stem cell mobilization by decreasing bone marrow SDF-1 and up-regulating CXCR4. Nat Immun. *3*, 687–694.

Pietramaggiori, G., Scherer, S., Alperovich, M., Chen, B., Orgill, D., and Wagers, A. (2009). Improved cutaneous healing in diabetic mice exposed to healthy peripheral circulation. J. Invest. Dermatol. *129*, 2265–2274.

Ploemacher, R., Van der Sluijs, J., Voerman, J., and Brons, N. (1989). An in vitro limiting-dilution assay of long-term repopulating hematopoietic stem cells in the mouse. Blood *74*, 2755–2763.

Ploemacher, R.E., Van der Sluijs, J.P., Van Beurden, C. a, Baert, M.R., and Chan, P.L. (1991). Use of limiting-dilution type long-term marrow cultures in frequency analysis of marrow-repopulating and spleen colony-forming hematopoietic stem cells in the mouse. Blood *78*, 2527–2533.

Punzel, M., Gupta, P., Roodell, M., Mortari, F., and Verfaillie, C.M. (1999a). Factor(s) secreted by AFT024 fetal liver cells following stimulation with human cytokines are important for human LTC-IC growth. Leukemia *13*, 1079–1084.

Punzel, M., Moore, K. a, Lemischka, I.R., and Verfaillie, C.M. (1999b). The type of stromal feeder used in limiting dilution assays influences frequency and maintenance assessment of human long-term culture initiating cells. Leukemia *13*, 92–97.

Punzel, M., Gupta, P., and Verfaillie, C.M. (2002). The microenvironment of AFT024 cells maintains primitive human hematopoiesis by counteracting contact mediated inhibition of proliferation. Cell Commun Adhes. *9*, 149–159.

Punzel, M., Liu, D., Zhang, T., Eckstein, V., Miesala, K., and Ho, A.D. (2003a). The symmetry of initial divisions of human hematopoietic progenitors is altered only by the cellular microenvironment. Exp Hematol. *31*, 339–347.

Punzel, M., Liu, D., Zhang, T., Eckstein, V., Miesala, K., and Ho, A.D. (2003b). The symmetry of initial divisions of human hematopoietic progenitors is altered only by the cellular microenvironment. Exp Hematol. *31*, 339–347.

Ramalho-Santos, M., and Willenbring, H. (2007). On the origin of the term "stem cell". Cell Stem Cell *1*, 35–38.

Rampon, C., and Huber, P. (2003). Multilineage hematopoietic progenitor activity generated autonomously in the mouse yolk sac: analysis using angiogenesis-defective embryos. Int J Dev Biol. *4*, 273–280.

Rettig, W., Chesa, P., Beresford, H., Feickert, H., Jennings, M., Cohen, J., Oettgen, H., and Old, L. (1986). Differential expression of cell surface antigens and glial fibrillary acidic protein in human astrocytoma subsets. Cancer Res. *46*, 6406–6412.

Rettig, W., Su, S., Fortunato, S., Scanlan, M., Raj, B., Garin-Chesa, P., Healey, J., and Old, L. (1994). Fibroblast activation protein: purification, epitope mapping and induction by growth factors. Int J Cancer. *58*, 385–392.

Rieger, M., Hoppe, P.S., Smejkal, B.M., Eitelhuber, A.C., and Schroeder, T. (2009). Hematopoietic cytokines can instruct lineage choice. Science *325*, 217–218.

Ries, J. (1907). Kinematographie der Befruchtung und Zellteilung. Archiv Für Mikroskopische Anatomie *74*, 1–31.

Roberts, E.W., Deonarine, A., Jones, J.O., Denton, a. E., Feig, C., Lyons, S.K., Espeli, M., Kraman, M., McKenna, B., Wells, R.J.B., et al. (2013). Depletion of stromal cells expressing fibroblast activation protein- from skeletal muscle and bone marrow results in cachexia and anemia. J Exp Med. *210*, 1137–1151.

Rosendaal, M., Hodgson, G.S., and Bradley, T.R. (1976). Haematopoietic stem cells are organised for use on the basis of their generation-age. Nature *264*, 68–69.

Roux, P., Münter, S., Frischknecht, F., Herbomel, P., and Shorte, S.L. (2004). Focusing light on infection in four dimensions. Cell Microbiol. *6*, 333–343.

Samokhvalov, I.M., Samokhvalova, N.I., and Nishikawa, S. (2007). Cell tracing shows the contribution of the yolk sac to adult haematopoiesis. Nature *446*, 1056–1061.

Scanlan, M., Raj, B., Calvo, B., Garin-Chesa, P., Sanz-Moncasi, M., Healey, J., Old, L., and Rettig, W. (1994). Molecular cloning of fibroblast activation protein alpha, a member of the serine protease family selectively expressed in stromal fibroblasts of epithelial cancers. Proc Natl Acad Sci U S A. *91*, 5657–5661.

Schofield, R. (1978). The relationship between the spleen colony-forming cell and the haemopoietic stem cell. Blood Cells *4*, 7–25.

Schroeder, T. (2008). Imaging stem-cell-driven regeneration in mammals. Nature *453*, 345–351.

Schroeder, T. (2011). Long-term single-cell imaging of mammalian stem cells. Nat Methods. *8*, 30–35.

Sekulovic, S., Gasparetto, M., Lecault, V., Hoesli, C. a, Kent, D.G., Rosten, P., Wan, A., Brookes, C., Hansen, C.L., Piret, J.M., et al. (2011). Ontogeny stage-independent and high-level clonal expansion in vitro of mouse hematopoietic stem cells stimulated by an engineered NUP98-HOX fusion transcription factor. Blood *118*, 4366–4376.

Shimizu, N., Noda, S., Katayama, K., Ichikawa, H., Kodama, H., and Miyoshi, H. (2008). Identification of genes potentially involved in supporting hematopoietic stem cell activity of stromal cell line MC3T3-G2/PA6. Int J Hematol. *87*, 239–245.

Sieburg, H.B., Cho, R.H., Dykstra, B., Uchida, N., Eaves, C.J., and Muller-Sieburg, C.E. (2006). The hematopoietic stem compartment consists of a limited number of discrete stem cell subsets. Blood *107*, 2311–2316.

Van der Sluijs, J., De Jong, J., Brons, N., and Ploemacher, R. (1990). Marrow repopulating cells, but not CFU-S, establish long-term in vitro hemopoiesis on a marrow-derived stromal layer. Exp Hematol. *18*, 893–896.

Smas, C.M., Chen, L., and Sul, H.S. (1997). Cleavage of membrane-associated pref-1 generates a soluble inhibitor of adipocyte differentiation. Mol Cell Biol. *17*, 977–988.

Spangrude, G.J., Heimfeld, S., and Weissman, I.L. (1988). Purification and characterization of mouse hematopoietic stem cells. Science *241*, 58–62.

Sugimura, R., He, X.C., Venkatraman, A., Arai, F., Box, A., Semerad, C., Haug, J.S., Peng, L., Zhong, X.-B., Suda, T., et al. (2012). Noncanonical Wnt signaling maintains hematopoietic stem cells in the niche. Cell *150*, 351–365.

Sugiyama, T., Kohara, H., and Noda, M. (2006). Maintenance of the Hematopoietic Stem Cell Pool by CXCL12-CXCR4 Chemokine Signaling in Bone Marrow Stromal Cell Niches. Immunity *25*, 977–988.

Sul, H.S. (2009). Minireview: Pref-1: Role in Adipogenesis and Mesenchymal Cell Fate. Mol Endocrinol. *23*, 1717–1725.

Superti-Furga, A., Rocchi, M., Schäfer, B., and Gitzelmann, R. (1993). Complementary DNA sequence and chromosomal mapping of a human proteoglycan-binding cell-adhesion protein (dermatopontin). Genomics *17*, 463–467.

Sutherland, H.J., Eaves, C.J., Lansdorp, P.M., Thacker, J.D., and Hogge, D.E. (1991). Differential regulation of primitive human hematopoietic cells in long-term cultures maintained on genetically engineered murine stromal cells. Blood *78*, 666–672.

Suzuki, J., Fujita, J., and Taniguchi, S. (1992). Characterization of murine hemopoietic-supportive (MS-1 and MS-5) and non-supportive (MS-K) cell lines. Leukemia *6*, 452–458.

Takeda, U., Utani, A., Wu, J., and Adachi, E. (2002). Targeted disruption of dermatopontin causes abnormal collagen fibrillogenesis. J Invest Dermatol. *119*, 678–683.

Talbot, F. (1931). Practical Cinematography and its Applications. (London: William Heinemann).

Tauber, A.I. (2003). Metchnikoff and the phagocytosis theory. Nat Rev Mol Cell Biol. *4*, 897–901.

Tavassoli, M. (1981). Structure and function of sinusoidal endothelium of bone marrow. Prog Clin Biol Res. *59B*, 249–256.

Thiemann, F., Moore, K., Smogorzewska, E., Lemischka, I., and Crooks, G. (1998). The murine stromal cell line AFT024 acts specifically on human CD34+ CD38-progenitors to maintain primitive function and immunophenotype in vitro. Exp Hematol. *26*, 612–619.

Thomas, E.D. (2000). Bone Marrow Transplantation: A Historical Review. *36*, 209–218.

Till, J.E., and McCulloch, E. a (1961). A direct measurement of the radiation sensitivity of normal mouse bone marrow cells. 1961. Radiat Res. *14*, 213–222.

Till, J.E., McCulloch, E.A., and Siminovitch, L. (1964). A stohastic Model of Stem Cell Proliferation based on the Growth of Spleen Colony-Forming Cells. Proc. Natn. Acad. Sci. U.S.A. *51*, 29–36.

Trentin, J.J. (1971). Determination of Bone Marrow Stem Cell Differentiation by Stromal Hemopoietic Inductive. Am J Pathol. *65*, 621–628.

Tyndall, A., and Gratwohl, A. (1997). marrow stem cell transplants in autoimmune disease. A consensus report written on behalf of the European League Against Rheumatism (EULAR) and the European. Br J Rheumatol. *36*, 390–392.

Ueno, H., Sakita-Ishikawa, M., Morikawa, Y., Nakano, T., Kitamura, T., and Saito, M. (2003). A stromal cell-derived membrane protein that supports hematopoietic stem cells. Nature Immunology *4*, 457–463.

Wagers, A.J. (2012). The Stem Cell Niche in Regenerative Medicine. Cell Stem Cell *10*, 362–369.

Wagner, W., Saffrich, R., Wirkner, U., Eckstein, V., Blake, J., Ansorge, A., Schwager, C., Wein, F., Miesala, K., Ansorge, W., et al. (2005). Hematopoietic progenitor cells and cellular microenvironment: behavioral and molecular changes upon interaction. Stem Cells *23*, 1180–1191.

Wang, L.D., and Wagers, A.J. (2011). Dynamic niches in the origination and differentiation of haematopoietic stem cells. Nature *12*, 643–655.

Weiss, L. (1976). The hematopoietic microenvironment of the bone marrow: an ultrastructural study of the stroma in rats. The Anatomical Record *186*, 161–184.

Weissman, I.L. (2002). The road ended up at stem cells. Immunol Rev. *185*, 159–174.

Weissman, I.L., and Shizuru, J. a (2008). The origins of the identification and isolation of hematopoietic stem cells, and their capability to induce donor-specific transplantation tolerance and treat autoimmune diseases. Blood *112*, 3543–3553.

Whitlock, C. a, and Witte, O.N. (1982). Long-term culture of B lymphocytes and their precursors from murine bone marrow. Proc Natl Acad Sci U S A. *79*, 3608–3612.

Wilson, A., and Trumpp, A. (2006). Bone-marrow haematopoietic-stem-cell niches. Nat Rev Immunol. *6*, 93–106.

Wilson, A., Laurenti, E., and Oser, G. (2008). Hematopoietic stem cells reversibly switch from dormancy to self-renewal during homeostasis and repair. Cell *135*, 1118–1129.

Wineman, J., Moore, K., Lemischka, I., and Müller-Sieburg, C. (1996). Functional heterogeneity of the hematopoietic microenvironment: rare stromal elements maintain long-term repopulating stem cells. Blood *87*, 4082–4090.

Winkler, I.G., Sims, N.A., Pettit, A.R., Barbier, V., Helwani, F., Poulton, I.J., Rooijen, N. Van, and Alexander, K.A. (2010). Bone marrow macrophages maintain hematopoietic stem cell (HSC) niches and their depletion mobilizes HSC. Blood *116*, 4815–4828.

Wolf, NS, and Trentin, J. (1968). Hematopoietic Colony Studies. V. Effect of hemopoietic organ stroma on differentiation of pluripotent stem cells. J Exp Med. *127*, 205–214.

Wu, a M., Till, J.E., Siminovitch, L., and McCulloch, E. a (1967). A cytological study of the capacity for differentiation of normal hemopoietic colony-forming cells. J Cell Physiol. *69*, 177–184.

Xu, M.J., Tsuji, K., Ueda, T., Mukouyama, Y.S., Hara, T., Yang, F.C., Ebihara, Y., Matsuoka, S., Manabe, a, Kikuchi, a, et al. (1998). Stimulation of mouse and human

primitive hematopoiesis by murine embryonic aorta-gonad-mesonephros-derived stromal cell lines. Blood *92*, 2032–2040.

Yoder, M.C., Papaioannou, V.E., Breitfeld, P.P., and Williams, D. a (1994). Murine yolk sac endoderm- and mesoderm-derived cell lines support in vitro growth and differentiation of hematopoietic cells. Blood *83*, 2436–2443.

Yoder, M.C., King, B., Hiatt, K., and Williams, D. a (1995). Murine embryonic yolk sac cells promote in vitro proliferation of bone marrow high proliferative potential colony-forming cells. Blood *86*, 1322–1330.

Yoder, M.C., and Hiatt, K. (1997). Engraftment of embryonic hematopoietic cells in conditioned newborn recipients. Blood *89*, 2176–2183.

Yoder, M.C., Hiatt, K., and Mukherjee, P. (1997). In vivo repopulating hematopoietic stem cells are present in the murine yolk sac at day 9.0 postcoitus. Proc Natl Acad Sci U S A. *94*, 6776–6780.

Yoshihara, H., Arai, F., Hosokawa, K., Hagiwara, T., Takubo, K., Nakamura, Y., Gomei, Y., Iwasaki, H., Matsuoka, S., Miyamoto, K., et al. (2007). Thrombopoietin / MPL Signaling Regulates Hematopoietic Stem Cell Quiescence and Interaction with the Osteoblastic Niche. Cell *1*, 685–697.

Zhang, J., Niu, C., Ye, L., Huang, H., He, X., Harris, S., Wiedemann, L.M., Mishina, Y., and Li, L. (2003). Identification of the haematopoietic stem cell niche and control of the niche size. Nature *425*, 836–841.

Zhang, Y., Proenca, R., Maffei, M., Barone, M., Leopold, L., and Friedman, J. (1994). Positional cloning of the mouse obese gene and its human homologue. Nature *372*, 452–32.

Zovein, A., Hofmann, J., Lynch, M., French, W., Turlo, K., Yang, Y., Becker, M., Zanetta, L., Dejana, E., Gasson, J., et al. (2008). Fate tracing reveals the endothelial origin of hematopoietic stem cells. Cell Stem Cell *3*, 625–636.

Zufferey, R., Donello, J., Trono, D., and Hope, T. (1999). Woodchuck hepatitis virus posttranscriptional regulatory element enhances expression of transgenes delivered by retroviral vectors. J Virol. *73*, 2286–2292.

9. Abbreviations

°C: degree Celsius

2-Me: 2-Mercaptoethanol

AA4.1: cell surface antigen AA4 or CD93,

AGM: *aorta-gonad mesonephros region*

AM region: dorsal aorta/mesenchyme region

BM: bone marrow

BMP4: bone morphogenic protein 4

Bmpr1a: Bone morphogenic protein receptor type 1a

BSA: bovine serum albumin

CA: Cobblestone area

CAG: chicken beta actin

CAFC: cobblestone area forming cell

CB: cord blood

CFC: colony forming cells

CFU: cobblestone forming unit

CFU-S: spleen colony forming unit

c-Kit: kit oncogene

CLP: common lymphoid progenitor

CMP: common myeloid progenitor

EDTA ethylene-diamin-tetraacetic acid

EL: embryonic liver

EPCR: endothelial protein C receptor

E-SLAM code: EPCR, CD48, CD150

ETP: earliest thymic progenitor

FACS: fluorescent-activated cell sorting

FCS: fetal calf serum

FL or Flt-3l: fms-related tyrosine kinase 3 ligand

FL: fetal liver

G1: gastrointestinal region

G-CSF: granulocyte colony-stimulating factor

GM-CSF: granulocyte macrophage colony-stimulating factor

GMP: granulocyte/monocyte progenitor

HC: hydrocortisone

HS: horse serum

HER model: Hematopoiesis is engendered randomly

HIM model: Hematopoietic Inductive Microenvironments

HOXB4: homeobox B4

HSCs: Hematopoietic stem cells

IL-3: interleukin 3

IL-6: interleukin 6

IL-6: interleukin 6

IL-7: interleukin 7

IL-8: interleukin 8

IT-HSC: intermediate-term hematopoietic stem cell

KSL: cKit+ or mast/stem cell growth factor receptor Kit, Sca1+ or stem cell
antigen 1, Lineage- cells

LDA LTC-IC: limiting dilution long-term culture initiating cell,

LIF: leukemia inhibitory factor

Lin: Lineage

LTC-IC: long-term culture initiating-cell

LT-HSC: long-term hematopoietic stem cell

Ly-bi HSCs: lymphoid-biased HSCs

MCP-1: monocyte chemoattractant protein 1

MEP: megakaryocyte/platelet progenitor

MIP-1a: macrophage inflammatory protein 1-alpha

MPP: multipotent progenitor

My-bi HSCs: myeloid-biased HSCs

NOD/SCID mice: non-obese diabetic severe combined immunodeficient

proB: B-cell progenitor

Pth: parathyroid hormone

qRT-PCR: quantitative real time polymerase chain reaction

Sca1: stem cell antigen 1

SCF: stem cell factor

SLAM code: CD150, CD48

SP: side population

SV40T: temperature-sensitive simian virus 40 large T antigen

Thy1: thymus cell antigen 1, theta

Tpo: thrombopoietin

TTT: Timm's Tracking Tool

UCB: umbilical cord blood

UG region: urogenital ridges region

VEGF: vascular endothelial growth factor

YS: yolk sac

10. Acknowledgements

I would like to first thank Dr Timm Schroeder for his supervision and mentorship during these 4 years of my PhD life. Timm, I would really like to thank you for having your office's door always open for me, for replying to my midnight emails within few minutes, for our fruitful conversations and for your support and guidance. Thank you also for your trust, time, energy and for the unique opportunity to make my hobby a proper job.

I would also like to thank the members of my thesis committee meetings (Prof Dr Heinrich Leonhardt, Prof Dr Gunnar Schotta and Dr Matthias Kieslinger) for their constructive feedback and for transforming our meetings to pleasant discussion!

Special thanks to Dr Teri Moore and Prof Dr Ihor Lemischka for sharing the quality of their lab in the Mount Sinai School of Medicine, NY and more importantly the warmth of their house in Harlem with me.

I have a very special thanks to my lab colleagues for creating a high-quality scientific niche; Sandra and Bianca for the endless technical support, Christian for the technical support and for intriguing discussions, Dan for being such a great colleague and character (not to mention your critical reading of this manuscript), Dirk for the great scientific and philosophical discussions, for sharing the same office, neighboring lab space and same rooms during meetings/etc, Max for your help and time with FACS and transplants, Joost for usually being a patient listener during our discussions, Bernhard and Olli for fulfilling my TTT needs, Philipp for FACS support, Adam for interesting discussions and volley-ball games, Laura for the funny moments and discussions and Simon for always being patient. Also, many thanks to Christoph Hinzen and Matthias Kieslinger for their valuable help in performing and organising the in vivo transplantations!

Last, but not least, I would like to thank Marina for her incredible support in scientific and every-day life, my friends for the great moments and memories during all these years (Platon, Petro, Tsavo, Panagioti, Koze, Nikos, Efi, Eleni, Maria, Gianna), my beloved family (Magda, Dimo, Ntoraki and soon Mimi) and my giagia for their endless support.

CURRICULUM VITAE

Name: Konstantinos D. Kokkaliaris

Date and Place of birth: 08-04-1984, Cholargos, Athens, Greece

Contact number: +30 6977128974, +44 (0)7531152936

E-mail: kokkaliaris@helmholtz-muenchen.de

kostaskokkal@yahoo.gr

EDUCATION

- **2002** Graduation from Xantos Lyceum, Chaidari, Athens, Greece (Excellent, 18.3/20)
- **2002** Accepted in the Faculty of Biology in the National and Kapodistrian University of Athens after successful National Entrance Examinations
- **2008** Defended Diploma Thesis (Excellent, 10) (Supervisor: Prof. Dr Loukas H. Margaritis)
- **2008** Diploma Degree in Biology (7.1/10), Faculty of Biology, National & Kapodistrian University of Athens, Athens, Greece
- **2008-2009**: MSc by Research on Life Sciences, The College of Medicine & Veterinary Medicine, University of Edinburgh, Edinburgh, Scotland, UK (Supervisor: Dr Lesley Forrester)
- **2009-2013**: PhD Candidate, Institute for Stem Cell Research, Helmholtz Center Munich & Ludwig Maximilian University of Munich, Munich, Germany (Supervisor: Dr Timm Schroeder)
  - **2012**: Research visit in the Mount Sinai School of Medicine, Department of Developmental and Regenerative Biology, The Black Family Stem Cell Institute, New York, NY, USA (Prof. Dr Ihor Lemischka and Prof. Dr Kateri Moore)
- **2014- today**: Post Doctoral fellow, Cell System Dynamics group, Department of Biosystems Science and Engineering, ETH Zurich, Basel, Switzerland (Supervisor: Prof Dr Timm Schroeder)

PUBLICATIONS

- Loeffler D**, Kokkaliaris KD** and Schroeder T **(2011)** Wnt to Notch relay signaling induces definitive hematopoiesis. *Cell Stem Cell,* 9(1): 2-4. Impact factor 2011: 25,943
- Jackson M, Axton RA, Taylor AH, Wilson JA, Gordon-Keylock SA, **Kokkaliaris KD**, Brickman JM, Schulz H, Hummel O, Hubner N, Forrester LM **(2012)** HOXB4 Can Enhance the Differentiation of Embryonic Stem Cells by Modulating the Hematopoietic Niche. *Stem Cells*, 30:150-160. Impact factor: **7,871**
- **Kokkaliaris KD,** Loeffler D and Schroeder T **(2012)** Advances in Tracking Hematopoiesis at the Single Cell Level. *Current Opinion in Hematology,* 19(4):243-9. Impact factor: **4,953**
- Montrone C, **Kokkaliaris KD**, Loeffler D, Lechner M, Kastenmüller G, Schroeder T, Ruepp A (**2013**) HSC-Explorer: A Curated Database for Hematopoietic Stem Cells. *PLoS One,* 8(7): e70348. Impact factor: **4,09**

- Margaritis LH, Manta AK, **Kokkaliaris KD**, Schiza D, Alimisis K, Barkas G, Georgiou E, Giannakopoulou O, Kollia I, Kontogianni G, Kourouzidou A, Myari A, Roumelioti F, Skouroliakou A, Sykioti V, Varda G, Xenos K, Ziomas K (**2013**) Drosophila oogenesis as a bio-marker responding to EMF sources. *Electromagn Biol Med.* 33(3):165-89. Impact factor: **1,15**
- Swiers G, Baumann C, O'Rourke J, Giannoulatou E, Taylor S, Joshi A, Moignard V, Pina C, Bee T, **Kokkaliaris KD**, Yoshimoto M, Yoder MC, Frampton J, Schroeder T, Enver T, Göttgens B, de Bruijn MF (**2014**) Early dynamic fate changes in haemogenic endothelium characterized at the single-cell level. *Nat Commun*, 4:2924. Impact factor: **10,74**

HONOURS & AWARDS

- **2010-2011**: Deutscher Akademischer Austausch Dienst – **DAAD** (German Academic Exchange Service), **Scholarship for doctoral studies**
- **2012**: **Boehringer Ingelheim Fonds** (Foundation for Basic Research in Medicine) **travel grant** for research visit in the Mount Sinai School of Medicine, Department of Developmental and Regenerative Biology, The Black Family Stem Cell Institute, New York, NY, USA

SKILLS

Experimental Techniques & Expertise:

- **Molecular Biology:** all basic cloning techniques, qRT-PCR, shRNA knockdown techniques, western blotting, generation of lentiviral vectors
- **Cell Biology:** Cell culture of clonal cell lines, culture of embryonic stem cells, cell transfection, cell death assays (orange acridine, TUNEL assay), immunofluorescence labelling, luciferase assays, flow cytometry
- **Imaging / Microscopy:** Optical and electron microscopy, wide-field microscopy, fluorescence microscopy, Confocal Laser Scanning Microscopy, Live Cell Time Lapse Imaging, Total Internal Reflection Fluorescence Microscopy (TIRFM), image data analysis (ImageJ, Imaris software) & Deconvolution (Huygens Software).
- **Laboratory Animals:** Certificate in Laboratory Animal Science for Researchers (**FELASA C** Diploma)

Computational Background

- European Computer Driving License - ECDL Core
- Expert in Microsoft Office 2003 and 2007, Internet, Adobe Photoshop
- Linux user (Ubuntu, Suse)

Eidesstattliche Erklärung

Ich versichere hiermit an Eides statt, dass die vorgelegte Dissertation von mir selbständig und ohne unerlaubte Hilfe angefertigt ist.

München, den ....26.09.2014......... ....

<div align="center">(Unterschrift)</div>

Erklärung

Hiermit erkläre ich, *

[X] dass die Dissertation nicht ganz oder in wesentlichen Teilen einer anderen Prüfungskommission vorgelegt worden ist.

[ ] dass ich mich anderweitig einer Doktorprüfung ohne Erfolg **nicht** unterzogen habe.

[ ] dass ich mich mit Erfolg der Doktorprüfung im Hauptfach ....

und in den Nebenfächern ....

bei der Fakultät für .... der ....

<div align="center">(Hochschule/Universität)</div>

unterzogen habe.

[ ] dass ich ohne Erfolg versucht habe, eine Dissertation einzureichen oder mich der Doktorprüfung zu unterziehen.

München, den.........26.09.2014......... ....

<div align="center">(Unterschrift)</div>

*) Nichtzutreffendes streichen